5-2007

Low-complexity iterative detection techniques for Slow-Frequency-Hop spread-spectrum communications with Reed-Solomon coding.

Harish Ramchandran
Clemson University, hramcha@ces.clemson.edu

LOW-COMPLEXITY ITERATIVE DETECTION TECHNIQUES FOR SLOW-FREQUENCY-HOP SPREAD-SPECTRUM COMMUNICATIONS WITH REED-SOLOMON CODING

A Dissertation
Presented to
the Graduate School of
Clemson University

In Partial Fulfillment
of the Requirements for the Degree
Doctor of Philosophy
Electrical Engineering

by
Harish Ramchandran
May 2007

Accepted by:
Dr. Daniel L. Noneaker, Committee Chair
Dr. Carl W. Baum
Dr. Michael B. Pursley
Dr. Michael M. Kostreva

ABSTRACT

Slow-frequency-hop (SFH) spread-spectrum communications provide a high level of robustness in packet-radio networks for both military and commercial applications. Reed-Solomon (R-S) coding has proven to be a good choice for countering the critical channel impairments of partial-band fading and partial-band interference in a SFH system. In particular, it is effective if information about the reliability of individual code-symbol decisions or the content of entire dwell intervals is obtained at the receiver and used in errors-and-erasures (EE) decoding of the R-S code words.

In this dissertation, we consider high-data-rate SFH communications for which the channel in each frequency slot is frequency selective, manifesting itself as intersymbol interference (ISI) at the receiver. The use of a packet-level iterative equalization-and-decoding technique is considered in conjunction with a SFH system employing R-S coding. In each packet-level iteration, MLSE equalization is used in each dwell interval and is followed by bounded-distance EE decoding of the R-S code words. Several per-dwell interleaver designs are considered for the SFH systems. It is shown that packet-level iterations result in a significant improvement in performance with only a modest increase in detection complexity for a variety of ISI channels. The use of differential encoding in conjunction with the SFH system and packet-level iterations is also considered, and it is shown to provide further improvements in performance with only a modest additional increase in detection complexity. The performance SFH systems employing packet-level iterations with and without differential encoding is also evaluated for channels with partial-band interference. Comparisons are made between the performance of this system and the

performance of SFH systems using some other codes and iterative decoding techniques.

DEDICATION

This dissertation is dedicated to the memory of my grandfather, Mr. U. Gopalakrishnan Nair, who passed away three years ago. He is one of the greatest human beings that I have met and has been influential on many fronts in my life. I would also dedicate this work to my loving parents who instilled in me a passion to excel and always encouraged me to strive for higher goals.

ACKNOWLEDGMENTS

I would like to thank my advisor Dr. Daniel Noneaker for his assistance during my entire graduate studies in Clemson. His patient guidance and many valuable insights helped me accomplish my research goals in a timely and systematic fashion. Many thanks are in order to Dr. Michael Pursley, Dr. Carl Baum and Dr. Michael Kostreva for serving on my dissertation committee and for taking the time to review my dissertation and providing feedback. Thanks to Drs. Pursley and Baum in particular for questions they raised which helped define the topic of Chapter 6. I would like to thank the Army Research Office and the Army Research Laboratory for providing me with financial assistance through graduate school. All the current and past students of the Wireless Communications Laboratory in Clemson have been great people to work and interact with. I would especially want to name Jason, Arvind, Tommy and Steve with whom I always had a lot of fun during our annual trips to attend the Milcom conference.

A special mention to soon-to-be Drs. Aditya Chaubey and Rahul Rao, who have not only been great friends but also people who exposed me to many new avenues and interests beyond academics. The long, sometimes heated but always interesting discussions at Keith Street and other places in Clemson qualify for moments in Clemson that I will remember for a long time. They along with Sajay, Laura, Srikant, Anushree, Sourabh, Rachana, Kunal, Vijay and Ananya have made my stay in Clemson thoroughly enjoyable and probably the best years of my life. I would also like to mention my longtime friends Santosh, Ramola and Hiten and my cousin Anisha who have been there for me everytime I needed them. Their motivation and encouragement has helped me climb many hurdles in life. And last but not the least I want to thank my dearest wife Rekha who supported me whole-heartedly during the long hours of work in the last year of my studies. I would not have been able to finish this dissertation without her love and support.

TABLE OF CONTENTS

Page

LIST OF TABLES

LIST OF FIGURES

Figure Page

Figure Page

CHAPTER 1

INTRODUCTION

Many applications of packet radio communications involve circumstances in which only limited coordination is possible among the nodes of the radio network. As a consequence, multiple-access interference frequently gives rise to the near-far interference condition at receivers in the network [1]. Moreover, the receivers are often subjected to non-network sources of partial-band interference of varied and unpredictable bandwidth and power. A high level of robustness can be achieved by the network in the face of these impairments if the nodes in the network employ slow-frequency-hop (SFH) spread-spectrum modulation with appropriate channel coding techniques.

In particular, Reed-Solomon (R-S) coding has proven to be an effective tool for countering multiple-access interference and other partial-band interference in SFH systems [2]. Effective receiver designs employing R-S decoding can be implemented without any estimates of either the signal-to-noise ratio or the signal-to-interference ratio at the receiver. R-S codes are most beneficial if they are used with errors-and-erasures (EE) decoding and a method of identifying and erasing code-symbol decisions of low reliability [2–5]. The effectiveness of this technique is responsible in large part for the widespread use of SFH spread spectrum in military packet radio communications [6, 7] as well as its use in some commercial ad hoc radio networks.

Current SFH packet radio networks operate at low-to-moderate link data rates for which the most common channel impairments are partial-band interference across the system bandwidth and frequency-flat fading within each hop frequency. For future SFH systems, however, the link data rates will be higher. Thus the channel is likely to be frequency selective within each frequency slot, resulting in significant intersymbol interference (ISI) at the receiver. Consequently, the receiver designs for future SFH systems must incorporate equalization in each dwell interval while preserving the robustness of existing SFH systems with respect to partial-band impairments. Such designs can also be exploited as enhancements of existing (lower data rate) SFH systems to improve performance in those instances in which a channel with a large delay spread is encountered. It is thus desirable that the resulting detection complexity is not much greater than the complexity required for receiver designs in current use.

In earlier work [8], we consider a SFH packet radio system with R-S coding that is subjected to ISI in each frequency slot. Maximum-likelihood sequence estimation (MLSE) equalization [9] is employed at the receiver, which is retrained on a hop-by-hop basis. Unreliable code symbols are identified using the parity-bit method [4] and erased for EE decoding. The performance of this system is compared with a system which does not use the parity-bit method and instead employs errors-only decoding of R-S code words. It is shown that the use of parity bits significantly improves the performance of the SFH systems for a wide variety of ISI channels.

Our previous work concerns a receiver that employs a single pass of equalization followed by EE decoding of each of the multiple R-S code words in a packet (i.e, *one-shot equalization and decoding*). In this dissertation, we consider reception techniques that employ iterative equalization and decoding in a manner that results in only a modest increase the detection complexity compared with one-shot equalization and decoding. The iteration is applied to the entire content of a packet, rather than individual R-S code words within the packet. Hence it is referred to as *packet-level iterative equalization and decoding*.

In this dissertation, we consider a packet-level iterative equalization-and-decoding technique in which MLSE equalization and bounded-distance EE decoding is employed in each iteration. Each dwell interval for a packet transmission contains one parity-encoded code symbol from each R-S code word in the packet. In each packet-level iteration at the receiver, the receiver employs MLSE equalization to detect the binary channel symbols in each dwell interval followed by EE decoding of those code words in the packet that could not be successfully decoded in the previous iterations. The channel-symbol polarities for the code symbols corresponding to code words successfully decoded in the current and previous iterations are fed back to the equalizer for use in the next iteration. This feedback is used as *a priori* information that enables state pinning [10, 11] which constrains the paths through the equalizer trellis in the new iteration in a way that aids in successful decoding of additional code words in the packet.

The code symbols in a dwell interval are transmitted consecutively in their parity-encoded binary representations in one of the packet transmission formats we consider with iterative equalization and decoding [12]. Both the performance and the detection complexity of packet-level iterative equalization and decoding are investigated for a variety of ISI channels, and they are compared with the performance and detection complexity of one-shot equalization and decoding. A modification to the packet transmission format is also considered in which the binary contents of each dwell interval are interleaved before transmission [13]. Several interleaver designs are considered in conjunction with packet-level iterative MLSE equalization and EE decoding.

For a SFH system with R-S coding, it is shown in Chapter 6 that poor performance in partial-band interference results if the bits forming the representation of a given code symbol are interleaved across multiple dwell intervals. Thus the bit-interleaving techniques considered in this dissertation satisfy the constraint that all the bits in the representation of a given code symbol are transmitted in the same dwell interval. It is shown that bit interleaving with this constraint results in significant performance improvement for a wide variety of multipath channels with only a modest increase in detection complexity.

The effect of state pinning on the minimum free distance of the equalizer trellis is determined analytically. Previous methods employed in finding minimum distance properties for a trellis without any state pinning [14–16] are suitably modified, and it is shown that state pinning results in an increase in the minimum free distance of the trellis. For a channel response of length greater than two, state pinning is shown to overcome a substantial portion of the worst-case asymptotic performance loss in SNR that results with one-shot MLSE equalization.

In this dissertation, we also consider a SFH system design that is motivated by previous results in which the serial concatenation of an outer binary code and an inner differential encoder separated by a pseudo-random interleaver yields codes with distance spectra that are asymptotically good with increasing block size [17, 18]. The SCC codes considered in [17] are shown to provide an interleaving gain, and near-maximum-likelihood iterative decoding at the receiver results in excellent performance in an AWGN channel. In the SFH systems we consider, the need to provide adequate protection against partial-band impairments introduces an additional constraint on the interleaver design as a consequence of the non-binary code-symbol alphabet of the R-S code. We show that in spite of this, the use of differential encoding in SFH systems with R-S coding can be exploited at the receiver to achieve improved performance.

The SFH systems that we consider with differential encoding employ a packet transmission format in which the binary contents of each dwell interval are bit interleaved and differentially encoded prior to transmission [19]. Packet-level iterative detection and EE decoding is employed at the receiver for such a system. A generalization of state pinning (denoted "branch pruning") is introduced to account for the effect of differential encoding, and it is used by the receiver in each iteration to constrain the equalizer based on feedback from the EE decoder. It is shown that differential encoding results in improved performance in AWGN channels and channels with moderate ISI. The performance improvements are achieved with a modest increase in detection complexity. The effect of branch pruning on the minimum free distance of the equalizer trellis is determined analytically for AWGN and multipath channels, and it is shown that branch pruning resulting from feedback results in an asymptotic gain in performance.

The performance of SFH systems employing packet-level iterations are also evaluated for channels in which the received signal is subjected to partial-band interference [20]. SFH systems which employ per-dwell bit interleaving with and without differential encoding are considered and the performance of each of those systems is compared with the performance of one-shot equalization and decoding. The performance comparison and detection complexities are determined for instances in which the received signal is subjected to partial-band interference and for both an AWGN channel and an ISI channel. It is shown that the benefits of using differential encoding in conjunction with packet-level iterative detection and decoding in the SFH system are preserved if partial-band interference is introduced into the channel.

The use of the parity-bit method [4] is considered for both symbol-by-symbol erasures and threshold-based dwell erasures in conjunction with communications over the partial-band-interference channel. More efficient parity-bit techniques are also considered in which blocks of multiple R-S code symbols in a dwell interval are encoded with a single parity bit and corresponding block erasures occur at the receiver [4]. (This results in different tradeoffs than those that arise in the use of test symbols for dwell erasures [4, 21].)

The performance of the dwell-erasure technique along with packet-level iterative detection is also compared with the performance of other previously introduced coding and decoding techniques for SFH systems that include both one-shot decoding techniques and iterative decoding techniques. It is shown that the performance of the SFH systems which employ R-S coding and packet-level iterative detection and decoding are superior to the earlier systems using one-shot detection and they are competitive with the other systems using "turbo" coding and iterative decoding.

The remainder of this dissertation is organized as follows. Related prior work is summarized in Chapter 2. In Chapter 3, the channel model that is employed for the performance evaluation of the SFH system designs is described. Chapter 4 describes the packet-level iterative MLSE equalization and EE decoding technique and a variety of bit interleaving designs for the SFH systems. Performance evaluation and detection complexities of the system designs are determined for a wide variety of ISI channels. Analytical results for the distance properties of the equalizer trellis is shown. In Chapter 5, the packet-level iterative technique is considered in conjunction with a SFH system which employs bit interleaving and differential encoding in each dwell interval. Performance comparison for systems with and without differential encoding is made for AWGN and a variety of ISI channels. Analytical results for the minimum free distance of the detector trellis is shown for a system which employs differential encoding. Chapter 6 shows the performance results of SFH systems employing packet-level iterations with and without differential encoding in a partial-band interference channel. Finally, conclusions are presented and future work discussed in Chapter 7.

CHAPTER 2

RELATED PRIOR RESEARCH

Iterative equalization and decoding has been widely examined in contexts corresponding to narrowband communications [22, 23], but its consideration in the context of SFH communications appears to have been limited to its use with serially concatenated convolutional (SCC) codes [24] and (in our work) with R-S codes. Most previous work on iterative detection techniques for SFH communications has focused instead on the performance of iterative decoding with single-path static or frequency-flat fading channels (in some instances in the presence of partial-band interference). Among the systems addressed are those using parallel concatenated convolutional (PCC) codes [25–27], SCC codes [28, 29], turbo product codes [30, 31], and bit-interleaved coded modulation [32]. Iterative channel estimation and decoding using convolutional codes is considered in [33] for a SFH system.

The use of PCC codes and iterative decoding is considered in [25–27] for SFH communications using both coherent and noncoherent communications. In the work it is assumed that the receiver has *a priori* knowledge of both the noise and interference power spectral densities but no *a priori* knowledge of which frequency slots are subjected to interference. It is shown that the use of a PCC code results in performance in partial-band interference superior to that of either of two SFH systems using non-iterative detection: R-S codes and errors-only decoding [34], and concatenated R-S and convolutional codes with test symbols [35]. SCC codes with M-ary PSK and inner differential encoding are considered in [29] for SFH systems, and good performance is achieved in partial-band interference by using an adaptation of the ratio-threshold test [3]. A SCC code with inner CPFSK modulation is considered in [28] for SFH communications in the presence of jamming. Turbo product codes are considered in [30, 31] for SFH communications. They are shown to provide performance comparable to that of PCC codes, but with a relatively low detection complexity. Bit-interleaved coded modulation with iterative decoding is considered in [32], and it is shown to be useful in SFH communications with fast fading.

A form of packet-level iterative detection is considered in [36] for a SFH packet radio system using R-S coding in partial-band interference, where feedback from bounded-distance decoding of R-S code words is used to make per-dwell erasures of code symbols for the remaining undecoded code words in the packet. This use of feedback is similar to the "error forecasting" technique introduced in [10] for detection of a packet containing multiple R-S code words, though the techniques addressed in the two papers differ in some respects.

The use of state pinning with packet-level iterative detection is considered in [10] and [11] for a packet format employing a concatenation of multiple outer R-S code words per packet and inner convolutional encoding. The results of successful errors-only decoding of some of the R-S code words in the packet is used to constrain the trellis search for subsequent iterations of Viterbi decoding of the inner code. Performance is considered only for an AWGN channel in the two papers. The use of state pinning in this manner can be viewed as an improvement of an earlier technique in which decoding of each R-S code word is attempted only once and only the trellis decoding of the inner code is iterated [37, 38]. Additional work employing error forecasting or state pinning is cited in [39]. In the previous work that addresses either technique in conjunction with concatenated coding, only a nonrecursive inner convolutional code is considered and only modest performance gains are achieved.

Numerous other decoding techniques employ iterated decoding attempts for individual code words in a packet format that includes multiple R-S code words [40–42]. Each decoding attempt of a constituent R-S code word is itself an iterative algorithm [43–46] in most of these techniques, which may impose an excessive computational burden on many radio receivers for code rates of interest in packet radio communications.

CHAPTER 3

CHANNEL MODEL

Each transmitted radio-frequency signal considered in this dissertation has the form

$$s(t) = v(t)\cos(2\pi f_c t + \nu(t) + \phi)$$

where $v(t)$ is an amplitude-modulation function and $\nu(t)$ is a phase-modulation function. (This form is sufficiently general to include frequency modulation and frequency hopping.) Thus the transmitted signal can be expressed as

$$s(t) = v_1(t)\cos(2\pi f_c t) - v_2(t)\sin(2\pi f_c t)$$

where $v_1(t) = v(t)\cos[\nu(t) + \phi]$ and $v_2(t) = v(t)\sin[\nu(t) + \phi]$.

The channel is a doubly selective, Gaussian, wide-sense-stationary, uncorrelated-scattering channel [47] with a discrete delay spectrum [48]. The transmitted signal is also distorted by additive thermal noise and interference at the receiver. Thus the received signal is given by

$$\begin{aligned} r(t) \;=\; & \sum_{i=0}^{M-1} \Big\{ \Big[v_1(t-\tau_i) g_i^{(I)}(t) - v_2(t-\tau_i) g_i^{(Q)}(t) \Big] \cos[2\pi f_c (t-\tau_i)] \\ & - \Big[v_2(t-\tau_i) g_i^{(I)}(t) + v_1(t-\tau_i) g_i^{(Q)}(t) \Big] \sin[2\pi f_c (t-\tau_i)] \Big\} \\ & + n(t) + i(t) \end{aligned}$$

where M is number of multipath components in the received signal, $n(t)$ is a white Gaussian noise process with doubled-sided power spectral density $N_0/2$, and $i(t)$ is an interference process. (The interference process is identically zero in all the results except those of Chapter 6. It is defined in that chapter.)

The time-varying multipath attenuation functions of the channel are given by

$$g_i^{(I)}(t) = h_i^{(I)}(t) + \rho_i^{(I)}(t) \quad \text{and} \quad g_i^{(Q)}(t) = h_i^{(Q)}(t) + \rho_i^{(Q)}(t)$$

for $i = 0, \cdots, M-1$,where $\{h_0^{(I)}(t), h_0^{(Q)}(t), \cdots, h_{M-1}^{(I)}(t), h_{M-1}^{(Q)}(t)\}$ are mutually independent, zero-mean, Gaussian random processes and $\{\rho_0^{(I)}(t), \rho_0^{(Q)}(t), \cdots, \rho_{M-1}^{(I)}(t), \rho_{M-1}^{(Q)}(t)\}$ are deterministic functions of time. The pair of random processes for the ith multipath component are characterized by their autocorrelation functions

$$E\left[h_i^{(I)}(t)h_i^{(I)}(x)\right] = E\left[h_i^{(Q)}(t)h_i^{(Q)}(x)\right] = \sigma_i^2 d(t-x)$$

where σ_i^2 is the power in either random process and $d(t)$ is the time-correlation function for all of the multipath components.

The transmitted and received signals and the channel's impulse response can also be represented in a baseband-equivalent form with respect to f_c [49]. The baseband-equivalent transmitted signal is given by

$$\tilde{s}(t) = \frac{1}{\sqrt{2}}\left\{v_1(t) + jv_2(t)\right\},$$

and the baseband-equivalent, time-varying impulse response of the channel is given by

$$\tilde{g}(t,\tau) = \sum_{i=0}^{M-1} \tilde{g}_i(t)\exp[-j2\pi f_c \tau_i]\delta(t-\tau_i) \tag{3.1}$$

where

$$\tilde{g}_i(t) = \left\{g_i^{(I)}(t) + jg_i^{(Q)}(t)\right\}.$$

The baseband-equivalent received signal is given by

$$\tilde{r}(t) = \int_{-\infty}^{\infty} \tilde{g}(t,\tau)\tilde{s}(\tau)d\tau + \tilde{n}(t) + \tilde{i}(t)$$

where $\tilde{n}(t)$ is a proper, complex-valued white Gaussian random process [50] with double-sided power spectral density N_0 and $\tilde{i}(t)$ is the baseband equivalent of the interference random process. Then

$$s(t) = \sqrt{2}\,\mathcal{R}e\{\tilde{s}(t)\exp[-j2\pi f_c t]\}$$

and

$$r(t) = \sqrt{2}\,\mathcal{R}e\{\tilde{r}(t)\exp[-j2\pi f_c t]\}.$$

The baseband-equivalent attenuation function of the ith multipath component in the received signal can be expressed as

$$\tilde{g}_i(t) = \tilde{h}_i(t) + \tilde{\rho}_i(t)$$

where $\tilde{h}_i(t) = h_i^{(I)}(t) + jh_i^{(I)}(t)$ and $\tilde{\rho}_i(t) = \rho_i^{(I)}(t) + j\rho_i^{(Q)}(t)$ are the baseband-equivalent attenuation functions of the diffuse part and the specular part of the multipath component, respectively.

In each example considered in this dissertation, the specular part of the attenuation function is a constant for each multipath component in the received signal. Thus the notation $\tilde{\rho}_i(t)$ is simplified to ρ_i. Moreover, the value of ρ_i is real in each example. The power attenuation of the specular part of the ith multipath component is thus ρ_i^2. The average power attenuation of the diffuse part is $2\sigma_i^2$, and the average power attenuation of the complete multipath component is $\rho_i^2 + 2\sigma_i^2$.

The magnitude attenuation of the diffuse part of the ith multipath component in the received signal follows a Rayleigh distribution at any time, and thus the magnitude attenuation of the complete multipath component follows a Rician distribution. A multipath component with zero diffuse signal power is referred to as a *static multipath component*, and a multipath component with zero specular signal power is referred to as a *Rayleigh-fading multipath component*. If all the multipath components are static, the channel is referred to as a *static channel*. Conversely, if all the multipath components exhibit Rayleigh fading, the channel is referred to as a *Rayleigh-fading channel*. Each example that is considered in this dissertation concerns either a static channel or a Rayleigh-fading channel.

The time-correlation function determines the rate of variation in the attenuation of the diffuse part of each multipath component. A two-sided exponential time-correlation function [51] is considered in all the examples of Rayleigh-fading channels in this dissertation. It is given by

$$d(t) = \exp(-2\pi B_d t),$$

where B_d is the half-power bandwidth of the Fourier transform of $d(t)$. If the information rate of the SFH system is denoted by R_b bits/s, the (normalized) *Doppler spread* of the channel is given by $D_T = B_d/R_b$. For a given information rate, the Doppler spread is proportional to the system's carrier frequency and the velocity between the transmitter and the receiver.

The SFH systems that are the focus of this dissertation use distinct carrier frequencies for the different frequency slots of the system. Thus at any time t, the baseband-equivalent impulse response of the channel with respect to the center frequency of a given frequency slot depends on the slot. This is apparent from the expression in equation (3.1), which depends on f_c. In each example in this dissertation, however, the center frequencies of any two frequency slots differ by an integer multiple of the inverse of the channel-symbol duration for the system. Moreover in most of the examples, each path delay τ_i is an integer multiple of the channel-symbol duration. For each such examples, the baseband-equivalent impulse response of the channel at any time t is the same with respect the center frequencies of all frequency slots.

CHAPTER 4

INTERLEAVING TECHNIQUES FOR SFH SYSTEMS WITH PACKET-LEVEL ITERATIVE DETECTION

4.1 Description of SFH Systems

For each SFH system considered in this chapter, the information content is encoded at the transmitter by an (n, k) singly extended R-S encoder [52]. Each packet consists of N_s code words and each code word contains n code symbols belonging to an $n = 2^m$-ary code alphabet. Each n-ary code symbol is represented by a distinct $(m + 1)$-bit binary sequence of even parity. (This parity-encoded representation is used to generate code-symbol erasures at the receiver [4].) The code words are written into an n-by-$(m+1) \times N_s$ block code-symbol interleaver such that each interleaver row contains the parity-encoded binary representation of one code symbol from each of the code words.

Some of the systems considered here include a second level of interleaving, which is referred to as *bit interleaving.* For each of these systems, with one exception, the binary contents of each row of the interleaving block are reordered prior to transmission. In the one exceptional system, the binary contents of each row are redistributed across the entire interleaving block. In all of the SFH systems, a packet is transmitted in n dwell intervals with the contents of each row of the resulting interleaving block transmitted in a different dwell interval. Each dwell interval consists of a preamble sequence of N_t bits followed by the $(m + 1)$ N_s bits from the corresponding row of the block interleaver and a guard interval of N_e bits in which no signal is transmitted. Thus in each system save the exception noted above, the contents of a dwell interval correspond to one code symbol from each of the N_s R-S code words. The binary contents of each dwell interval (including the preamble sequence) are transmitted using BPSK modulation. The generic transmitter for the SFH systems considered in this chapter is shown in Figure 4.1.

Each dwell interval is transmitted in a frequency slot that is determined by a frequency-hopping pattern given by $\{f_0 = f_c + k_0\Delta f, ..., f_{n-1} = f_c + k_{n-1}\Delta f\}$ where f_c is the center frequency of the lowest-frequency slot, Δf is the offset between the center frequencies of adjacent frequency slots and $k_i \in \{0, ..., S-1\}$. If the duration of each binary channel symbol transmitted using BPSK modulation is T, then $\Delta f = 2/T$. Thus if the total system bandwidth is B_t, the number of frequency slots available is $S = B_t T/2$. For a packet transmitted at time $t = 0$, the transmission is thus given by

$$s(t) = \sqrt{2P}\sum_{i=0}^{n-1}\sum_{j=0}^{N_t+(m+1)N_s-1}(-1)^{b_{i(N_t+(m+1)\ N_s)+j}}$$
$$\times p_T(t-(i(N_t+(m+1)\ N_s+N_e)+j)T)\cos(j2\pi f_i t+\phi_i) \tag{4.1}$$

where p_T is the unit-amplitude pulse over $[0,T]$, P is the transmitted power, b_l is the lth binary channel symbol, and ϕ_i is the carrier phase offset in the ith dwell interval.

The transmission occurs over the multipath, fading channel described in Chapter 3. The *average signal-to-noise ratio* at the receiver is thus given by

$$\frac{\overline{\mathcal{E}_b}}{N_0} = \frac{PT}{N_0}\frac{n(N_t+(m+1)\ N_s)}{mkN_s}\sum_{l=0}^{M-1}(\rho_l^2+2\sigma_l^2). \tag{4.2}$$

In the results presented in this chapter, no interference process appears at the receiver.

There are two stages of data reception in each dwell interval. In the first stage, the dwell interval's preamble is used as a training sequence to obtain a discrete-time equivalent impulse response of the channel. The receiver includes in-phase and quadrature filters matched to the waveform for the transmitted preamble, and the over-sampled filter outputs are used to determine the maximum-energy, symbol-rate discrete-time estimate of the channel's baseband-equivalent impulse response at the center frequency for the dwell interval [8]. The number of taps in the resulting channel model is a pre-determined parameter of the receiver. (A value of four taps is used for all the examples in this dissertation, except where otherwise noted in Chapter 6.)

The estimated impulse response provides the equalizer's complex-valued channel coefficients for the dwell interval. The channel coefficients for each dwell interval are obtained once for each packet, and they are used in the equalizer for that dwell interval throughout the attempt to detect the packet. Since the channel coefficients include phase information, the data detection is coherent.

In the second stage of reception, the received signal is passed through in-phase and quadrature branches of the receiver. In each branch the signal is demodulated and passed through a baseband filter which is matched to the rectangular data pulse. The filter outputs are sampled once per channel-symbol interval and the sequence of complex-valued samples is generated for each of the binary channel symbols corresponding to the data contents of the dwell interval. The equalizer training and data-sample generation are employed in each of the SFH systems described below. The generic receiver for the systems considered in this chapter is shown in Figure 4.2.

Seven packet formats and a total of nine combinations of packet format and receiver are considered in this chapter. The nine combinations are designated as systems A through I, and their respective characteristics are shown in Table 4.1. In systems A through G, a rectangular block code-symbol interleaver is employed. That is, each R-S code word in the packet is written in its parity-encoded binary representation as $(m+1)$ consecutive columns of the block interleaver (prior to any bit interleaving that may be used). Systems H and I use diagonal block code-symbol interleaving instead. The contents of the first row are the same as in rectangular block interleaving so that the

System	Code-Symbol Interleaver	Bit Interleaver	Packet-Level Iteration
A	rectangular	none	no
B	rectangular	none	yes
C	rectangular	regular, per dwell	yes
D	rectangular	pseudo-random, per dwell	yes
E	rectangular	odd-even, per dwell	yes
F	rectangular	distance-swap, per dwell	yes
G	rectangular	s-random, packet-wide	yes
H	diagonal	none	no
I	diagonal	none	yes

Table 4.1 Characteristics of SFH systems considered in Chapter 4.

order of the code symbols in the dwell interval is $1, 2, ..., N_s$ after block interleaving. For the second row, a circular right shift by $(m + 1)$ bits (i.e,, the parity-encoded representation of one code symbol) is applied to the interleaving pattern of the first row. Thus the order of the code symbols in the second row is $N_s, 1, 2, ..., N_s - 1$ after block interleaving. For each subsequent row of the diagonal block interleaver, the interleaving pattern is obtained by an $(m + 1)$-bit circular right shift of the interleaving pattern in the previous row. The interleaving pattern thus repeats in every N_s rows.

The first SFH system considered (referred to as *system A*) does not use bit interleaving so that the code symbols in each row of the block interleaver are transmitted consecutively in the corresponding dwell interval using their binary parity-encoded representations. The receiver in system A employs maximum-likelihood sequence estimation (MLSE) for equalization of the data samples in each dwell interval [9], and the outputs of the equalizer are the hard decisions for the corresponding binary channel symbols in the dwell interval. The equalizer structure for each dwell interval can be represented by a trellis diagram with the branch labels for the paths in the trellis determined by the complex coefficients of the estimated channel impulse response for the dwell interval. The Viterbi algorithm is employed using the trellis with the squared-Euclidean-distance metric to implement MLSE equalization in the dwell interval [53]. An example of such a trellis structure is shown in Figure 4.3 in which the training stage for a given dwell interval has resulted in a two-path model as the estimate of the baseband-equivalent channel. The initial time step of the trellis is constrained to a unique state determined by the preamble sequence.

The detected channel symbols from each dwell interval are used to form the detected $(m+1)$-bit parity-encoded representation for each code symbol, and the detected representation is tested for even parity. If parity check fails, the corresponding code symbol is replaced by an erasure symbol for use in decoding. The contents of the packet are deinterleaved by writing the detected n-ary code symbols and the erasure symbols from each dwell interval into a row of an n-by-N_s rectangular block deinterleaver. Each column of the deinterleaving block thus represents the detected code symbols and erasure symbols for one (n, k) R-S code word. The contents of each column are passed to a bounded-distance EE decoder for the R-S code. One-shot equalization and decoding is employed. (That is, there is only one MLSE equalization performed for each dwell interval and only one EE decoding attempt for each R-S code word.) Thus system A is represented by Figures 4.1 and 4.2 with all the dashed elements excluded.

The second SFH system that is considered uses the same packet transmission format as system A. The receiver employs packet-level iterations of MLSE equalization with state pinning and EE decoding, however [12]. We refer to this system as *system B*. In the first packet-level iteration the equalizer uses the entire equalizer trellis in each dwell interval, and code symbols that fail parity check are replaced by erasure symbols. The detected code symbols and erasure symbols are deinterleaved using an n-by-N_s block deinterleaver, and bounded-distance EE decoding is employed for each R-S code word. Thus the first packet-level iteration in the receiver of system B is equivalent to the reception employed in system A.

The first packet-level iteration can result in failure of bounded-distance decoding for one or more code words in the packet, however. If any such failures occur, further iterations of equalization and decoding are employed in system B. In each subsequent iteration, the equalizer for each dwell interval is provided with feedback in the form of the channel-symbol polarities for the code symbols corresponding to code words that were correctly decoded in the earlier packet-level iterations. (Thus the receiver in system B is illustrated by Figure 4.2 with the dashed feedback loop included but both the bit interleaver block and the bit deinterleaver block excluded.)

As in the first iteration, the equalizer for a given dwell interval in subsequent packet-level iterations uses the Viterbi algorithm employing the samples from the channel for that dwell interval. It differs from the first iteration, however, in that the Viterbi algorithm is constrained to only those paths through the equalizer trellis that are consistent with the feedback information. The constraint can be expressed as a restriction to a subset of the trellis states at the end of those time steps for which the channel-symbol polarity has been fed back: hence the use of the term "state pinning" to describe the technique [11]. State pinning is illustrated in Figure 4.4 for the equalizer trellis for a two-path channel in which the feedback information ($b_1 = 1, b_2 = 0, b_4 = 1, b_5 = 0$) is provided from successful decoding of R-S code words in previous packet-level iterations. The equalizer's hard decisions for the remaining unknown bits are employed as before for EE decoding of the R-S code words that were not successfully decoded in the earlier iterations. Packet-level iterations of equalization and decoding continue until all the code words in the packet are successfully decoded or no additional code words are successfully decoded in an iteration.

A modification of system B is also considered in which bit interleaving is applied to the contents of each dwell interval prior to transmission. Bit interleaving is accomplished by reordering the $(m+1)N_s$ bits that represent the contents of each row of the transmitter's rectangular block interleaver. At the receiver, the same technique of packet-level iterative equalization and decoding is employed as in system B except that the hard-decision outputs from the equalizer for each dwell interval are bit deinterleaved before detected code symbols and erasures are determined for the corresponding row of the receiver's rectangular block deinterleaver. Conversely, the feedback decisions from the decoder are bit interleaved for each dwell interval for use by the equalizer in the next packet-level iteration. Bit interleaving has the effect of spreading the feedback from each packet-level iteration more uniformly across each dwell interval for the equalization in subsequent iterations. In system B, which lacks bit interleaving, each correct code-word decision results in state pinning for $(m+1)$ consecutive time intervals in the equalizer trellis in the subsequent iteration. In the modified system with bit interleaving, in contrast, the pinned states are scattered throughout each dwell's equalizer trellis.

Systems using four different bit-interleaver designs of this type are considered here. The first system uses *regular bit interleaving*, and it is referred to as *system C*. In system C, the bit interleaver shown in Figure 4.5 is applied to each row of the rectangular interleaving block. This results in $m+1$ groups of N_s consecutive bits in each row of the interleaving block, with each group containing one bit from the parity-encoded binary representation of each of the N_s code symbols in the dwell interval. (The regular bit interleaver is illustrated for $m = 5$, i.e., for a 32-ary R-S code.) The same bit-interleaving pattern is used for all dwell intervals in the packet. Another system, referred to as *system D*, uses *pseudo-random bit interleaving*. In system D, the regular bit interleaver is applied first to the contents of each dwell interval . A pseudo-random reordering is then applied to the N_s bits within each of the $m + 1$ groups. The same reordering is applied to all $m + 1$ groups in a given dwell interval, but different randomization patterns are applied to different dwell intervals.

More structured per-dwell bit-interleaver designs are used in two other SFH systems in place of per-dwell pseudo-random reordering within each group. *System E* uses *odd-even bit interleaving*. The regular bit interleaver is applied to the first dwell interval of the packet, and the ordering within each dwell interval is not altered further. The interleaving pattern for the second dwell interval is obtained starting with the pattern for the first dwell interval. Bits are then swapped for positions one and two, positions three and four, and so forth. (The description assumes that N_s is even, though the modification for odd N_s is straightforward.) The same reordering is applied for all the $(m + 1)$ groups in the dwell interval. The interleaving pattern for the third dwell interval is obtained starting with the pattern for the second dwell interval. Within each group, the bits are then swapped for positions two and three, four and five, and so forth, and the bits are swapped for positions one and N_s. Again, the same reordering is applied for all the $(m + 1)$ groups in the dwell interval. The interleaving pattern for each subsequent dwell interval is based on a comparable modification of the pattern for the previous dwell interval, using the swapping pattern of the second dwell interval for even-numbered dwell intervals and the swapping pattern of the third dwell interval for all odd-numbered dwell intervals. If $N_s = 12$, for example, the interleaving pattern repeats every twelve dwell intervals.

A method referred to as *distance-swap bit interleaving* is used in *system F*. It is applicable if N_S is even, and it is determined by the positive integer factors of $N_s/2$, which are denoted in increasing order as $\{i_1, \cdots, i_p\}$. The regular bit interleaver is applied to the first dwell interval of the packet. The interleaving pattern for the second dwell interval is obtained starting with the pattern for the first dwell interval. Bits are then swapped for positions one and $i_1 + 1$, positions two and $i_1 + 2$, and so forth until every bit position in the first group has been part of exactly one swap. The same reordering is applied to the other groups in the dwell interval. The interleaving pattern for the third dwell interval is obtained starting with the pattern for the second dwell interval using the same approach but with swaps at a distance of i_2. Increased swapping distances are employed for subsequent dwell intervals, up to a distance of i_p. After that the swapping distances for subsequent dwell intervals cycles through $\{i_1, \cdots, i_p\}$. For example, suppose $N_s = 12$ and there are thirty-two dwell intervals. Then the set of swapping distances is $\{1, 2, 3, 6\}$, each distance is used with the swapping technique for either six or seven dwell intervals, and the interleaving pattern repeats every twenty dwell intervals.

A bit-interleaver design is also considered in which the bit interleaving is not restricted to the contents of individual dwell intervals. Instead, an s-random interleaver [54] with $s = 12$ is applied to all the encoded binary symbols in the interleaving block for the packet. Each dwell interval may thus contain binary symbols from more than one code symbol of a given code word, in contrast with the packet format of each of the other SFH systems considered here. The SFH system with s-random bit interleaving is referred to as *system G*, and it also uses packet-level iterative equalization and decoding at the receiver.

Two SFH systems are considered that use diagonal block code-symbol interleaving instead of rectangular block code-symbol interleaving. *System H* employs diagonal block code-symbol interleaving with no bit interleaving, and it uses one-shot equalization and decoding at the receiver. *System I* also employs diagonal block code-symbol interleaving with no bit interleaving, but it uses packet-level iterative equalization and decoding at the receiver. Systems H and I thus differ from systems A and B, respectively, only in the form of block code-symbol interleaving they use.

4.2 Effect of State Pinning on Minimum Distance of Equalizer Trellis

Optimal sequence detection (MLSE equalization) for a binary antipodal sequence received over a static intersymbol-interference channel with additive white Gaussian noise can be implemented efficiently by applying the Viterbi algorithm to a trellis that represents all possible sequences of ISI-distorted binary symbols [9]. One-shot MLSE equalization suffers from an asymptotic performance loss relative to communication over a single-path AWGN channel, where the loss is characterized by the limiting increase in the signal-to-noise ratio required to achieve a given probability of bit error or probability of first event error. Specifically, an asymptotic performance loss occurs with MLSE equalization if the ISI channel consists of three or more paths, and the loss depends on the impulse response of the channel [9]. For example, a three-path channel can result in an asymptotic performance loss as great as 2.34 dB, and a four-path channel can result in an asymptotic loss as great as 4.2 dB [14,15].

The asymptotic performance loss of one-shot MLSE equalization for a given channel's impulse response is determined by the minimum Euclidean distance between paths that determine an error event in the equalizer's trellis. Packet-level iteration results in state pinning in each dwell interval's equalizer trellis in the second and subsequent iterations, which eliminates some error events that can occur in the original trellis. This often results in an increase in the minimum Euclidean distance for remaining error events in the state-pinned trellis and hence the asymptotic probability of error for the equalizer is reduced for a given joint distribution of the channel-symbol statistics.

The change in packet-detection performance that results with packet-level iterative equalization and decoding is only partly due to the effect of state pinning on the set of Euclidean distances for each dwell interval's equalizer trellis, however. State pinning also determines the number of bit errors and the locations of the bit errors in possible error events at a given Euclidean distance, and the subsequent results of R-S code-word decoding depend on both characteristics of the error events that occur in each dwell interval's equalizer. Furthermore, decoding successes and failures from earlier iterations alter the *a posteriori* joint distribution function of the statistics for the channel symbols that are unknown at the start of the current equalizer iteration. Thus even the pairwise error probability for a given error event differs for each equalizer iteration in which the error event can be realized. Among these factors, the effect of state pinning on the minimum Euclidean distance in the equalizer trellis is the most amenable to analysis, and it provides the most straightforward insights into the benefits of packet-level iterative equalization and decoding. Thus it is the focus of this section.

The subsequent development concerns a static channel consisting of L paths, where the ith path has delay iT and (complex) baseband-equivalent attenuation h_i for $0 \leq i \leq L-1$. Without loss of generality, it is assumed that

$$\sum_{i=0}^{L-1} |h_i|^2 = 1.$$

The equalizer for one dwell interval is considered, and it is assumed that the training stage results in a perfect model of the channel's impulse response. The minimum squared Euclidean distance among error events in the *unpinned* equalizer trellis for a given channel response can be determined by an application of transfer-function techniques. The quantity of interest here is the *smallest* possible minimum squared Euclidean distance among all L-path channels, however, and the corresponding channel is referred to as the *worst-case channel* of L paths.

The squared Euclidean distance and the impulse response of the worst-case L-path channel is determined by considering the ternary error sequence defining each error event and finding the minimum eigenvalue and the corresponding eigenvector of an associated positive-definite, symmetric, Toeplitz matrix [14,15]. The number of distinct error sequences can be quite large for dwell-interval lengths of practical interest, but a breadth-first tree search with appropriate pruning rules can be used to substantially reduce the number of error sequences that must be considered [16]. The minimum squared Euclidean distance is equal to four for each channel for which $L = 1$ or $L = 2$. The worst-case minimum squared Euclidean distance is less than four if $L \geq 3$, however, resulting in a corresponding asymptotic loss in the performance of MLSE equalization [14]. Moreover, the worst-case minimum squared Euclidean distance is a decreasing function of L. (Note that the values cited in [14] for worst-case distances are incorrect and too large for $L = 7$ through $L = 10$. The correct worst-case distance for $L = 7$ is given in [16], and tighter upper bounds for $L = 8$ through $L = 10$ are given at the end of this section.)

Now suppose that state pinning results in an equalizer trellis in which the polarity of the kth channel symbol is unknown but the polarities of the L_1 immediately preceding channel symbols and L_2 immediately succeeding channel symbols are known *a priori*. For a given channel impulse response and given values of L_1 and L_2, the minimum squared Euclidean distance among error events that result in erroneous detection of the channel symbol depends in general on the position of the channel symbol within the dwell interval (and thus within the trellis of the dwell interval's equalizer). However, it is no less than the minimum squared Euclidean distance for a channel symbol in a trellis of infinite length. We assume an infinite-length trellis in the rest of this section and thus ignore beneficial "end effects" for symbols near the beginning or end of a dwell interval. Thus the worst-case minimum squared Euclidean distance among error events that result in erroneous detection of the kth channel symbol does not depend on k. It is denoted by $d^2_{\min}(L_1, L_2)$, and it is referred to as the *worst-case effective minimum squared Euclidean distance* with respect to a channel symbol with L_1 preceding known symbols and L_2 succeeding known symbols. Clearly, it is a non-decreasing function of both L_1 and L_2, and it is at least as great as the worst-case distance without state pinning (i.e., $d^2_{\min}(0, 0)$).

Several general results concerning $d^2_{\min}(L_1, L_2)$ can be proven. Let $\underline{b}$ and $\underline{\tilde{b}}$ denote the vectors of transmitted channel symbols that determine two paths through the equalizer trellis such that the two paths form an error event in the trellis. Specifically, let $\underline{b}$ and $\underline{\tilde{b}}$ correspond to different decisions regarding the kth channel symbol (i.e., $\tilde{b}_k = -b_k$). Let $\underline{x}$ and $\underline{\tilde{x}}$ denote the corresponding vectors of expected received symbols, with respective elements

$$x_k = \sum_{i=0}^{L-1} h_i \, (-1)^{b_{k-i}} \quad \text{and} \quad \tilde{x}_k = \sum_{i=0}^{L-1} h_i \, (-1)^{\tilde{b}_{k-i}} \quad \text{f}\mathit{or\ each}\ k.$$

If the error event begins at time q (i.e., it begins with the qth channel symbol) and spans p time steps, the squared Euclidean distance for the error event is

$$d^2(\underline{x}, \underline{\tilde{x}}) = \sum_{i=q}^{q+p-1} |x_k - \tilde{x}_k|^2.$$

If the L_1 channel symbols preceding the kth channel symbol are known *a priori*, their polarities are denoted by $(\hat{b}_{k-L_1}, \cdots, \hat{b}_{k-1})$. If the L_2 channel symbols preceding the k channel symbol are known *a priori*, their polarities are denoted by $(\hat{b}_{k+1}, \cdots, \hat{b}_{k+L_2})$.

If at least $L-1$ consecutive states are pinned on each side of the unknown channel symbol, then it is easily shown that the worst-case effective minimum squared Euclidean distance with respect to the channel symbol is equal to four.

Thus there is no asymptotic loss in MLSE equalization relative to detection in a single-path channel for that channel symbol.

Theorem 1 *If $L_1 \geq L-1$, the state-pinned trellis contains only one state at time k.*

Proof: The state at time k is determined by the $L-1$ most recent channel symbols. Thus exactly one state at time k satisfies the constraints.

$\square$

Theorem 2 *If $L_1 \geq L-1$ and $L_2 \geq L-1$, there is only one error event that can result in erroneous detection of the unknown channel symbol, and the squared Euclidean distance is equal to four. Thus $d^2_{\min}(L_1, L_2) = 4$.*

Proof: From Theorem 1, an error event affecting the kth channel symbol must begin at time step k. Clearly, the two paths that determine the error event must differ in the kth channel symbol.

Since $L_2 \geq L-1$, the error event must terminate at time step $k+L$ with $\underline{b} = (b_k, \hat{b}_{k+1}, \cdots, \hat{b}_{k+L-1})$ and $\underline{\tilde{b}} = (-b_k, \hat{b}_{k+1}, \cdots, \hat{b}_{k+L-1})$.

The error event is thus determined uniquely, and consequently

$$d^2_{\min}(L_1, L_2) = d^2(\underline{x}, \underline{\tilde{x}}) = \sum_{i=0}^{L-1} |h_i - (-h_i)|^2 = 4.$$

$\square$

If instead $L_1 = L-2$ and $L_2 \geq L-2$, or vice-versa, the number of error events that result in erroneous detection of the unknown channel symbol is greater than one. The squared Euclidean distance for each of the error events is greater than or equal to four, however. Thus for an arbitrary L-path channel, knowledge of the polarities of the $L-2$ channel symbols preceding and succeeding each unknown channel symbol in the equalizer trellis is sufficient to recover the loss in minimum distance resulting from intersymbol interference.

Theorem 3 *If $L_1 \geq L-2$ and $L_2 \geq L-2$, erroneous detection of the unknown channel symbol must result from an error event for which the squared Euclidean distance is at least four. For at least one such error event, the squared Euclidean distance is equal to four. Thus* $d^2_{\min}(L_1, L_2) = 4$.

<u>Proof</u>: Using the notation defined above,

$$|x_q - \tilde{x}_q|^2 = |2\ h_0|^2 = 4|h_0|^2,$$

$$|x_{k+j} - \tilde{x}_{k+j}|^2 = |2\ h_j|^2 = 4|h_j|^2 \ \text{ for } 1 \leq j \leq L-2,$$

and

$$|x_{q+p-1} - \tilde{x}_{q+p-1}|^2 = |2\ h_{L-1}|^2 = 4|h_{L-1}|^2.$$

Since $p \geq (k-q) + L$,

$$d^2(\underline{x}, \underline{\tilde{x}}) \geq \sum_{i=0}^{L-1} 4|h_i|^2 = 4.$$

Moreover, for the error event considered in Theorem 2, $d^2(\underline{x}, \underline{\tilde{x}}) = 4$. Thus $d^2_{\min}(L_1, L_2) = 4$.

$\square$

If $L_1 < L-2$ or $L_2 < L-2$, no general result concerning the worst-case effective minimum distance can be readily obtained for an arbitrary L-path channel. Instead we adopt the technique of [14], restricting attention to error sequences that satisfy the constraints imposed by the known channel-symbol polarities. The technique could be employed in the context of the tree-search approach of [16]. The constraints of state pinning invalidate some of the pruning rules of [16], however, and the exclusion of those rules can result in much larger stopping times for the search. Instead, we employ the heuristic of considering only error sequences of length no greater than $5L$. This approach does not guarantee the discovery of the true worst-case distance for given values of L_1 and L_2. In practice, however, the worst-case error sequences found in each search are much shorter than $5L$, which provides some confidence that they are in fact true worst-case sequences. The following theorems ensure that this approach need only be applied for $\frac{(L-2)(L-1)}{2} - 1$ combinations of L_1 and L_2 (excluding $L_1 = L_2 = 0$) in order to determine the worst-case effective minimum distance for all values of L_1 and L_2.

Theorem 4 *For a given L_2, the value of $d^2_{\min}(L_1, L_2)$ is the same for all $L_1 \geq L - 2$.*

Proof: Suppose first that $L_1 = L - 2$, and consider an error event that begins at time $q < k$. Of necessity, $q < k - (L-2)$ so that

$$\underline{b} = (b_q, b_{q+1}, \cdots, b_{k-(L-1)}\hat{b}_{k-(L-2)}, \cdots, \hat{b}_{k-1}, b_k, b_{k+1}, \cdots, b_{q+p})$$

and

$$\underline{\tilde{b}} = (-b_q, \tilde{b}_{q+1}, \cdots, \tilde{b}_{k-(L-1)}\hat{b}_{k-(L-2)}, \cdots, \hat{b}_{k-1}, -b_k, \tilde{b}_{k+1}, \cdots, \tilde{b}_{q+p}).$$

Then

$$\underline{b}^{'} = (b_k, b_{k+1}, \cdots, b_{q+p})$$

and

$$\underline{\tilde{b}}^{'} = (-b_k, \tilde{b}_{k+1}, \cdots, \tilde{b}_{q+p})$$

correspond to different decisions regarding the polarity of the kth channel symbol and form another error event that satisfies the state-pinning constraints. Furthermore,

$$d^2(\underline{x}^{'}, \underline{\tilde{x}}^{'}) \leq d^2(\underline{x}, \underline{\tilde{x}}).$$

Thus $d^2_{\min}(L_1, L_2)$ is determined by an error event of the form of $\underline{b}^{'}$ and $\underline{\tilde{b}}^{'}$. Moreover, each such error event also satisfies the state-pinning constraints for any $L_1 > L - 2$. Thus $d^2_{\min}(L_1, L_2)$ is the same for all $L_1 \geq L - 2$.

$\square$

Theorem 5 *For each pair of non-negative integers m and n, $d^2_{\min}(m,n) = d^2_{\min}(n,m)$.*

Proof: The proof follows the "reversed error sequence" result of [16, Section III.C] with the additional consideration of state-pinning constraints. Suppose $L_1 = n$ and $L_2 = m$. Furthermore, suppose that

$$\underline{b} = (b_q, \cdots, b_{k-1}, b_k, b_{k+1}, \cdots, b_{q+p})$$

and

$$\underline{\tilde{b}} = (\tilde{b}_q, \cdots, \tilde{b}_{k-1}, -b_k, \tilde{b}_{k+1}, \cdots, \tilde{b}_{q+p})$$

form an error event that satisfies the state-pinning constraints.

Consider the error event formed by

$$\underline{b}^{'} = (b^{'}_{2k-q-p}, \cdots, b^{'}_{k-1}, b^{'}_k, b^{'}_{k+1}, \cdots, b^{'}_{2k-q}) = (b_{q+p}, \cdots, b_{k+1}, b_k, b_{k-1}, \cdots, b_q)$$

and

$$\underline{\tilde{b}}^{'} = (\tilde{b}^{'}_{2k-q-p}, \cdots, \tilde{b}^{'}_{k-1}, \tilde{b}^{'}_k, \tilde{b}^{'}_{k+1}, \cdots, \tilde{b}^{'}_{2k-q}) = (\tilde{b}_{q+p}, \cdots, \tilde{b}_{k+1}, -b_k, \tilde{b}_{k-1}, \cdots, \tilde{b}_q).$$

The latter error event satisfies some state-pinning constraints with $L_1 = n$ and $L_2 = m$, and the two paths result in different decisions for the kth channel symbol. Moreover, the value of $d^2(\underline{x}, \underline{\tilde{x}})$ that results if the channel's impulse response is $\{h_0, \cdots, h_{L-1}\}$ is equal to the value of $d^2(\underline{x}^{'}, \underline{\tilde{x}}^{'})$ that results if the channel's impulse response is $\{h_{L-1}, \cdots, h_0\}$. The relationship is reciprocal. Thus

$$d^2_{\min}(m,n) = d^2_{\min}(n,m).$$

$\square$

Theorem 6 *For any l, $d^2_{\min}(0,l) = d^2_{\min}(l,0) = d^2_{\min}(0,0)$.*

Proof: With $L_2 = 0$, there is always a minimum-distance error event that begins with the kth channel symbol. Thus $d^2_{\min}(l, 0) = d^2_{\min}(0, 0)$ for any l. (See the proof of Theorem 4 above.) By Theorem 5, $d^2_{\min}(0, l) = d^2_{\min}(l, 0)$ for any l.

$\square$

The method is illustrated by considering the collection of all three-path channels ($L = 3$) and determining the worst-case effective minimum squared Euclidean distance for each combination of L_1 and L_2. The reduction in the worst-case minimum squared Euclidean distance relative to a single-path channel is expressed in decibels. That is, it is given as $10 \log_{10}[d^2_{\min}(L_1, L_2)/4]$. The results for three-path channels are shown in Table 4.2. For this table and the others shown here, the last value in each column is unchanged if the column is extended downward. Similarly, the last value in each row is unchanged if the row is extended to the right.

$L_1 \backslash L_2$	0	1
0	-2.3 dB	-2.3 dB
1	-2.3 dB	0 dB

Table 4.2 Worst-case asymptotic loss due to ISI with a three-path channel.

Similar results are shown in Table 4.3 for the collection of four-path channels and in Table 4.4 for the collection of five-path channels. For four-path channels, the worst-case asymptotic loss is reduced by 1.5 dB if the polarities of only one preceding and one succeeding channel symbol are known prior to equalization for each unknown channel symbol. More than 3 dB of the 4.2 dB worst-case asymptotic loss is recovered if the polarity of either the second preceding or second succeeding channel symbol is also known *a priori* for each unknown channel symbol. For five-path channels, more than 4.8 dB of the

5.7 dB worst-case asymptotic loss is recovered if the polarities of the two preceding and two succeeding channel symbols are known prior to equalization for each unknown channel symbol.

$L_1 \backslash L_2$	0	1	2
0	-4.2 dB	-4.2 dB	-4.2 dB
1	-4.2 dB	-2.7 dB	-1.1 dB
2	-4.2 dB	-1.1 dB	0 dB

Table 4.3 Worst-case asymptotic loss due to ISI with a four-path channel.

$L_1 \backslash L_2$	0	1	2	3
0	-5.7 dB	-5.7 dB	-5.7 dB	-5.7 dB
1	-5.7 dB	-3.5 dB	-2.3dB	-2.3 dB
2	-5.7 dB	-2.3 dB	-0.86 dB	-0.86 dB
3	-5.7 dB	-2.3 dB	-0.86 dB	0 dB

Table 4.4 Worst-case asymptotic loss due to ISI with a five-path channel.

Similar results can be obtained for a collection of channels with higher values of L and in each case the asymptotic performance loss due to ISI decreases as L_1 or L_2 increases. For the special case in which no states are pinned ($L_1 = L_2 = 0$), the asymptotic performance loss due to ISI is given for $L = 3$ through $L = 10$ in [14]. The results are incorrect for $L = 7$ through $L = 10$, where it is claimed that the error sequence polynomial $e(D) = 1 + D$ results in the worst case minimum distance for these channel lengths. The correct normalized worst-case minimum distance for $L = 7$ is 0.1307, as shown in [16], resulting in a worst-case asymptotic loss of 8.84 dB due to ISI. The erroneous minimum distance of 0.152 is reported in [14]. An error sequence polynomial that results in this worst case minimum distance is

$e(D) = 1 - D - D^2 + D^3 + D^4 - D^5$. For $L = 8$ through $L = 10$, the same error sequence polynomial results in upper bounds of 0.0701, 0.0478 and 0.0340 respectively, for the worst-case minimum distance. These correspond to lower bounds of 11.54 dB, 13.24 dB and 14.6 dB respectively, on the worst-case asymptotic loss due to ISI. The corresponding (erroneous) minimum distances reported in [14] are 0.1202, 0.0977 and 0.0812 respectively.

4.3 Measures of System Performance

Two factors determine the value of a digital communication technique in most applications: the error probability that is achieved, and the cost in computation and delay at the receiver. The most useful measure of link error probability in a packet radio network is the probability of failed or erroneous reception of a packet. The bounded-distance EE decoding considered in this paper results in a probability of undetected decoding error that is much lower than the probability of detected decoding failure if a reasonable limit is placed on the maximum number of code-symbol erasures for any code word. (Additional protection against undetected errors in the packet can be provided by using a cyclic redundancy-check (CRC) code as an outer code [52]). Thus the link performance measure we employ is the probability that detection of the packet is terminated while at least one code word has not been successfully decoded. In the rest of the dissertation this measure is referred to simply as the *probability of packet error*. In particular, for each example in this chapter the link performance is characterized in terms of the signal-to-noise ratio that is required to achieved a specified probability of packet error.

Each packet-level iteration results in a (restricted) execution of the equalization algorithm for each dwell interval and an additional EE decoding attempt for some of the code words in the packet. Thus packet-level iteration results in increased detection complexity as well as variation in the detection complexity from packet to packet. For a given packet, in each iteration the number of operations executed by the MLSE equalizer in a dwell interval depends on the number of bits that are pinned in the iteration and the location of the pinned bits within the dwell interval.

In general, the proportionate savings in additions, compare-select operations, and memory writes due to state pinning can be either smaller or greater than the fraction of bits that are pinned in the iteration. But for one straightforward implementation, the overall equalizer complexity is approximately proportional to the fraction of bits that are not pinned in the iteration (which is in turn proportional to the fraction of code words not successfully decoded in previous iterations). Moreover, the number of EE decoding attempts in an iteration is exactly proportional to the fraction of code words that were not successfully decoded in the previous iterations.

Thus the total number of EE decoding attempts for a packet is a suitable proxy for the overall complexity of detecting the packet in the receiver. Moreover, if equalization for individual dwell intervals and EE decoding of individual code words in a packet are performed sequentially, the complexity is proportional to the delay incurred in packet detection. The number of EE decoding attempts *per code word* for a packet is therefore used as the measure of the detection complexity for the packet in the remainder of the discussion. The average detection complexity is thus given by the average number of EE decoding attempts *per code word*. Note that systems A and H (which use one-shot equalization and decoding) employ exactly one EE decoding attempt per code word, and thus each has a detection complexity of one for every packet. In contrast, the detection complexity of each system using packet-level iteration can be greater than one.

4.4 Performance of the SFH Systems

In this section we evaluate the performance of each of the system designs described in Section 4.1. Recall that the system that uses one-shot MLSE equalization and bounded-distance EE decoding is denoted system A. The system that uses packet-level iterative equalization and decoding without bit interleaving is denoted system B. The modifications of system B that include regular bit interleaving, pseudo-random bit, odd-even-swap, distance-swap interleaving within each dwell interval are denoted systems C, D, E and F, respectively. The system where the encoded binary contents of the entire packet are interleaved prior to transmission using an s-random interleaver is denoted system G. The replacement of rectangular block code-symbol interleaving with diagonal block code-symbol interleaving in systems A and B results in systems H and I, respectively.

In each of the examples, we consider a packet consisting of twelve (n,k) extended R-S codewords. Each dwell interval contains a preamble sequence of 26 bits. (The preamble sequence used in the examples is (11101111000100101110111100), which corresponds to one of the "midamble" training sequences specified in the GSM cellular standard.) There are twelve code symbols in each dwell interval and an extra bit of parity is added to each code symbol. Except where otherwise noted, the value of n is 32 and the value of k is 16. Thus there are 98 binary channel symbols in each dwell interval (including the preamble sequence) and 960 bits of information in each packet. The guard interval at the end of each dwell is four times the channel-symbol duration. The SFH packet transmission takes place over 32 dwell intervals, except where otherwise noted, and the carrier frequency for the transmission hops over 440 available frequency slots.

4.4.1 Comparison of Performance of the SFH Systems

The performance of SFH systems A through G is shown for a two-path static channel in Figure 4.6. The two paths have equal strengths, and their path delays are 0 and T. For a probability of packet error of 0.01, the system with packet-level iteration that does not employ bit interleaving (system B) results in a performance improvement of 0.4 dB over the system with one-shot equalization and decoding (system A). The system with regular bit interleaving (system C) provides a performance improvement of 1.15 dB over system A, and the system with pseudo-random bit interleaving (system D) results in a performance improvement of 1.45 dB over system A. The system with odd-even swap interleaving (system E) and the system with distance-swap interleaving (system F) result in a performance that is the same as the performance of system D. The system using s-random packet interleaving (system G) provides an improvement in performance of 1.25 dB over system A.

System A requires one EE decoding attempt per code word, as noted in the previous section. In contrast, the detection complexity of each system using packet-level iteration is greater than one. This is illustrated by considering the performance with the two-path channel that is shown in Figure 4.6. For a probability of packet error of 0.01, the average detection complexity of system B increases from one EE decoding attempt to 1.0047 EE decoding attempt per R-S code word in a packet. At the same probability of packet error, system C has an average detection complexity of 1.4 EE decoding attempts and system D has an average detection complexity of 1.43 EE decoding attempts per code word. The average detection complexities for system E, F and G are 1.44, 1.42 and 1.29 EE decoding attempts per R-S code word, respectively.

The performance of SFH systems A, B, C and D is shown in Figure 4.7 for a static channel with three equal-strength paths. The delays of the three paths are 0, T, and $2T$. The performance of one-shot equalization and decoding (system A) for a single-path static channel is also shown for comparison. The effect of intersymbol interference on system performance can be seen by comparing the performance of system A with the single-path channel and its performance with the three-path channel. For a probability of packet error of 0.01, the performance of system A is 3.25 dB poorer with the three-path channel than with the AWGN channel.

The poorer performance of system A in intersymbol interference is consistent with an examination of the factors affecting system performance. Specifically, the asymptotic (high signal-to-noise ratio) performance with the three-path channel considered here is 1.76 dB poorer than the performance in an AWGN channel if the performance measure is the probability of a first error event in MLSE equalization [9]. The error events that are dominant at high signal-to-noise ratio (those at a minimum Euclidean distance for each channel) have a more detrimental effect on packet detection with the three-path channel than with the AWGN channel. If the channel has a single path, each such error event results in a single channel-symbol error which results in the erasure of a single R-S code word with a high probability. In contrast, each minimum-distance error event for the three-path channel results in two channel-symbol errors. This in turn results in either one undetected code-symbol error or the erasure of two code symbols from different code words in the packet with a high probability. Moreover, the effect of error events at distances greater than the minimum distance is significant at the error probability of interest, and these have a more detrimental effect for the three-path channel than for the single-path channel. Finally, the accuracy of the per-dwell channel estimation (equalizer training) is poorer for the three-path channel than for a single-path channel.

The performance with the three-path channel is shown in Figure 4.7 for three of the SFH systems that use packet-level iterative equalization and decoding. For a probability of packet error of 0.01, system B results in performance that is 0.6 dB better than the performance of system A. System C provides a performance improvement of 1.4 dB over system A, and the system D results in a performance improvement of 1.5 dB over system A. In Figure 4.8, the performance of system D and the other three SFH systems employing per-dwell bit interleaving and packet-level iteration is shown for the same three-path static channel. System E provides a performance improvement of 1.6 dB over system A and system F results in performance improvement of 1.48 dB over system A. The system using s-random packet interleaving (system G) provides an improvement in performance of 1.53 dB over system A. Thus for this channel the use of bit interleaving and packet-level iteration recovers about half of the performance loss that intersymbol interference causes in the system with one-shot equalization and decoding.

For a probability of packet error of 0.01, system B has an average detection complexity of 1.0071 EE decoding attempts per code word with the three-path static channel, and system C has an average detection complexity of 1.5123 decoding attempts per code word. For the same probability of packet error, system D has an average detection complexity of 1.594 decoding attempts per code word. The corresponding values for system E, system F and system G are 1.63, 1.61 and 1.59 EE decoding attempts per code word, respectively. Thus for the three-path static channel considered in the example, the 1.6 dB performance improvement provided by system E is achieved at the cost of an increase in the average detection complexity of approximately 60%. Thus packet-level iterative detection combined with bit interleaving results in significant performance gains at the cost of only a moderate increase in the average detection complexity over one-shot equalization and coding for this channel.

The probability of packet error for the SFH systems is shown in Figure 4.9 for a four-path static channel. The four paths have equal strength, and their delays are 0, T, $2T$ and $3T$. For a probability of packet error of 0.01, System B results in a performance improvement of 0.4 dB over system A, and it increases the average detection complexity from one EE decoding attempt to 1.0041 EE decoding attempt per R-S code word in a packet. System C results in a performance improvement of 1.55 dB over system A at the cost of an average of 1.528 decoding attempts per code word. System D provides an improvement of 1.6 dB over system A with an average detection complexity of 1.5648 EE decoding attempts per code word. System E results in an improvement in performance of 1.7 dB over system A at the cost of an average detection complexity of 1.6 EE decoding attempts per code word. System F and system G both provide a improvement of 1.6 dB at a cost in complexity of an average of 1.576 and 1.55 EE decoding attempts per code word, respectively. Thus for the two-path, three-path and four-path static channels, the packet-level iteration with bit interleaving results in significant performance improvement over either one-shot detection or packet-level iterations with no bit interleaving, and the penalty in the average detection complexity is modest. System E, which uses odd-even bit interleaving, provides the best performance among all the bit interleaving methods for the static multipath channels, though the differences in performance and average complexity among systems C through G are small. Each bit-interleaving format is beneficial in a system with packet-level iteration, and thus systems C through G all result in much better performance than system B.

The tradeoff between performance and complexity favors the systems using packet-level iteration even more decidedly if performance with Rayleigh-fading multipath channels is considered. The average probability of packet error for a given system is determined largely by the receiver's detection outcomes for packets transmitted when the channel is subjected to deep fading, and the different systems can result in very different performance for such channels. The receiver in each system is able to successfully detect most packets transmitted when the channel is *not* subjected to deep fading, however, and most packets are detected in one iteration in this instance. Since the latter channel conditions occur with a high probability, the different systems can exhibit substantially differences in the average probability of packet error with only a small difference in the average detection complexity with fading channels.

This is illustrated by considering the performance of systems A through F, which is shown in Figure 4.10 for a Rayleigh-fading channel that consists of two paths with equal average power. The path delays are 0 and T, and the normalized Doppler spread of the channel is given by $D_T = 1.5 \times 10^{-4}$. For a probability of packet error of 0.01, System B results in a performance improvement of 0.3 dB over system A at the cost of an average of 1.007 EE decoding attempts per R-S code word. System C provides a gain of 1.05 dB over system A, and the average number of EE decoding attempts per code word increases to 1.008. System D, System E and System F result in a performance gain of 1.2 dB over system A with an average detection complexity of 1.009 decoding attempts per code word. System G (not shown in the figure) provides performance which is comparable to the performance of systems D, E and F with a comparable average detection complexity.

The performance of systems A, B, C and D is shown in Figure 4.11 for a three-path Rayleigh-fading channel with equal average power in the paths. The performance of systems D, E, F and G for the same channel is shown in Figure 4.12. The delays for the three paths are 0, T and $2T$, and the normalized Doppler spread of the channel is given by $D_T = 1.5 \times 10^{-4}$. For a probability of packet error of 0.01, system B results in a performance improvement of 0.7 dB over system A at the cost of an average of 1.0039 EE decoding attempts per code word. For the same probability of packet error, system C results in a performance improvement of 1.6 dB over system A with an average detection complexity of 1.011 EE decoding attempts per code word. System D results in a performance improvement of 1.6 dB over system A with an average detection complexity of 1.010 EE decoding attempts per R-S code word. Systems E and F also result in a performance improvement of 1.6 dB over system A for a probability of packet error of 0.01, but system G results in a performance improvement of only about 1 dB. The performance gains of system E and system F are achieved at an average cost of 1.010 EE decoding attempts per code word, while system G has an average detection complexity of 1.008 EE decoding attempts per code word. Thus, for this channel restricting the bit interleaving to within each dwell interval yields better performance than applying a s-random interleaver to the contents of the entire packet.

In Figure 4.13, the probability of packet error is illustrated for systems A through G with a Rayleigh-fading channel that consists of four paths with equal average power. The path delays are 0, T, $2T$ and $3T$, and the normalized Doppler spread of the channel is given by $D_T = 1.5 \times 10^{-4}$. System B results in a performance improvement of 0.17 dB over system A at the cost of an average of 1.0009 EE decoding attempts per R-S code word for a probability of packet error of 0.01. System C provides a gain of 1.8 dB over system A, and the average number of EE decoding attempts per code word increases to 1.0052. Systems D, E and F each result in a performance gain of 2.7 dB over system A with an average detection complexity of 1.014 decoding attempts per code word. System G provides a gain in performance of 2.1 dB over system A at an average cost of 1.010 EE decoding attempts per R-S code word.

From these examples it is seen that if the multipath channel exhibits Rayleigh fading, packet-level iteration with per-dwell bit interleaving yields performance gains over one-shot equalization and decoding and packet-level iteration without bit interleaving is similar to the gains obtained for static multipath channels of comparable delay spreads. The increase in the average detection complexity compared with either one-shot equalization and coding or packet-level iteration without bit interleaving is much less than for the static channels, however. In contrast with the results for static channels, the use of bit interleaving across dwell intervals results in somewhat poorer performance than the use of per-dwell bit interleaving for Rayleigh-fading channels with a large delay spread.

The effect of using diagonal code-symbol interleaving is illustrated by considering the performance of systems H and I in several multipath channels. The performance of systems A, B, H and I is shown in Figure 4.14 for the equal-strength, three-path static channel considered above. (Recall that systems H and I are modifications of systems A and B, respectively, with diagonal code-symbol interleaving replacing rectangular code-symbol interleaving.) As shown in Figure 4.14, systems A and H result in identical performance and systems B and I result in identical performance. The performance improvement of system I over system H is obtained with an increase of 1% in the average detection complexity, which is comparable to the complexity increase of system B over system A.

The performance of systems A, B, H and I is shown in Figure 4.15 for the three-path Rayleigh fading channel considered above. For a probability of packet error of 0.01, system H results in a performance improvement of 0.5 dB over system A and system I results in a performance improvement of 0.9 dB over system B. The average detection complexity for system I is 1.002 EE decoding attempts per code word, which is slightly less than the average detection complexity of 1.0039 EE decoding attempts for system B.

The better performance of systems H and I compared with systems A and B, respectively, in the Rayleigh-fading channel is a result of the variation in the channel's impulse response over the duration of a dwell interval. The channel coefficients determined during the training stage have a decreasing accuracy as the end of each dwell interval is approached, and consequently the channel symbols are detected with a higher probability of error in the latter part of each dwell interval. If a code symbol is represented by bits in the latter part of a dwell interval, it is subjected to a correspondingly high probability of error or erasure. Diagonal code-symbol interleaving provides a form of diversity protection against the time-varying channel response that results in a lower average probability of code-word error among the code words in the packet. (No corresponding diversity gain occurs with a static multipath channels since it's impulse response does not vary with time.)

The diversity protection provided by diagonal interleaving is also illustrated by considering the performance of systems A, B, H and I for the four-path Rayleigh-fading channel considered above, as shown in Figure 4.16. The use of system H results in a performance improvement of 1.6 dB over system A and system I results in a performance improvement of 1.8 dB over system B at a probability of packet error of 0.01. The average detection complexity of system I is 1.0034 decoding attempts which is slightly greater than the complexity of 1.0009 decoding attempts for system B. Similar performance improvements and relative detection complexities are observed for the two-path Rayleigh-fading channel considered above. Thus the performance gains due to the diversity protection of diagonal code-symbol interleaving are obtained at essentially no cost in the average detection complexity.

The results for the static and fading channels demonstrate that the use of per-dwell pseudo-random bit interleaving in conjunction with packet-level iteration (such as used in systems D, E and F) results in performance that is consistently comparable to or better than the performance of any of the other systems considered. The cost of the performance gain is a modest increase of a few percent to a few tens of percent in the average detection complexity compared with the other systems. The performance of systems D, E and F is much better than the performance of system B, system C or system H for all channels considered. It is also several tenths of a dB better than the performance of system C (with regular interleaving) for the static channels and for the Rayleigh-fading channel with the largest delay spread. The performance of systems D, E, and F is also somewhat better than the performance of system G for the fading channels, and it is much better than the performance of system I for the static channels.

The benefit of per-dwell pseudo-random bit interleaving in a SFH system with packet-level iteration is even more pronounced if the channel exhibits rapid fading. This is illustrated in Figure 4.17 in which the performance of systems B, C and D is shown for another three-path Rayleigh-fading channel with equal average power in the paths. The delays for the three paths are again 0, T and $2T$. The normalized Doppler spread of the channel is given by $D_T = 6 \times 10^{-4}$, however, so that the rate of variation in the channel's impulse response is four times as great as in the fading channels considered previously. The impulse response varies significantly within the span of a dwell interval, which results in an error floor at probability of packet error of 0.03 for system B.

The introduction of per-dwell bit interleaving produces a marked reduction in the error floor. For the system with regular bit interleaving (system C), the error floor occurs at a probability of packet error of less than 10^{-3}. At a packet error probability of 10^{-2}, system C has an average detection complexity of 1.0125 EE decoding attempts per code word. If pseudo-random bit interleaving is used instead (system D), the error floor is reduced further. For a packet error probability of 10^{-2}, system D has a performance improvement of 2.2 dB over system C at an average cost of 1.019 EE decoding attempts per code word. Systems E and F also achieve the same performance as system D with the same average detection complexity.

4.4.2 Performance of the SFH Systems with Various R-S Codes

The various SFH systems considered in this chapter exhibit the same relative performance when considered with R-S codes of different block lengths or different code rates. The effect of the code's block length of the performance of the various systems is illustrated by considering the performance of systems A, B, C, and D with a packet format consisting of twelve code words from a $(64, 32)$ extended R-S code. Each packet contains 2304 bits of information, and each code symbol has a parity-encoded binary representation of seven bits. Hence each dwell interval contains 110 binary channel symbols, including the preamble sequence of length 26 symbols. There are 64 dwell intervals in each packet transmission, and there are 390 frequency slots in the SFH system. Note that the $(64, 32)$ R-S code has the same rate as the $(32, 16)$ R-S code, though the instantaneous information rate of the packet is slightly greater with the $(64, 32)$ code when the overhead of the transmission format is taken into account.

The performance of systems A, B, C and D with the $(64, 32)$ code is shown in Figure 4.18 for an equal-strength, two-path static channel. The path delays for the channel are 0 and T. The performance improvement that is obtained by using packet-level iteration and bit interleaving with the $(64, 32)$ code is consistent with the performance improvement observed with the $(32, 16)$ code. For a packet error probability of 0.01, system B results in a performance improvement of 0.35 dB over system A with an average detection complexity of 1.009 EE decoding attempts per R-S code word. System C provides an improvement of 0.6 dB over system A at an average cost of 1.64 EE decoding attempts per code word. For the same packet error probability, system D exhibits a performance improvement of 0.95 dB, but it requires an average of 1.56 EE decoding attempts per code word to achieve this gain in performance.

In Figure 4.19, the performance of the SFH systems with the $(64, 32)$ R-S code is shown for the two-path, Rayleigh-fading channel with equal average strength per path. The normalized Doppler spread of the channel is given by $D_T = 1.5 \times 10^{-4}$ and the channel delays are 0 and T. For a probability of packet error of 0.01, system B results in a performance improvement of 0.4 dB over system A with an average detection complexity of 1.0028 decoding attempts per code word. With system C a performance gain of 0.8 dB is obtained with an increase in the average detection complexity to 1.0097 decoding attempts, and with system D a performance gain of 1.2 dB is obtained at an average complexity cost of 1.0155 EE decoding attempts per R-S code word.

The effect of the code rate on the various SFH systems is illustrated by considering the performance of systems A, B, C, and D with a $(32, 20)$ extended R-S code and with a $(32, 12)$ extended R-S code. As before, there are twelve code words in each packet. If the $(32, 20)$ code is used, each packet consists of 1200 information bits. If instead the $(32, 12)$ code is used, each packet contains 720 bits of information. The other system parameters are the same as those considered for the systems with the $(32, 16)$ R-S code. For both the $(32, 12)$ and $(32, 20)$ codes, the relative performance gain obtained with packet iteration and each bit interleaving technique is consistent with the performance gains observed for the $(32, 16)$ code.

In Figure 4.20, the performance for the SFH systems with the $(32, 20)$ R-S code is shown for the equal-strength, two-path static channel. For a packet error probability of 0.01, system B results in a performance improvement of 0.35 dB over system A with an average complexity of 1.0038 EE decoding attempts per R-S code word. System C provides an improvement of 1.15 dB over system A at an average cost of 1.34 EE decoding attempts per code word. For the same packet error probability, system D has a performance improvement of 1.4 dB, but it requires an average of 1.38 EE decoding attempts per code word to achieve this gain in performance.

The performance of systems A,B, C and D is shown with the $(32, 12)$ R-S code for the same two-path static channel in Figure 4.21. At a probability of packet error of 0.01, System B results in a performance improvement of 0.4 dB over system A at the cost of an average of 1.0045 EE decoding attempts per R-S code word. System C provides a gain of 1.2 dB over system A, and the average number of EE decoding attempts per code word increases to 1.39. System D results in a performance gain of 1.45 dB over system A with an average detection complexity of 1.42 EE decoding attempts per code word. Thus for a two-path static channel the performance/complexity tradeoff among the SFH systems using the various R-S codes considered in this subsection is consistent with the tradeoff between performance and complexity that was observed early for systems using the $(32, 16)$ R-S code.

The performance of the SFH systems with a $(32, 20)$ R-S code and with a $(32, 12)$ R-S code is shown in Figures 4.22 and 4.23, respectively, for the same Rayleigh-fading channel. For both the code rates, the performance improvement of systems B,C and D over system A is consistent with the performance improvement shown with the $(32, 16)$ R-S code. In particular, system D results in a performance improvement of 2.2 dB over system A in Figure 4.22 at an average cost of 1.008 EE decoding attempts per code words for a probability of packet error of 0.01. In Figure 4.23, the performance improvement of system D is 1.3 dB with an increase in the average detection complexity to 1.008 EE decoding attempts per R-S code word for the same probability of packet error.

The performance of system D in the two-path static channel is shown in Figure 4.24 for all four R-S codes considered in this chapter. For this channel, the system employing the $(32, 12)$ R-S code results in the worst performance. The performance with the $(32, 16)$ code and the $(32, 20)$ code is better by 0.5 dB and 0.65 dB, respectively, than the performance with the $(32, 12)$ code for a probability of packet error of 0.01. The performance with the $(64, 32)$ code is 0.6 dB better than the performance of $(32, 12)$ code for the same packet error probability. For each code, system D results in a comparable percentage increase in the average detection complexity over one-shot detection with the same code. Comparison of the absolute average detection complexities for the different codes depends on the choice of algebraic decoding algorithm and is not addressed here.

In Figure 4.25, the performance of system D is shown for the two-path Rayleigh-fading channel for all four R-S codes. For this channel, the system employing the $(32, 20)$ R-S code results in the worst performance. The performance with the $(32, 16)$ code and the $(32, 12)$ code is 1.0 dB and 1.7 dB better, respectively, than the performance with the $(32, 20)$ code for probability of packet error of 0.01. The system employing the $(64, 32)$ R-S code results in a performance improvement of 1.9 dB compared with the performance with the $(32, 12)$ code for the same probability of packet error.

A comparison of the results for the $(32, k)$ R-S codes in Figures 4.24 and 4.25 demonstrates that for the performance measure used here, the best choice of k depends on the channel. The highest code rate results in the best performance in the static channel, and the lowest code rate results in the best performance in the fading channel. Nonetheless, for all channels, code rates and block lengths, substantial performance improvement is obtained by employing bit interleaving and packet-level iterative equalization and decoding.

4.4.3 Performance with an Explicit Constraint on the Detection Complexity

The focus of the performance comparison employed thus far in the chapter is the *average* detection complexity of the SFH systems. Systems employing packet-level iteration, however, exhibit variable detection complexity (and equivalently, variable detection delay) from packet to packet. Each iteration for a packet reduces the number of R-S code words that have not yet been successfully decoded by one or more code words. Thus any of the systems employing packet-level iteration may perform as many as $N_s \times (N_s + 1)/2$ EE decoding attempts for a given packet. For the examples that are considered, $N_s = 12$. Hence there can be as many as 78 EE decoding attempts for a given packet. This results in a worst-case detection complexity that is 6.5 times greater than the fixed detection complexity with one-shot equalization and decoding. The worst-case detection complexity of packet-level iteration can be reduced if an additional stopping criterion is imposed. Specifically, we consider an additional criterion that the detection attempt for a given packet is terminated if the number of EE decoding attempts for the packet exceeds a predetermined maximum (which is of necessity less than 78 for our examples).

The choice of the maximum allowable number of EE decoding attempts for a packet provides a trade-off between performance and detection complexity. The tradeoff is illustrated in Figure 4.26 for the three-path static channel considered above. The probability of packet error is shown in Figure 4.26 for systems B and C with no explicit limit on the number of EE decoding attempts per packet. The probability of packet error is also shown for system C with limits of 18 and 24 EE decoding attempts for a packet. If the maximum number of EE decoding attempts for a packet is restricted to 18, the performance of system C is degraded by 0.8 dB for a probability of packet error of 0.01 in comparison with its performance if no limit is imposed. The average detection complexity is reduced from 1.51 to 1.081 EE decoding attempts per code word, however, and the worst-case computation for a packet is reduced more than four-fold from 78 to 18 EE decoding attempts. If the maximum number of allowable EE decoding attempts per packet is 24, the performance of system C is 0.4 dB worse than its performance with no limit. But the average detection complexity is reduced from 1.51 to 1.31 decoding attempts per code word, and the worst-case computation is reduced more than three-fold from 78 to 24 EE decoding attempts.

The tradeoff between performance and detection complexity with system D is illustrated in Figure 4.27. The probability of packet is shown for systems B and D and the four-path Rayleigh-fading channel described above. The probability of packet error is shown for both systems with no limit in the number of EE decoding attempts. It is also shown for system D with limits of 13 and 15 EE decoding attempts for a packet. If the maximum number of EE decoding attempts for a packet is limited to 15, the performance of system D is degraded by 0.3 dB in comparison with its performance if there is no limit. The average detection complexity is reduced from 1.014 to 1.008 EE decoding attempts per code word. If a limit of 13 EE decoding attempts per packet is used instead, the average detection complexity of system D is reduced to 1.002 EE decoding attempts per code word and the performance is degraded by 0.7 dB. The imposition of limits of 15 and 13 EE decoding attempts for a packet result in approximately a five-fold reduction and exactly a six-fold reduction, respectively, in the worst-case computation for a packet.

In Figure 4.28, the tradeoff between performance and detection complexity is shown for system E for the four-path static channel described above. The probability of packet error is shown for systems B and E with no limit on decoding complexity. Also, shown is the performance of system E with with limits of 18 and 24 on the maximum number of EE decoding attempts for a packet. If the number of EE decoding attempts is restricted to 18, the performance of system E is degraded by 0.7 dB and the average detection complexity is decreased from 1.6 EE decoding attempts to 1.125 EE decoding attempts per R-S code word. Imposing a limit of 24 EE decoding attempts per packet degrades performance by 0.35 dB, but the average detection complexity is reduced to 1.272 EE decoding attempts per R-S code word. The worst-case computation for a packet is reduced more than four-fold with a limit of 18 decoding attempts and more than three-fold when a limit of 24 decoding attempts is imposed. Thus, imposing limits on the number of EE decoding attempts provides a similar trade off between performance and complexity for Systems C, D and E. Thus most of the performance benefits of bit interleaving and packet-level iteration can be retained while substantially reducing the worst-case computational burden at the receiver by selection of an appropriate stopping criterion.

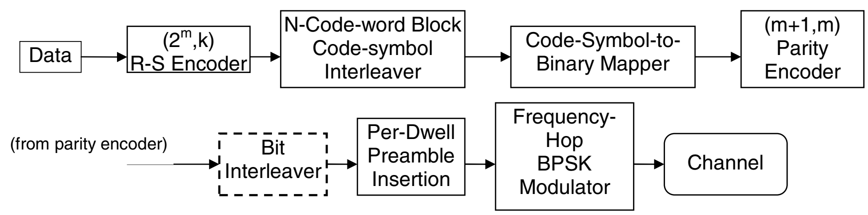

Figure 4.1 Generic transmitter for the SFH systems in Chapter 4.

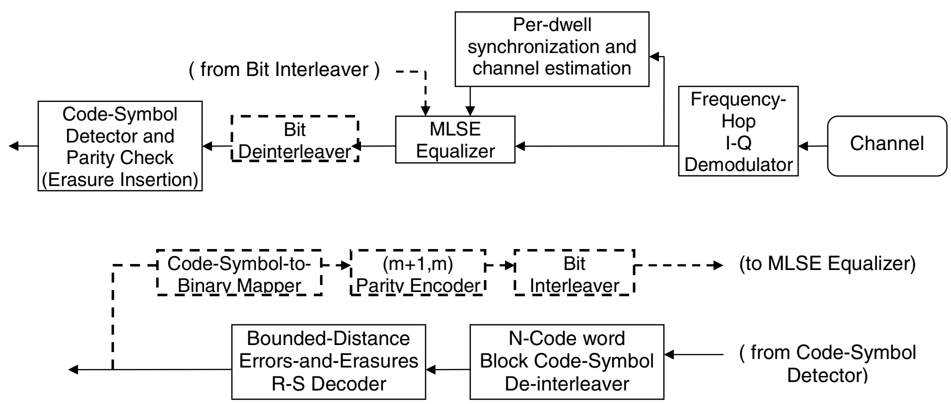

Figure 4.2 General receiver for the SFH systems in Chapter 4.

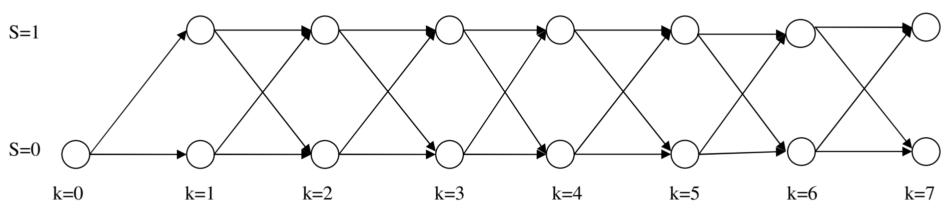

Figure 4.3 A two-state equalizer trellis without state pinning.

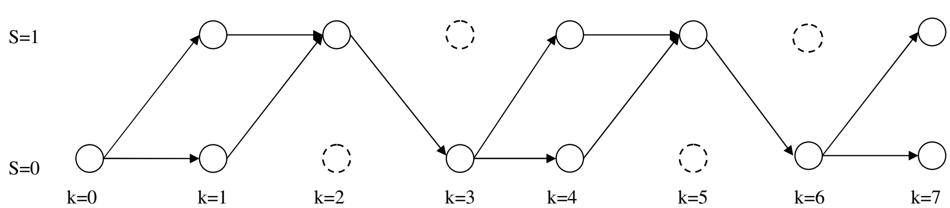

Figure 4.4 A two-state equalizer trellis with pinned states.

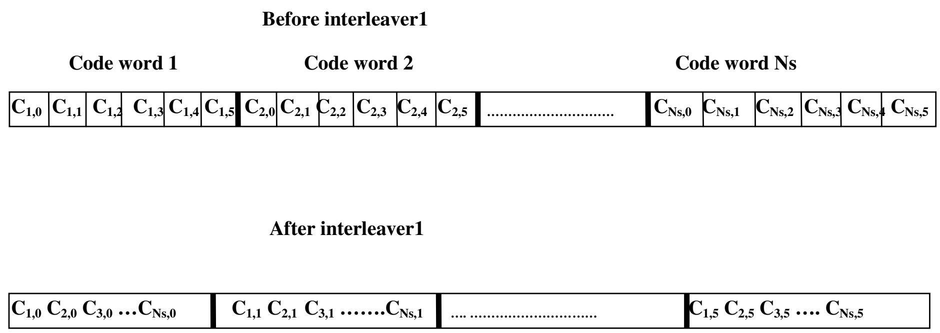

Figure 4.5 Regular bit interleaving for a dwell interval.

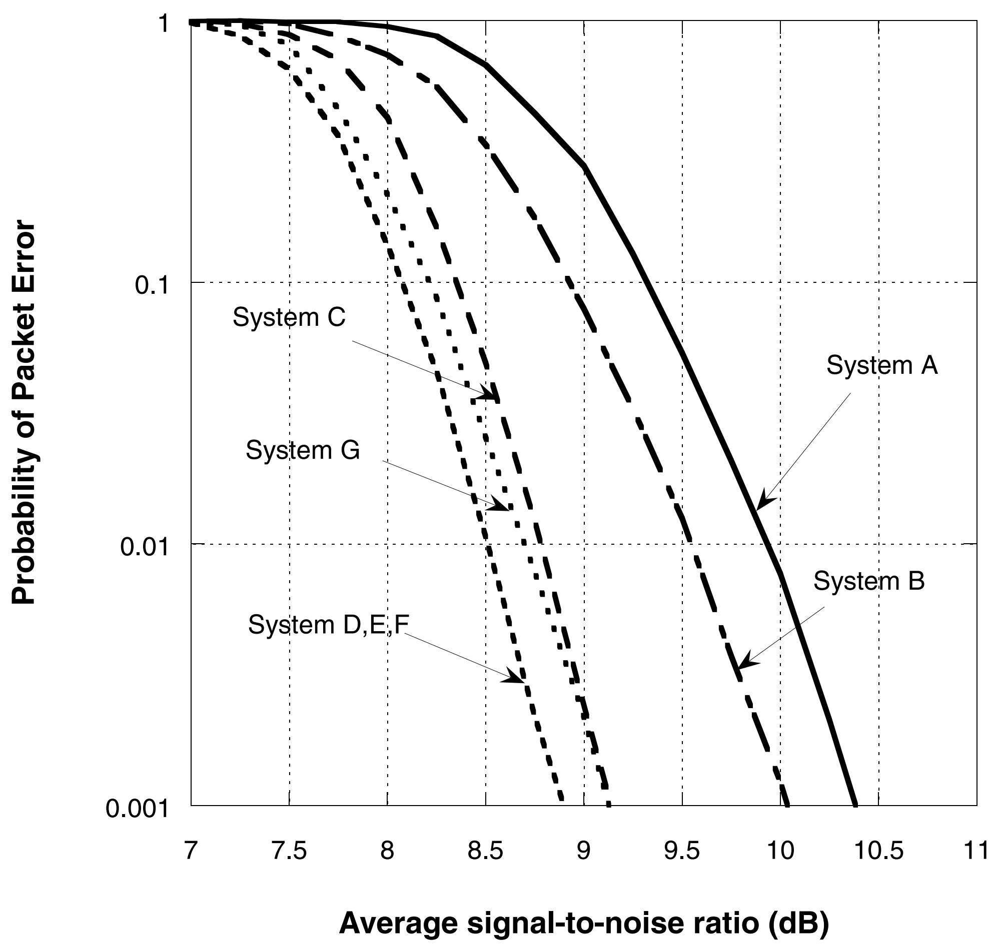

Figure 4.6 Probability of packet error with two-path static channel.

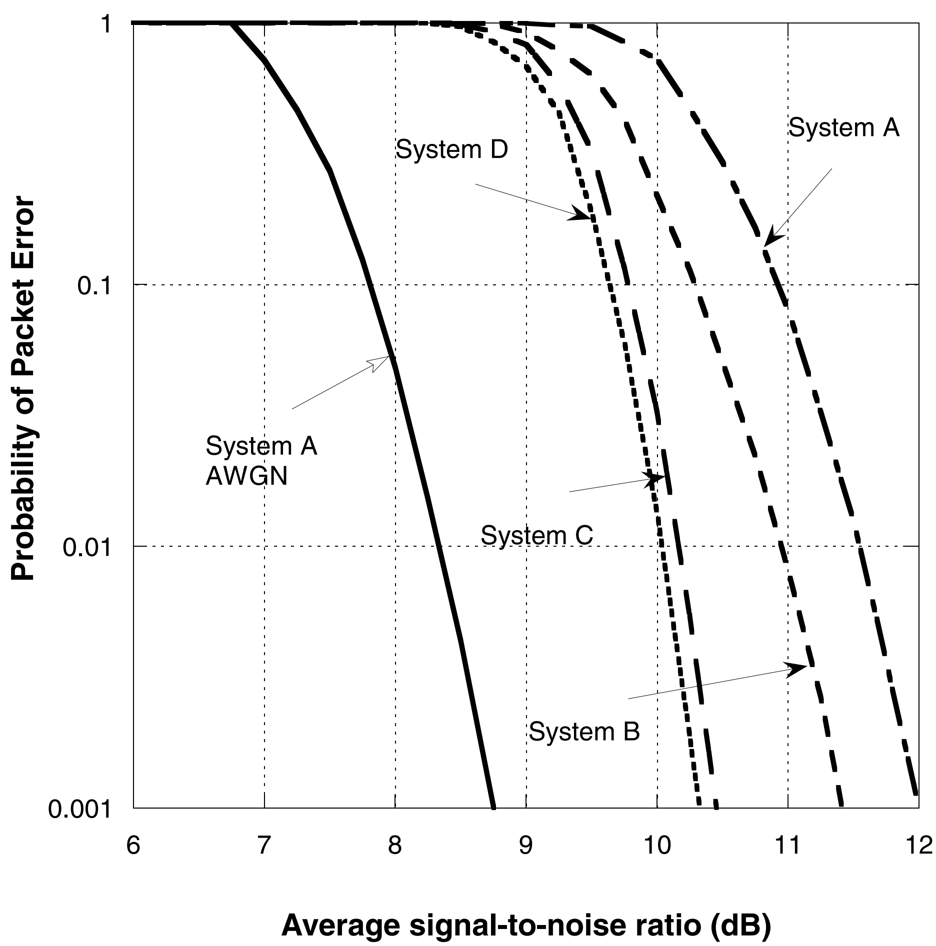

Figure 4.7 Probability of packet error with three-path static channel for systems A–D.

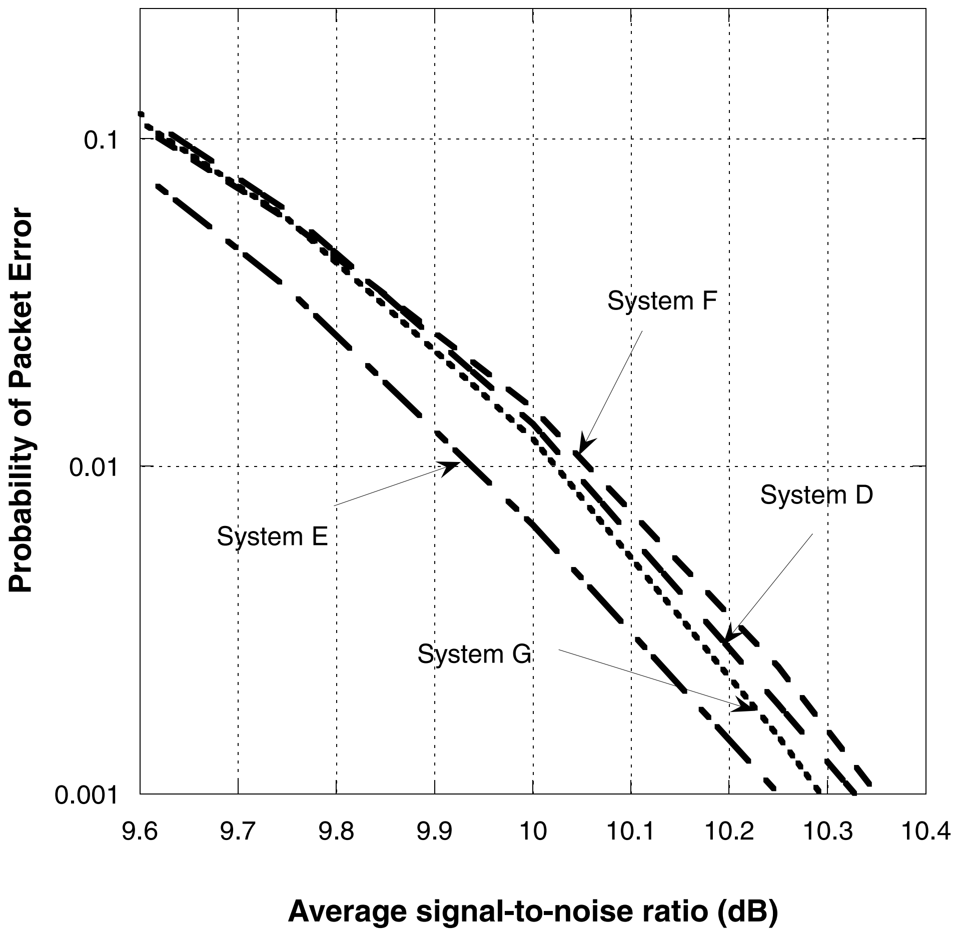

Figure 4.8 Probability of packet error with three-path static channel for systems D–G.

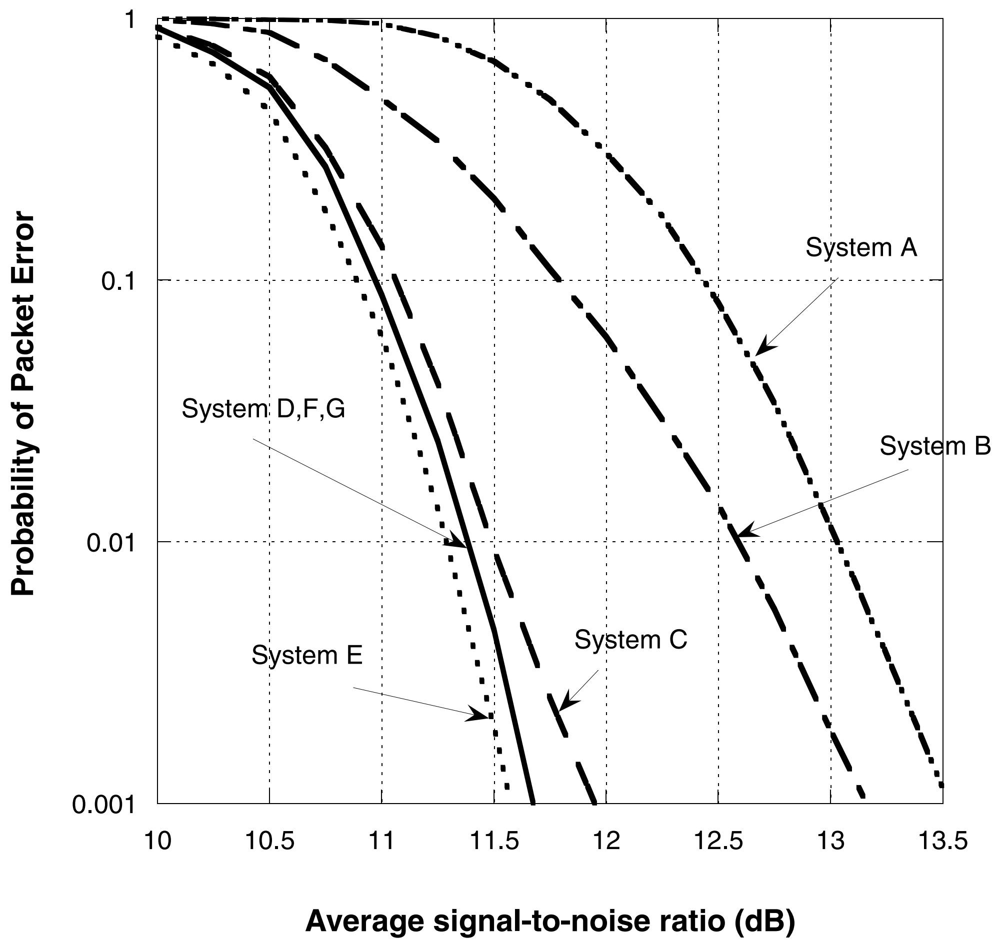

Figure 4.9 Probability of packet error with four-path static channel.

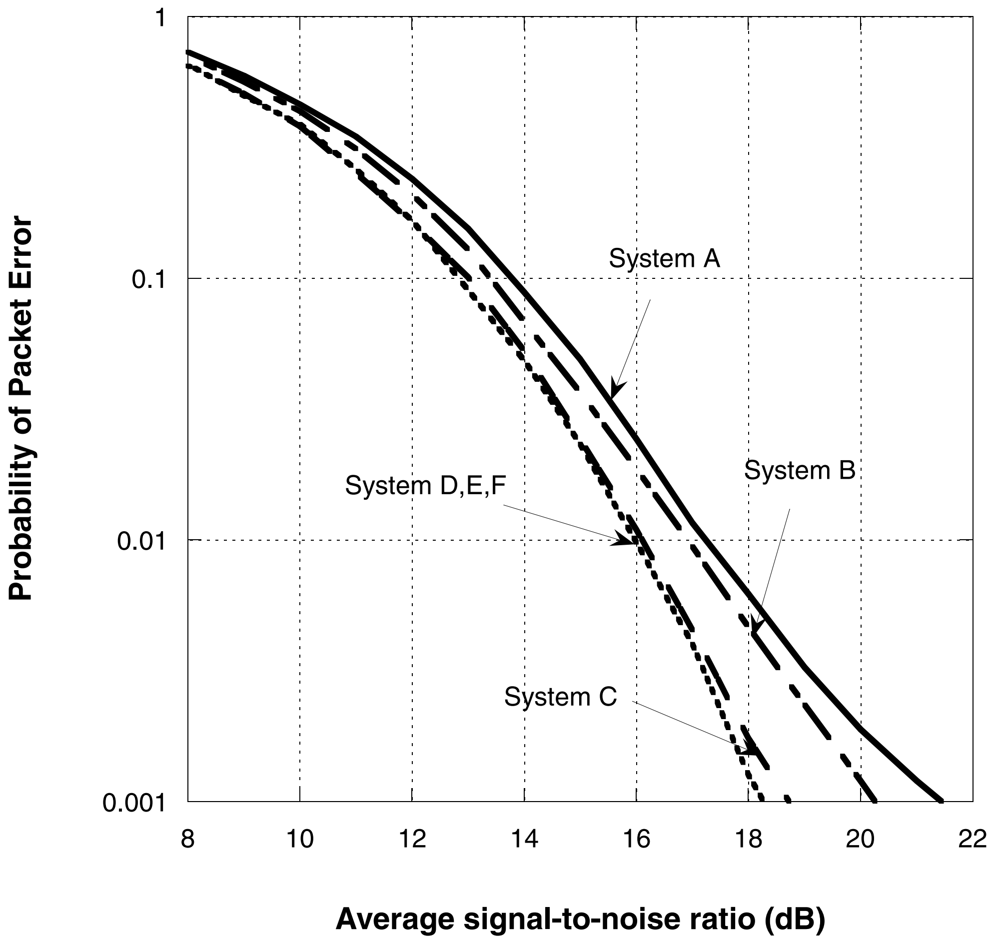

Figure 4.10 Probability of packet error with two-path Rayleigh-fading channel.

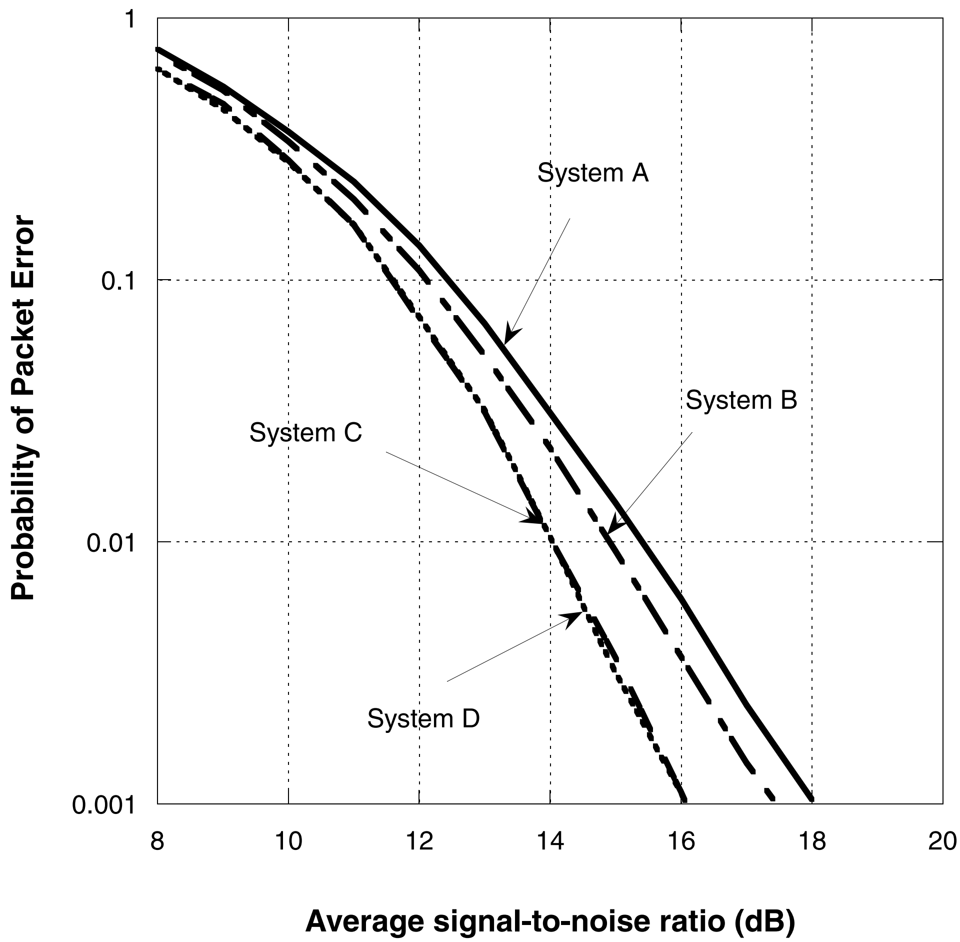

Figure 4.11 Probability of packet error with three-path Rayleigh-fading channel for systems A–D.

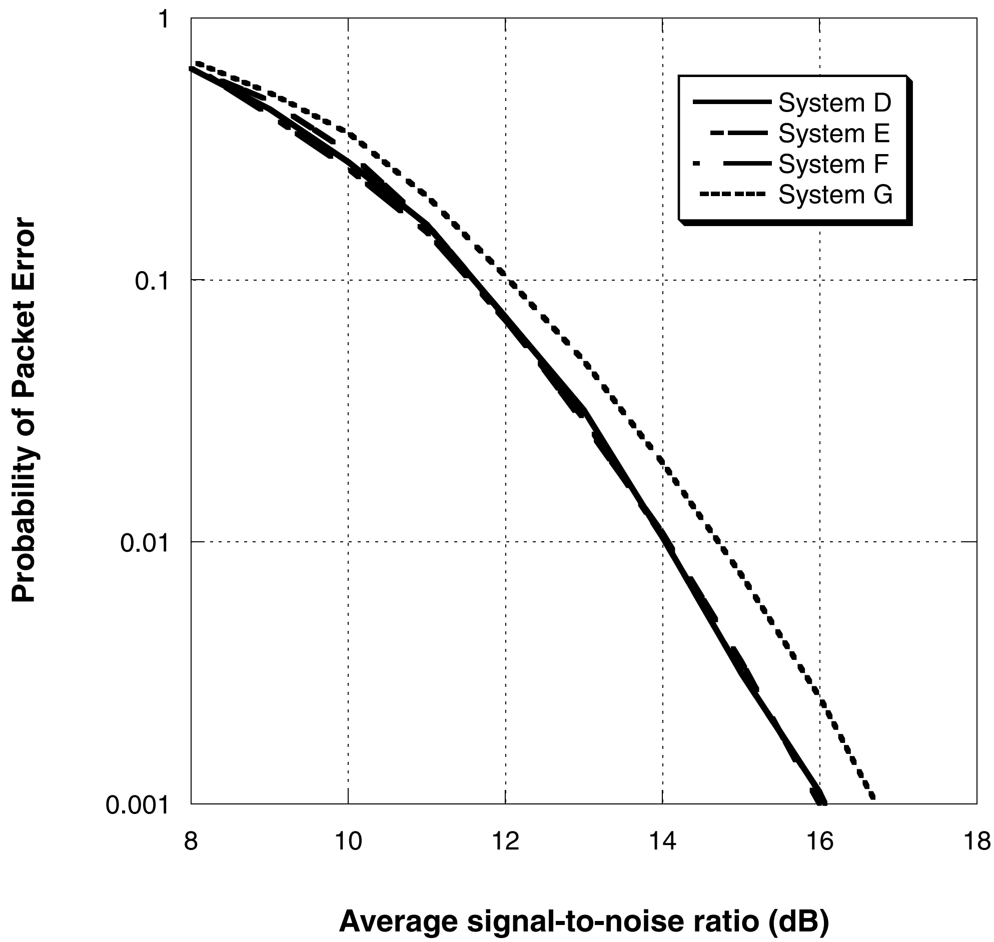

Figure 4.12 Probability of packet error with three-path Rayleigh-fading channel for systems D–G.

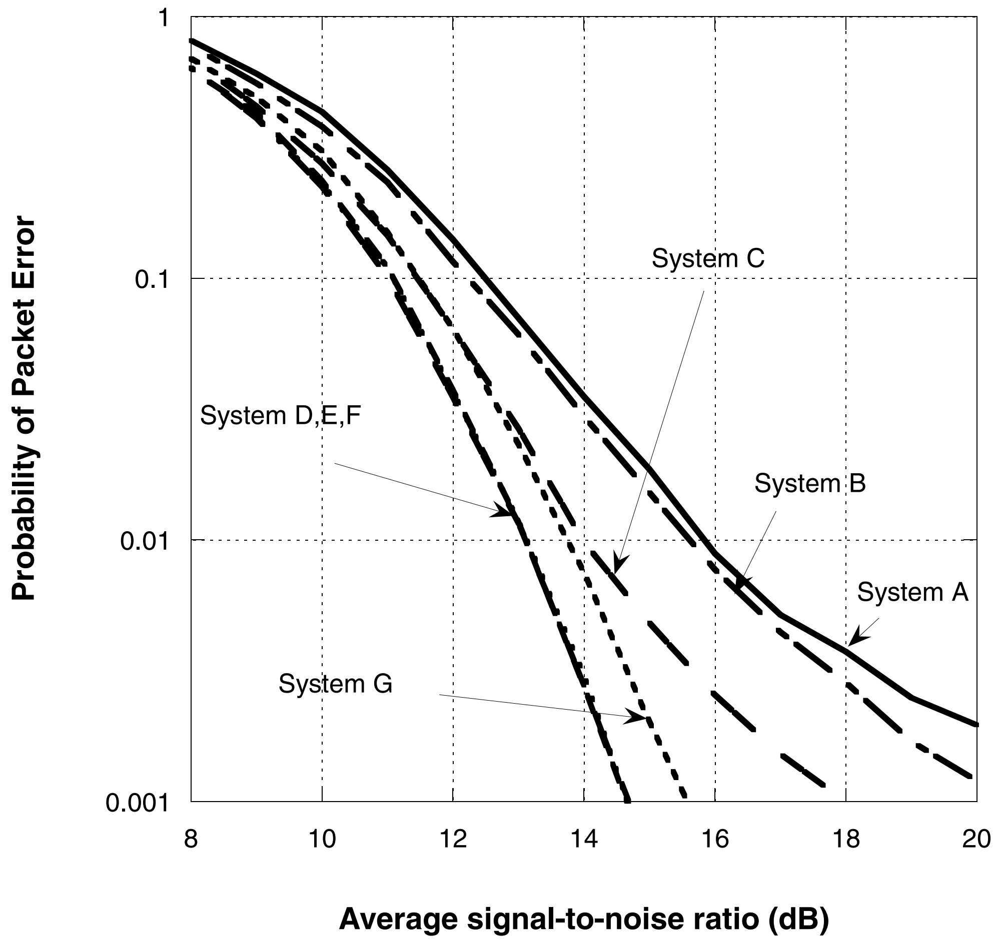

Figure 4.13 Probability of packet error with four-path Rayleigh-fading channel.

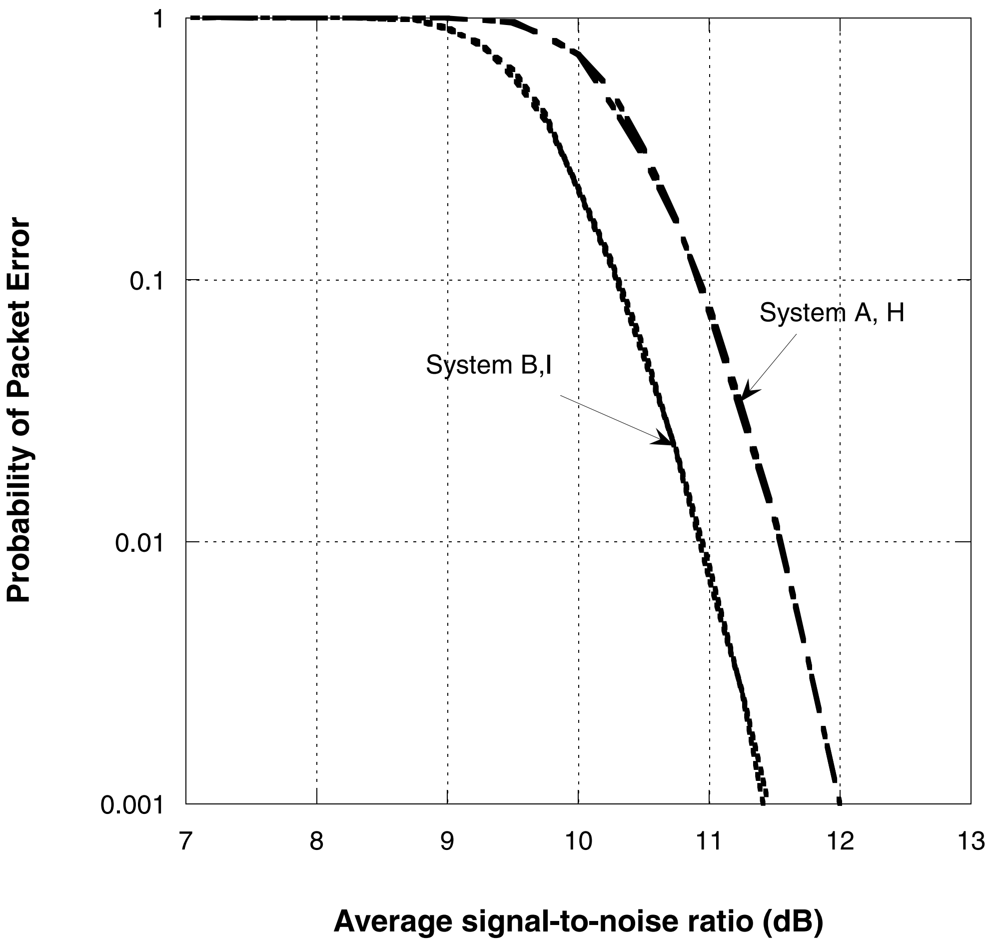

Figure 4.14 Probability of packet error with three-path static channel for systems A, B, H and I.

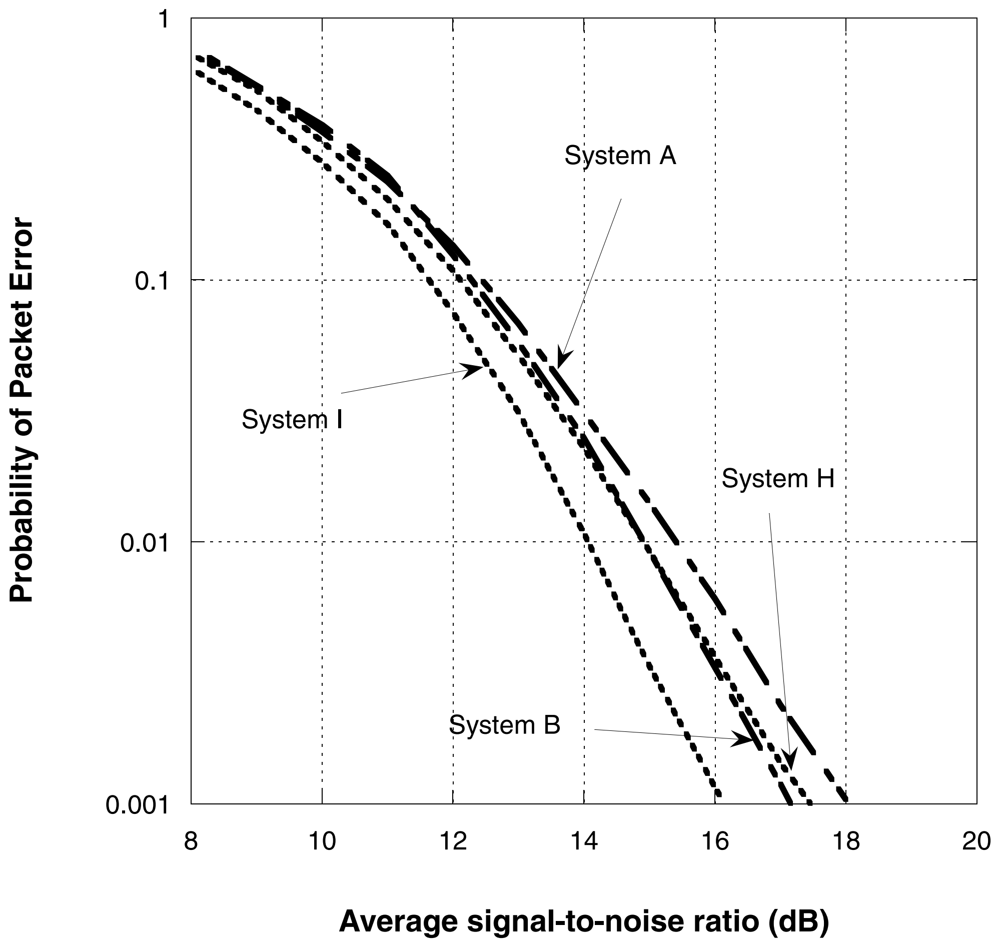

Figure 4.15 Probability of packet error with three-path Rayleigh fading channel for systems A, B, H and I.

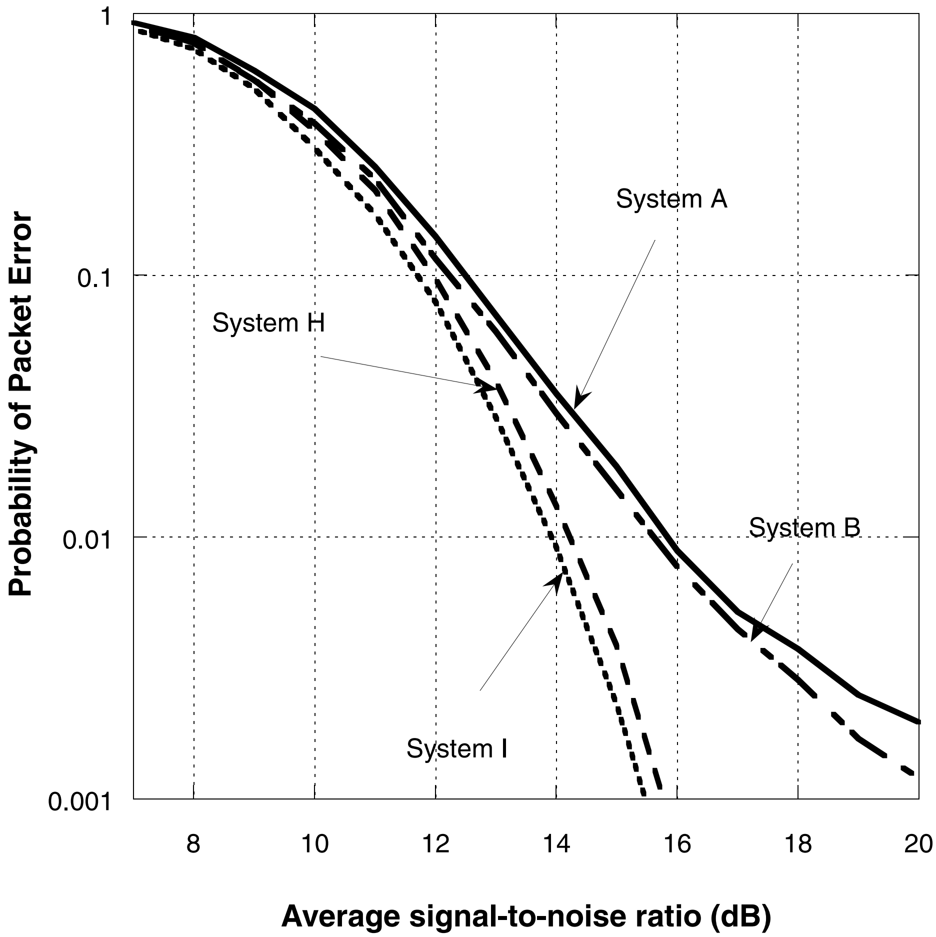

Figure 4.16 Probability of packet error with four-path Rayleigh-fading channel for systems A, B, H and I.

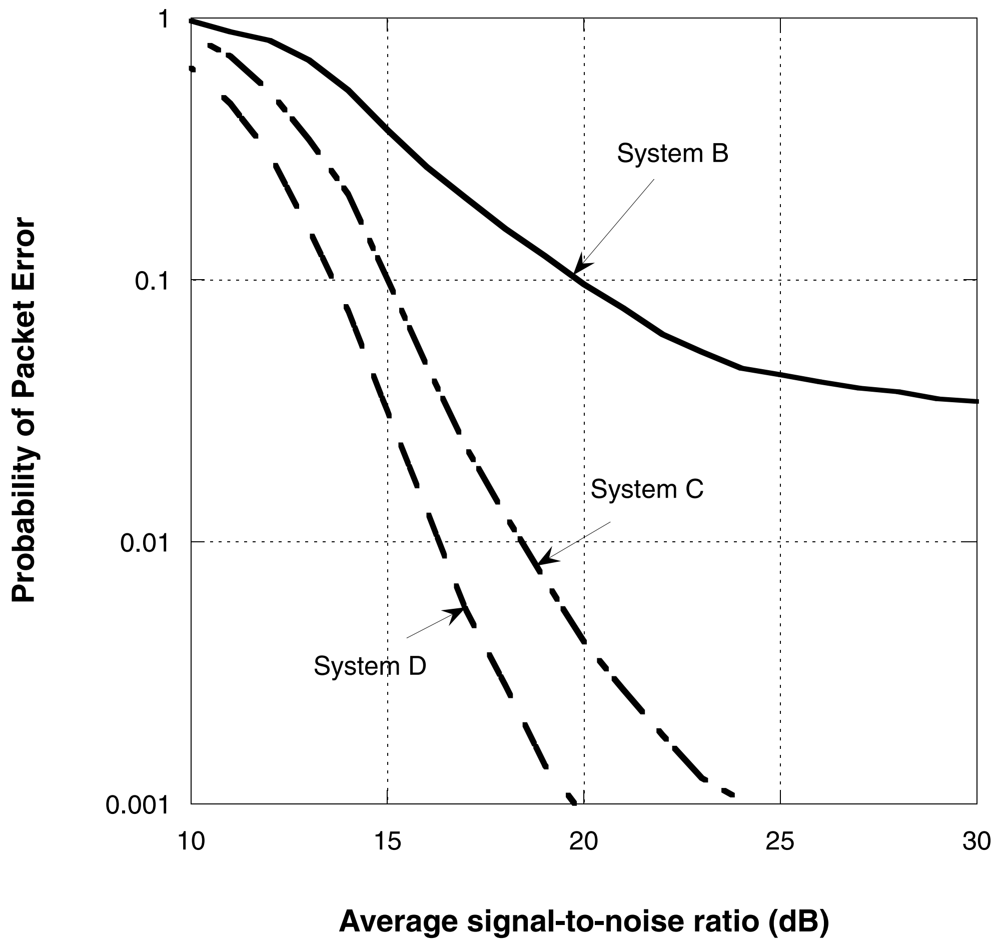

Figure 4.17 Probability of packet error with three-path Rayleigh-fading channel and large Doppler spread.

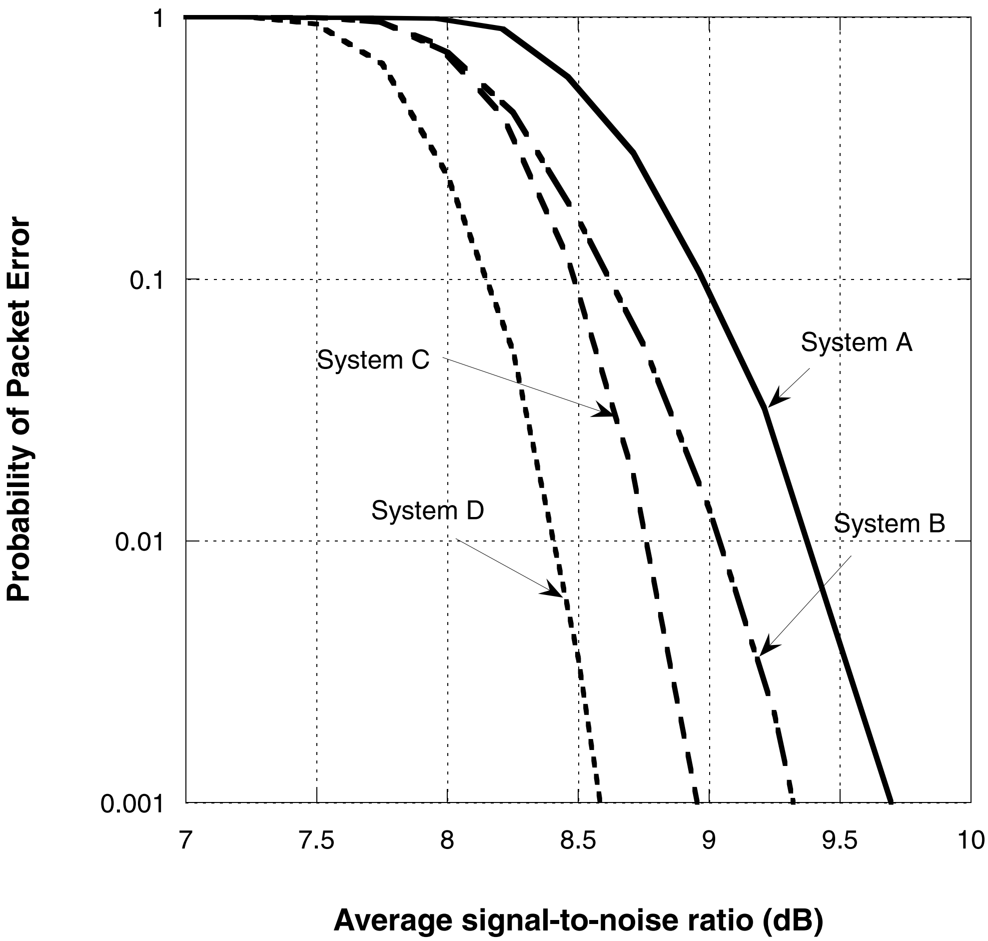

Figure 4.18 Probability of packet error with two-path static channel and (64,32) R-S code.

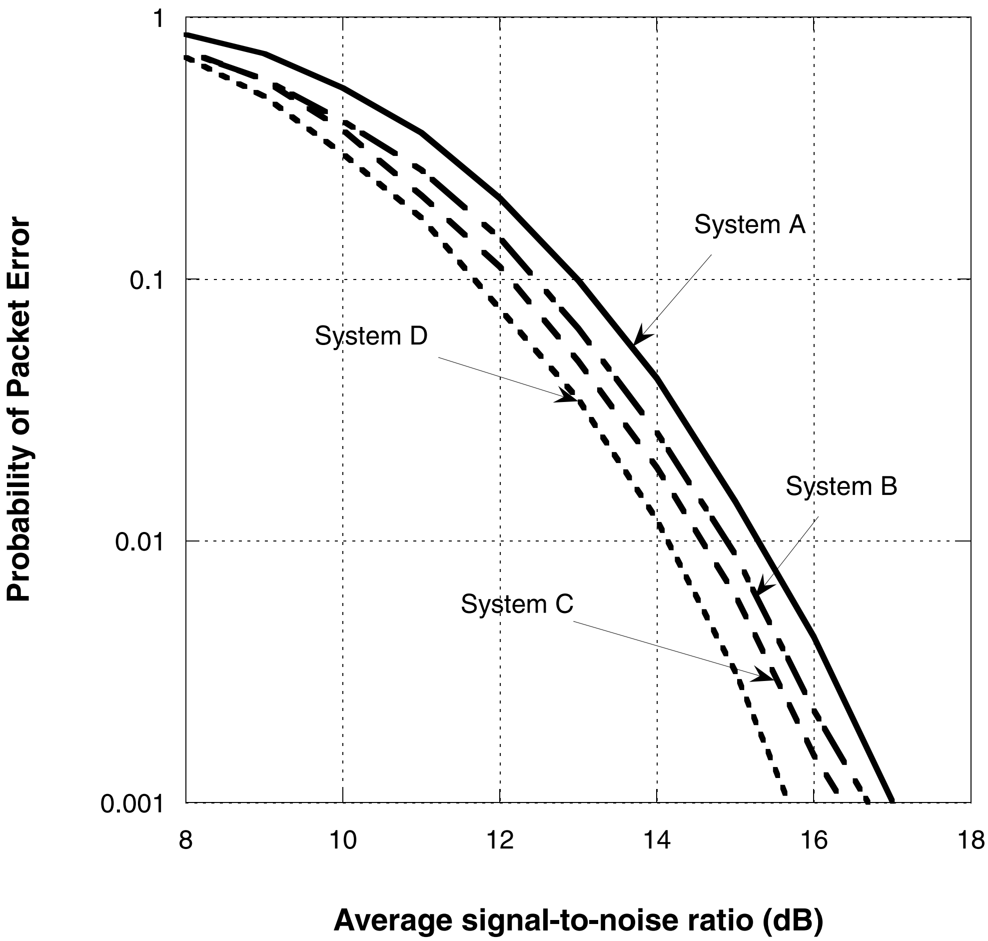

Figure 4.19 Probability of packet error with two-path Rayleigh-fading channel and (64,32) R-S code.

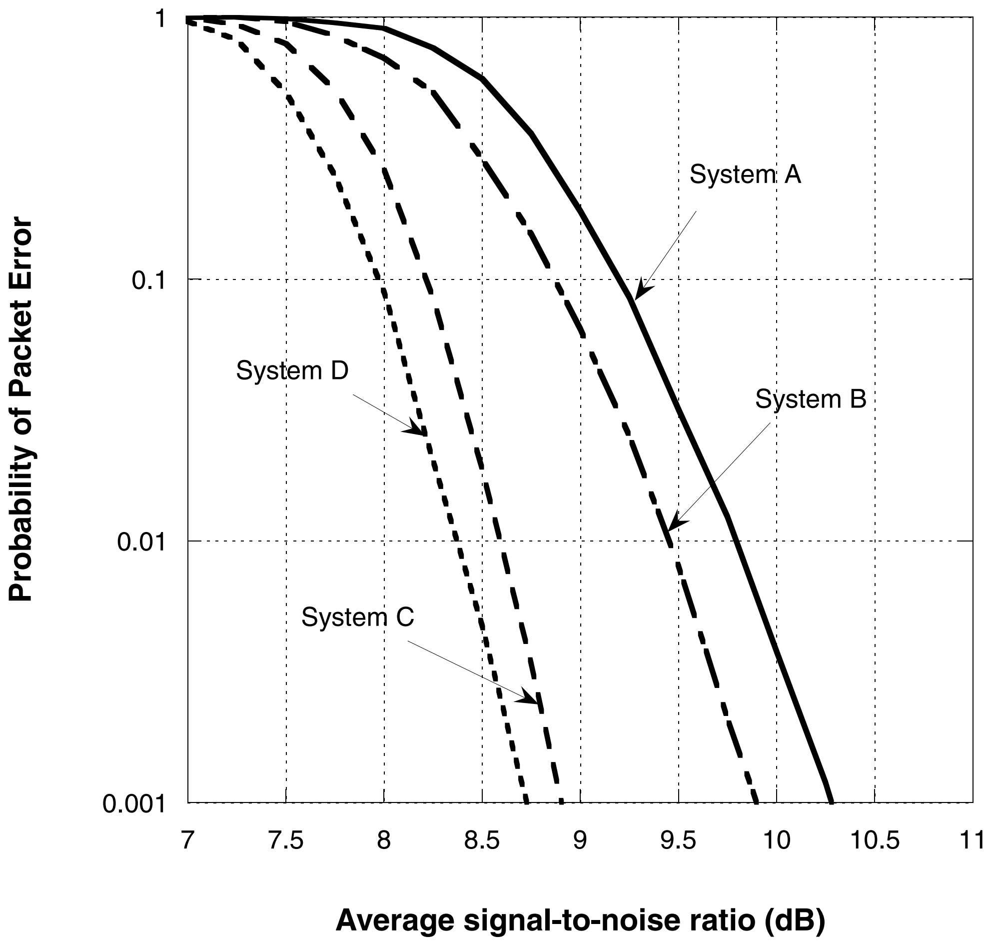

Figure 4.20 Probability of packet error with two-path static channel and (32,20) R-S code.

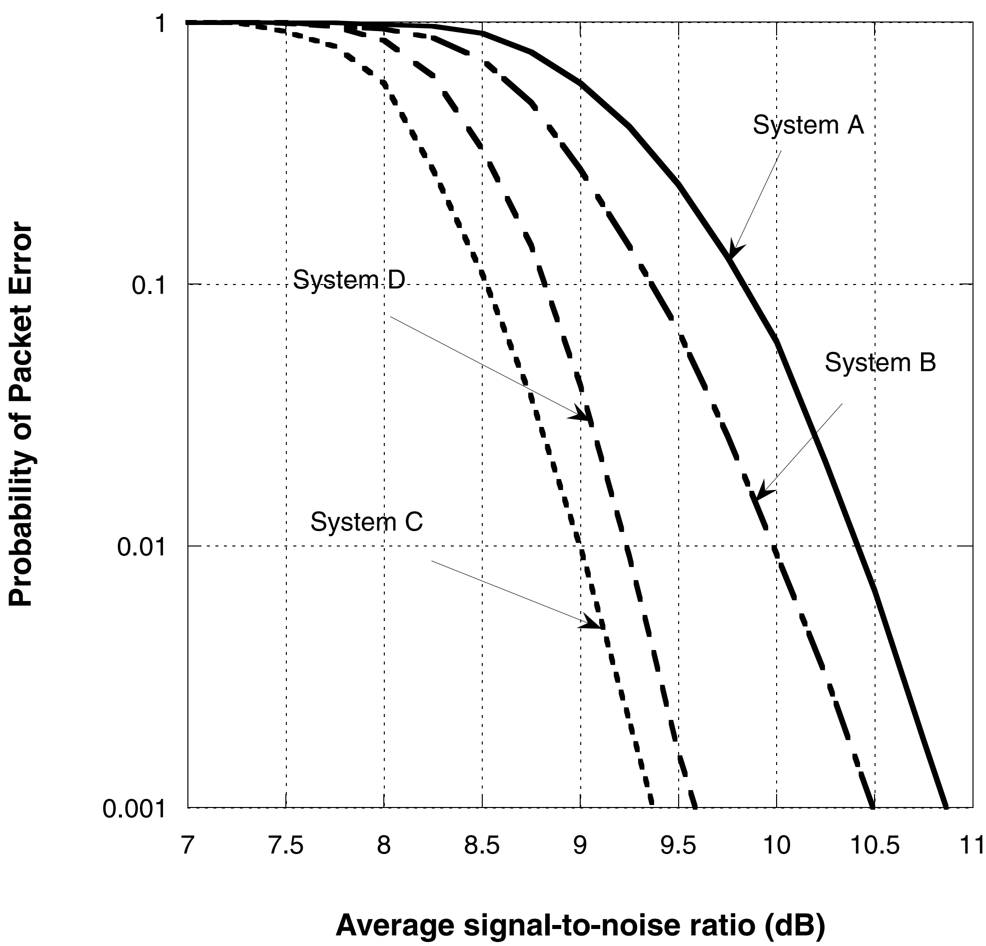

Figure 4.21 Probability of packet error with two-path static channel and (32,12) R-S code.

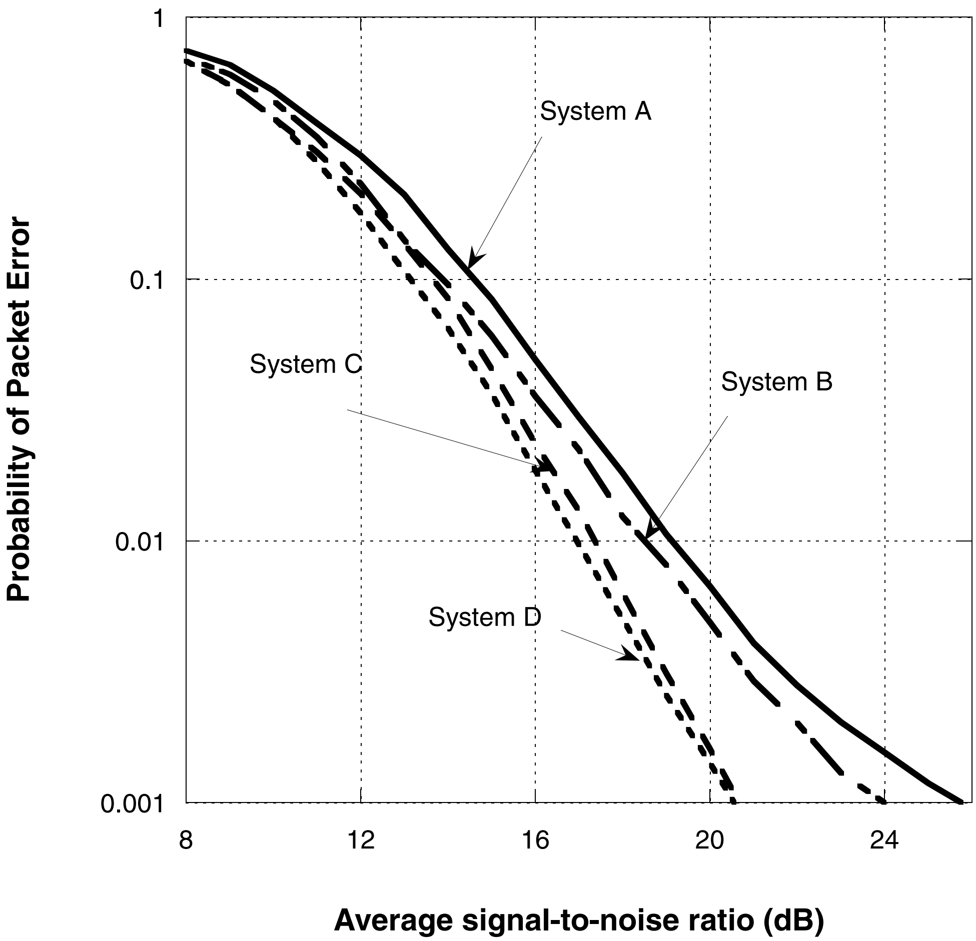

Figure 4.22 Probability of packet error with two-path Rayleigh-fading channel and (32,20) R-S code.

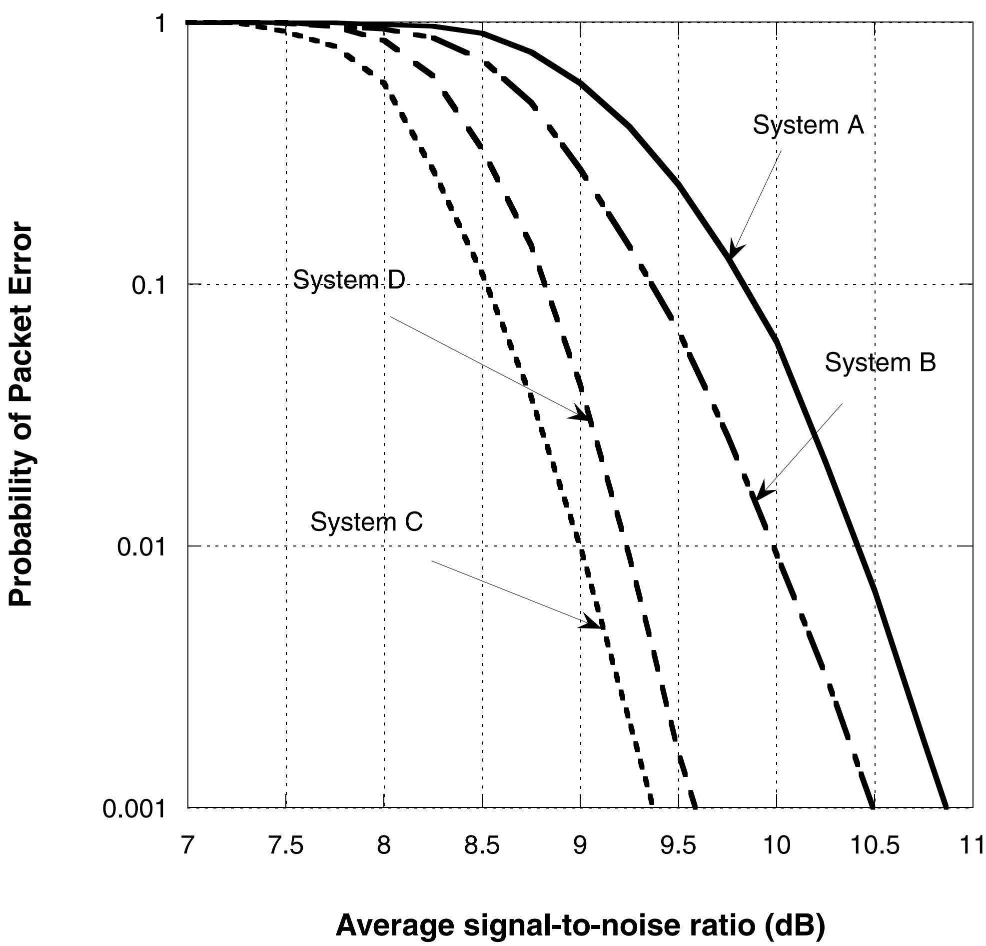

Figure 4.23 Probability of packet error with two-path Rayleigh-fading channel and (32,12) R-S code.

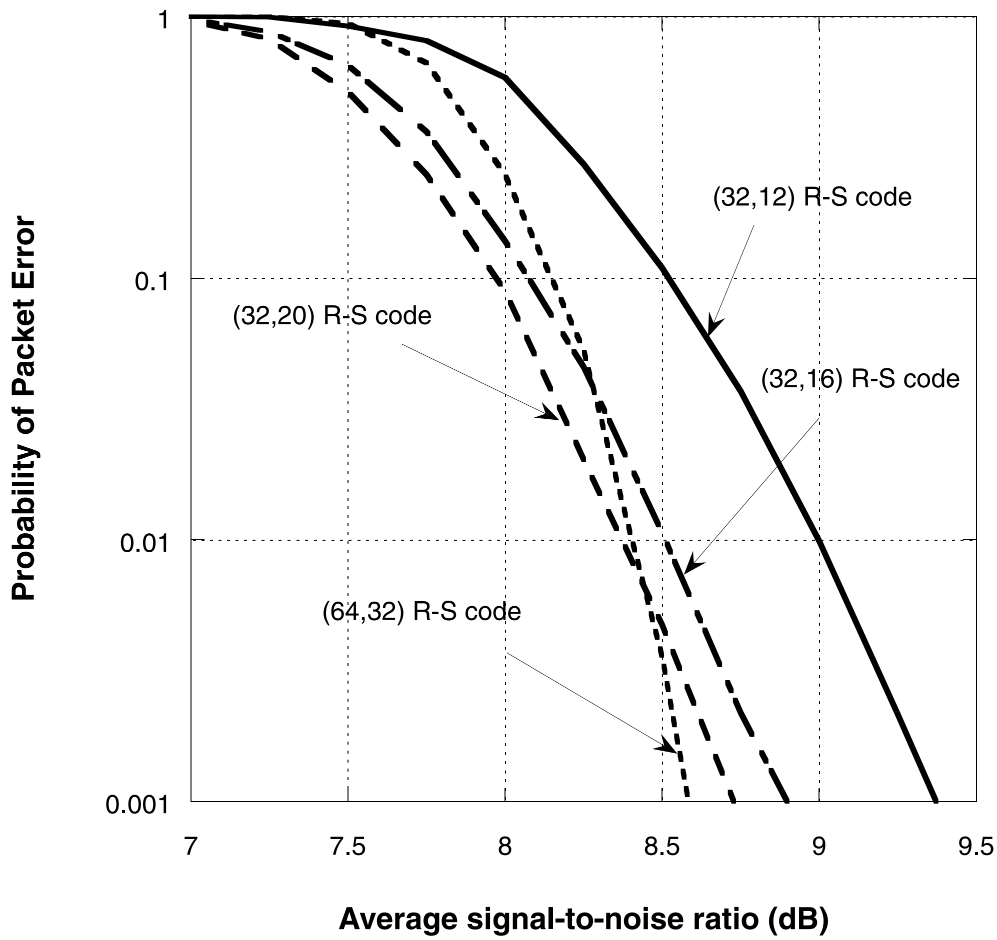

Figure 4.24 Probability of packet error for system D with two-path static channel and various R-S codes.

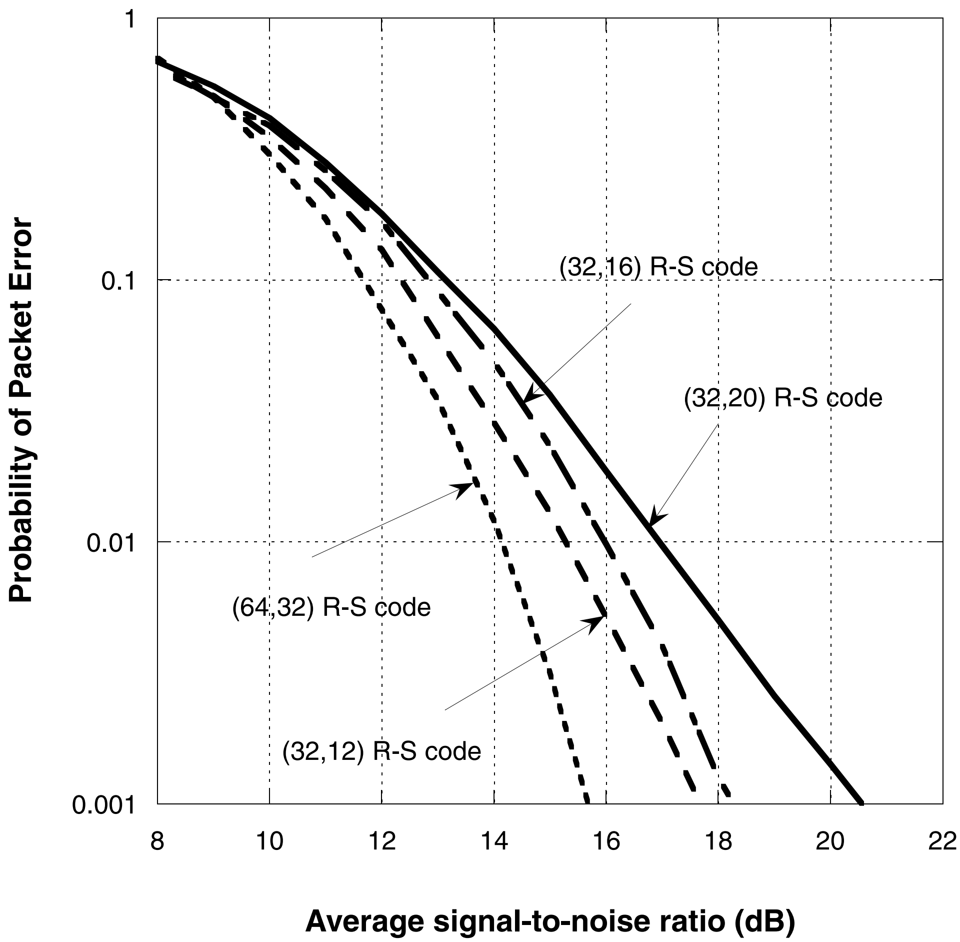

Figure 4.25 Probability of packet error for system D with two-path Rayleigh-fading channel and various R-S codes.

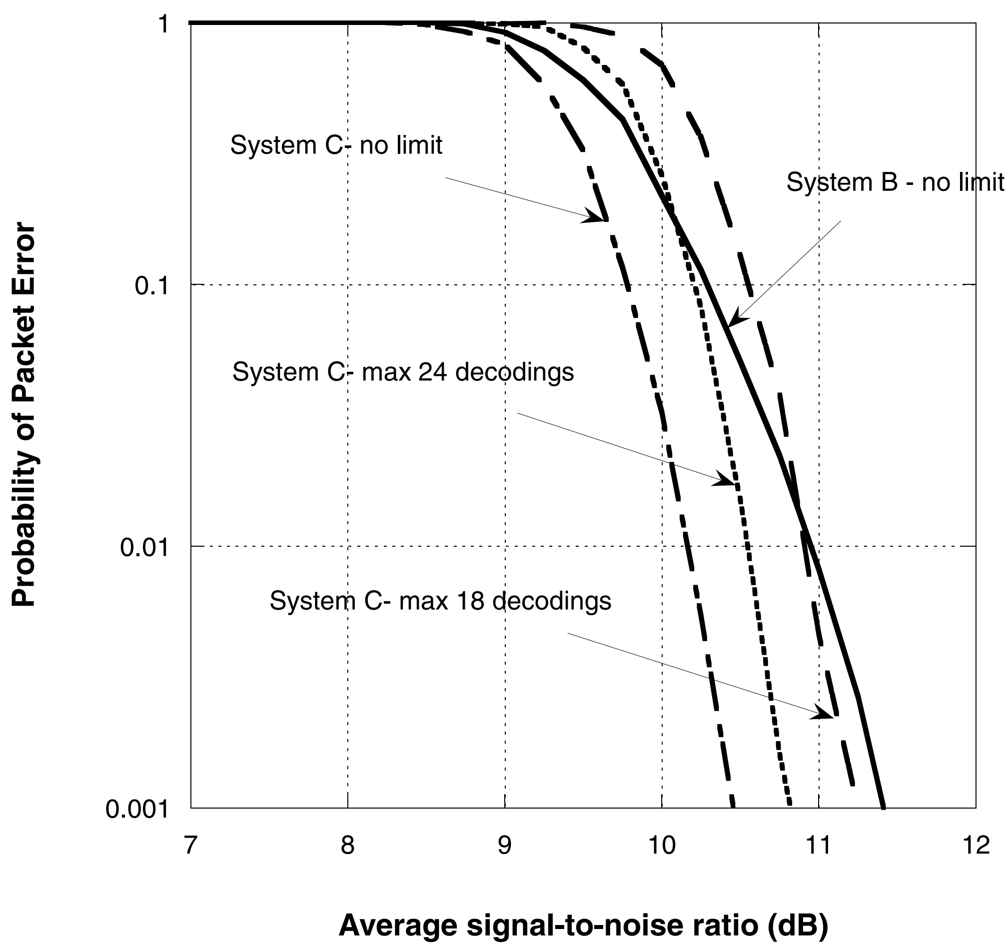

Figure 4.26 Probability of packet error with three-path static channel and limit on decoding delay.

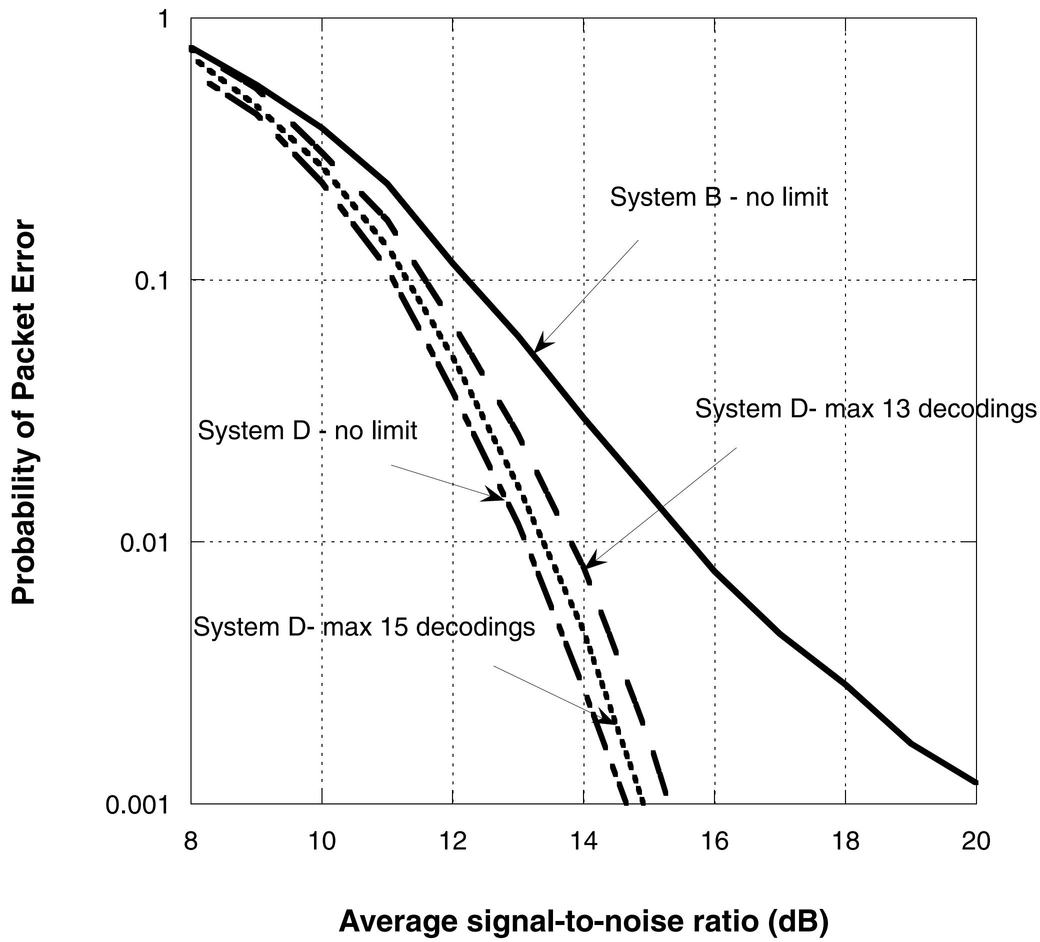

Figure 4.27 Probability of packet error with four-path Rayleigh-fading channel and limit on decoding delay.

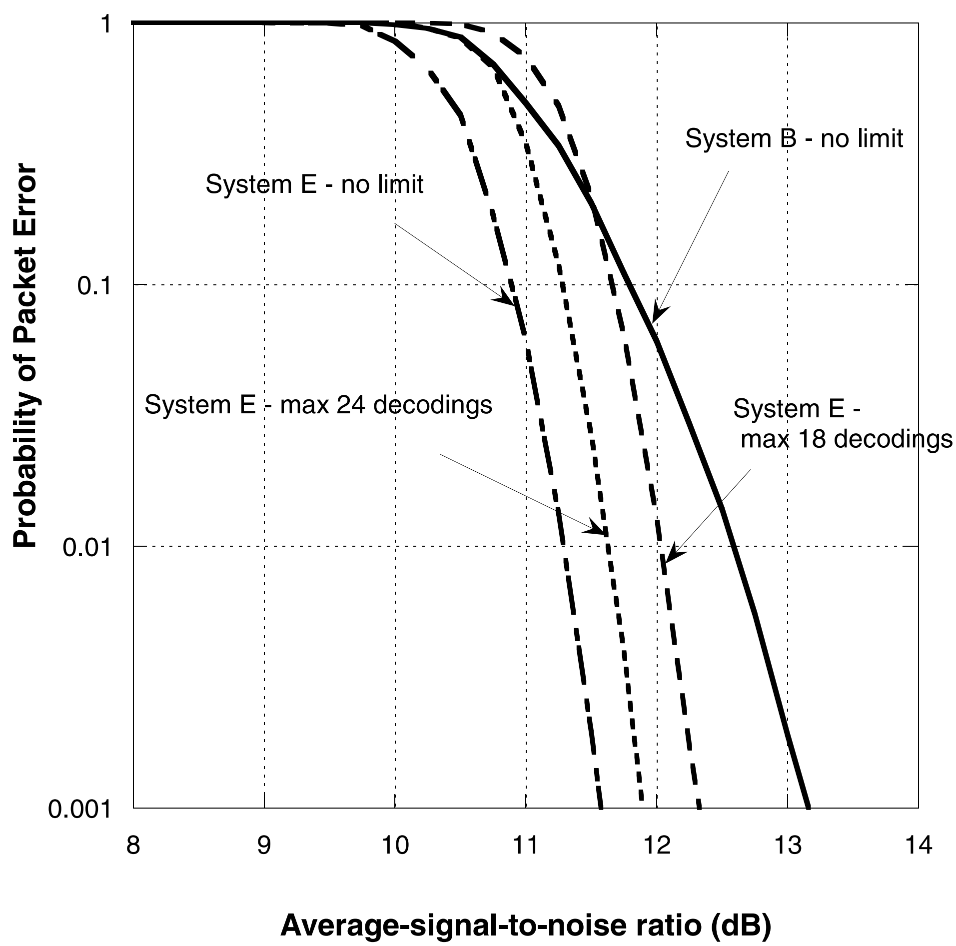

Figure 4.28 Probability of packet error with four-path static channel and limit on decoding delay.

CHAPTER 5

DIFFERENTIAL ENCODING IN SFH SYSTEMS WITH PACKET-LEVEL ITERATIVE DETECTION

5.1 Description of the SFH System with Differential Encoding

Each of the SFH systems considered in the previous chapter employs a transmission format in which the binary content of each row of a block interleaver is transmitted using BPSK modulation. Consequently, the transmitted binary sequence for a dwell interval exhibits memory only as a result of the parity constraint on the bits forming the representation of a given R-S code word. In system D, in particular, rectangular block code-symbol interleaving is followed by a form of pseudo-random binary interleaving within each row of the interleaver block.

In this chapter we consider a modification of system D in which the binary data contents of each row of the interleaver are differentially encoded prior to transmission using BPSK modulation. (Equivalently, the binary data contents of each row of the interleaver are transmitted using differential BPSK modulation.) The reference polarity for differential encoding in each row is determined by the polarity of the last bit of the training sequence in the corresponding dwell interval. The modified system is referred to as *system J*. The use of differential encoding in system J introduces additional memory into the transmitted sequence for each dwell interval.

The transmitter for system J is shown in Figure 5.1. Thus for a packet transmitted starting at time $t = 0$, the transmission is given by

$$s(t) = \sqrt{2P} \sum_{i=0}^{n-1} \sum_{j=0}^{N_t+(m+1)N_s-1} (-1)^{d_{i(N_t+(m+1)\ N_s)+j}}$$
$$\times p_T(t - (i(N_t + (m+1)\ N_s + N_e) + j)T) \cos(j2\pi f_i t + \phi_i). \qquad (5.1)$$

The preamble sequence for the ith dwell interval is given by $\{d_{i(N_t+(m+1)\ N_s)+j}\}$, $0 \leq j \leq N_t - 1$. The differentially encoded binary data for the ith dwell interval is given by $d_{i(N_t+(m+1)\ N_s)+j} = d_{i(N_t+(m+1)\ N_s)+j-1} \oplus b_{i(N_t+(m+1)\ N_s)+j}$ for $N_t \leq j \leq N_t + (m+1)N_s - 1$, where $b_{i(N_t+(m+1)\ N_s)+j}$ is the jth bit of the ith row of the interleaver block. The rest of the terms in equation (5.1) are as defined in Chapter 4 for equation (4.1).

The transmission occurs over the multipath, fading channel described in Chapter 3. The *signal-to-noise ratio* at the receiver is defined as in equation (4.2) in Chapter 4. No interference process appears at the receiver for the results presented in this chapter.

The receiver for system J employs the same technique with system D in the previous chapter, that is, packet-level iterations of MLSE equalization and bounded-distance EE. It is thus shown in Figure 4.2 with all of the dashed boxes included. The labeling of the equalizer trellis for each dwell interval is modified to account for differential encoding, however. This is illustrated in Figure 5.2, which shows the structure of a two-state equalizer trellis for a given dwell interval at the receivers of system D and system J. The vector (h_0, h_1) here represents the receiver's estimate of the channel's baseband-equivalent discrete-time impulse response.

In the absence of differential encoding, as in system D, the receiver's equalizer trellis for the estimated two-state channel is labeled as shown in Figure 5.2 (a). The branch label for each state transition has the form b_l/x, where b_l is the corresponding polarity of the lth bit (a data bit) in the transmitter's interleaver block and x is the normalized expected (noise-free) received sample value for the corresponding polarity b_l and channel state. If instead the differential encoding of system J is used, the equalizer trellis is labeled as shown in Figure 5.2 (b). Each branch label has the form $b_l/d_l/x$, where b_l

and x are as before and d_l is corresponding polarity of the lth differentially encoded bit.

Within each packet-level iteration, detection of the binary contents of each row of the block interleaver and EE decoding of each R-S code word are performed in a similar manner in the receivers of system D and system J. They differ only in the binary label sequence (the detected sequence) for a given survivor path in the dwell interval's trellis after Viterbi equalization. Equivalently, the two receivers can be viewed as detecting the same channel-symbol sequence for a given survivor path but with differential decoding subsequently applied to the hard-decision output in the receiver of system J.

The introduction of differential encoding in system J alters the manner in which the equalizer uses feedback information in the second and subsequent packet-level iterations. For each code word that has been decoded successfully in an earlier iteration, knowledge of the corresponding code symbols determines the polarities of the bits in the corresponding binary representation of the code symbols prior to differential encoding. Thus in subsequent iterations, the equalizer for a given dwell interval restricts the Viterbi algorithm in a manner that can be expressed as a restriction to a subset of trellis *branches* at some time steps. Hence the technique employed in conjunction with differential encoding is referred to as *branch pruning*.

Branch pruning in the trellis for a dwell interval is illustrated by considering the same two-state channel used as an example in chapter 4. The feedback ($b_1 = 1, b_2 = 0, b_4 = 1, b_5 = 0$), provided from successful decoding of R-S code words in previous packet-level iterations, results in the pruned trellis shown in Figure 5.3. This contrasts with the state-pinned trellis in Figure 4.4 that results from the same feedback in the system without differential encoding. Thus the effect of a R-S code word decision on the equalizer trellis in subsequent iterations differs for system D and system J. This is true even with a single-path channel, for which the detection trellis still contains two states in the system with differential encoding. Note that the state pinning used in systems without differential encoding can be viewed as a form of branch pruning, but the branch pruning used in systems with differential encoding cannot be described in terms of state pinning.

In this chapter (and in Chapter 6), we examine the effect that per-dwell differential encoding has on the performance of SFH communications with packet-level iterative detection by comparing the performance of system J with the performance of several of the SFH systems introduced in Chapter 4. The characteristics of each SFH system considered in this chapter are shown in Table 5.1.

System	Code-Symbol Interleaver	Bit Interleaver	Differential Encoding	Packet-Level Iteration
A	rectangular	none	no	no
B	rectangular	none	no	yes
D	rectangular	pseudo-random, per-dwell	no	yes
H	diagonal	none	no	no
I	diagonal	none	no	yes
J	rectangular	pseudo-random per-dwell	yes	yes

Table 5.1 Characteristics of SFH systems considered in Chapter 5.

5.2 Effect of Branch Pruning on Minimum Distance of Equalizer Trellis

The choice of whether or not to use differential encoding in the SFH system results in a tradeoff between the asymptotic performance of the system using one-shot detection and the asymptotic performance of the system using packet-level iteration. This is illustrated by considering the asymptotic performance of systems D and J in a single-path AWGN channel in which the receiver is provided with a perfect estimate of the channel in each dwell interval. The minimum squared Euclidean distance among error events at the receiver is four in either system, but there are two minimum-distance error events with respect to b_k rather than one in the system with differential encoding. Thus the asymptotic probability of error in the detection of b_k is twice as great in system J as in system D. Consequently, the asymptotic probability of packet error is greater for system J than for system D by a multiplicative factor that approaches $2^{d_{\mathrm{RS}}}$, where d_{RS} is the minimum distance of the R-S code. The penalty in decibels that this factor represents approaches zero asymptotically, as the signal-to-noise ratio approaches infinity for a given packet size and code rate, however.

For all subsequent packet-level iterations in system D, the minimum squared Euclidean distance of an error event associated with an unknown bit b_k is equal to four regardless of known polarities that have been fed back for other data bits in the same dwell interval. In contrast, branch pruning due to feedback of known bit polarities in system J alters the Euclidean distances of the two-state detection trellis for each dwell interval during the subsequent iteration. This is made clear by considering the representative time step shown in Figure 5.2 (b).

It is apparent that if the branches are pruned to reflect a known bit polarity, no error event can begin at the starting state of the time step and no error event can end at the ending state of the time step. Moreover, the time step must contribute a value of four to the squared Euclidean distance for any error event that encompasses the time step. Consequently, if a differentially encoded bit b_k is unknown but the differentially encoded bits labeling the immediately preceding L_1 and immediately succeeding L_2 trellis steps are provided as feedback, the minimum squared Euclidean distance to an associated error event for the unknown bit in the branch-pruned trellis is given by

$$d_{\min}^2 = (4 + 4\min\{L_1, L_2\}). \tag{5.2}$$

(If it is the first unknown bit position in the dwell interval, then $L_1 = \infty$.)

If most R-S code words in a packet have been decoded successfully in the previous iterations, the trellis positions of the remaining unknown bits are usually well separated due to interleaving. Thus a large effective minimum distance is achieved for these bits in subsequent sequence detection using the pruned trellis. The asymptotic performance is dominated by outcomes in which decoding failure occurs for a single code word in the packet, in which case the effective minimum squared distance is exactly 4 N_s for each remaining unknown bit. It can be shown that the introduction of differential encoding and packet-level iteration results in an improvement in performance that approaches 10 $\log_{10}(N_s)$ dB as the probability of packet error approaches zero. Moreover, the detection complexity asymptotically approaches $(N_s + 1)/N_s$. Consequently for a given joint distribution function of the samples from the channel, the introduction of differential encoding and packet-level iteration results in an arbitrarily large asymptotic performance gain at a vanishingly small asymptotic penalty in detection complexity.

The systems with and without differential encoding also differ in their equalizer distance properties for the second and subsequent iterations if the channel has multiple paths. This is illustrated by considering a two-path equal-strength static channel with $h_0 = h_1 = 1/\sqrt{2}$, where once again, it is assumed that the receiver used a perfect estimate of the channel in each dwell interval. In the system without differential encoding, the effect of a known bit polarity on the distance spectrum of the equalizer trellis is deterministic. From Figure 5.2 (a), it is apparent that the two branches that remain after one of the two states is pinned are at a squared Euclidean distance of two.

In the system with differential encoding, in contrast, the effect of a known bit polarity on the distance spectrum depends on the polarity in general, and hence, it is probabilistic. From Figure 5.2 (b), the two branches that remain after branch pruning are at a squared Euclidean distance of eight if the known data bit is a zero for the example two-path channel, but they are at a distance of zero if the known data bit is a one.

Now consider the general two-path static channel (h_0, h_1). For an unknown bit b_k in the equalizer trellis, consider the circumstance in which the polarities of the L_1 preceding bits and L_2 succeeding bits in the dwell interval have been provided as feedback from an earlier iteration of equalization and decoding. (Recall that this refers to the polarities of the bits prior to differential encoding b_k rather than the polarities of the channel symbols d_k.) In the following development we assume the bit polarities are independent and equally likely *a priori*. We define the random variables

$$X_1 = \sum_{i=k-L_1}^{k-1} b_i$$

and

$$X_2 = \sum_{i=k+1}^{k+L_2} b_i$$

which are independent. Each has a binomial distribution. I.e.,

$$\Pr(X_1 = i) = \binom{L_1}{i} \left(\frac{1}{2}\right)^{L_1} \tag{5.3}$$

and

$$\Pr(X_2 = i) = \binom{L_2}{i} \left(\frac{1}{2}\right)^{L_2}. \tag{5.4}$$

Consider the stage of the equalizer trellis illustrated in Figure 5.3. Again, if an error event results in a detection error for b_k, either the error event terminates in time step k or it originates in time step k. Let Z_1 denote the minimum squared Euclidean distance among error events terminating in time step k (within the constraint of the branch pruning in the L_1 preceding time steps). Let Z_2 denote the minimum squared Euclidean distance among error events originating in time step k (within the constraint of the branch pruning in the L_2 succeeding time steps). Then Z_1 and Z_2 are independent, and

$$\begin{aligned} Z_1 &= 4(|h_0|^2 + |h_1|^2) + 4|h_0 - h_1|^2 \times X_1 + 4|h_0 + h_1|^2 \times (L_1 - X_1) \\ &= 4\left[1 + |h_0 + h_1|^2 \times L_1\right] + 4 \times X_1 \left[|h_0 - h_1|^2 - |h_0 + h_1|^2\right] \end{aligned}$$

and

$$Z_2 = 4\left[1 + |h_0 + h_1|^2 \times L_2\right] + 4 \times X_2 \left[|h_0 - h_1|^2 - |h_0 + h_1|^2\right].$$

For the single-path channel this simplifies to

$$Z_1 = 4\left[1 + L_1\right]$$

and

$$Z_2 = 4\left[1 + L_2\right].$$

Note that for this special case, Z_1 and Z_2 don't depend on the polarities of the known bits. In contrast, for the channel with two equal-strength paths and baseband-equivalent impulse response ($h(D) = \frac{1}{\sqrt{2}} + \frac{1}{\sqrt{2}} D$),

$$Z_1 = 4\left[1 + 2 \times L_1\right] - 8 \times X_1$$

and

$$Z_2 = 4\left[1 + 2 \times L_2\right] - 8 \times X_2.$$

The first two moments of random variables Z_1 and Z_2 are given by

$$E[Z_1] = 4 + \left(4|h_0 - h_1|^2 + 4|h_0 + h_1|^2\right) \times L_1/2,$$

$$E[Z_2] = 4 + \left(4|h_0 - h_1|^2 + 4|h_0 + h_1|^2\right) \times L_2/2,$$

$$\text{Var}[Z_1] = 64L_1|h_0|^2|h_1|^2$$

and

$$\text{Var}[Z_2] = 64L_2|h_0|^2|h_1|^2.$$

The effective minimum squared Euclidean distance for b_k is thus a random variable given by $Z = \min\{Z_1, Z_2\}$. Without loss of generality, we can assume that $L_1 \leq L_2$. From the Chebyshev inequality it follows that

$$\begin{aligned} \Pr\left(Z < (1-\eta)\, E[Z_1]\right) &\leq \frac{\text{Var}[Z_1]}{\eta^2 E[Z_1]^2} \\ &\leq \frac{16(|h_0|^2|h_1|^2)}{(|h_0 - h_1|^2 + |h_0 + h_1|^2)^2 L_1 \eta^2}, \end{aligned}$$

and thus $\Pr\{Z < (1-\eta)\; E[Z_1]\}$ approaches zero as $L_1 \to \infty$ for any $\eta > 0$. Furthermore, $\lim_{L_1 \to \infty} E[Z_1] = \infty$. Thus the effective minimum distance approaches infinity stochastically as $\min\{L_1, L_2\}$ approaches infinity. This is in sharp contrast with the SFH system that does not employ differential encoding, for which the effective minimum distance with any ISI channel never exceeds the minimum distance achieved for one-shot detection with a single-path channel. Consequently, if the packet size is large enough and the signal-to-noise ratio is high enough to ensure that most code words in the packet are decoded during the first iteration with a high probability, the minimum distance among error events with respect to most remaining unknown bits is large in the second and subsequent packet-level iterations of equalization and decoding. This in turn contributes to a high probability of decoding of the remaining code words in the later iterations and a correspondingly low probability of packet detection failure.

Similar results can be shown for the equalizer of the SFH system employing differential encoding and packet-level iteration with ISI channels of more than two paths. Specifically, it can be shown for any L-path channel the effective minimum distance of error events corresponding to an unknown bit b_k approaches infinity stochastically as the value of $\min\{L_1, L_2\}$ approaches infinity.

5.3 Evaluation of Performance for SFH System with Differential Encoding

In this section, we evaluate the performance of SFH systems B, D and J for a variety of static and fading channels. (Recall that the system which uses packet-level MLSE equalization and bounded-distance EE decoding, but no bit interleaving and differential encoding is denoted system B. The modification of system B that include pseudo-random bit interleaving within each dwell interval is denoted system D. The system which employs pseudo-random bit interleaving in each dwell interval and differential encoding along with packet-level iterative detection is denoted system J). The measures of performance and detection complexity are defined in Section 4.3. In the results in this section, no limit is placed on the number of EE decoding attempts per packet (other than the limit inherent in the packet-level iterative technique).

A (32,16) R-S code is considered in each of the examples, except where otherwise noted. We focus on three packet sizes for use with the (32,16) code: a small packet consisting of 12 code words, a medium-sized packet consisting of 100 code words and a large packet consisting of 500 code words. (A packet size of 25 code words is also considered in one example.) For the small packet size there are 960 information bits per packet. Each dwell interval contains a preamble sequence of 26 bits. Since there are twelve code symbols in each dwell interval and an extra bit of parity is added to each code symbol there are 98 binary channel symbols in each dwell interval (including the preamble sequence). Each medium-sized packet contains 8000 information bits and each dwell interval contains a preamble sequence of 217 bits, so there are 817 binary channel symbols in each dwell interval. For the large packet size, there 40,000 bits of information in each packet. Each dwell interval contains a preamble sequence of 1085 bits, so that there are 4085 binary channel symbols in each dwell interval. Thus the three packet formats have the same efficiency. The dwell transmission takes place over 32 dwell intervals. The carrier frequency for SFH transmission hops over the available frequency slots in the spectrum according to a random hopping pattern. The number of available frequency slots is 440.

5.3.1 Performance in an AWGN channel

The performance of systems B, D and J is shown in Figure 5.4 for a single-path static (AWGN) channel and the small packet size. For a probability of packet error of 0.01, system J results in a performance improvement of 0.42 dB over system D and system J results in an improvement of 0.48 dB over system B. Thus the addition of differential encoding to bit interleaving within a dwell interval results in a noticeable improvement in the performance of packet-level iterative detection.

One-shot packet-level detection serves as the benchmark for detection complexity, since it requires one EE decoding attempt per R-S code word. An average of 1.002 EE decoding attempts per code word is required to achieve a probability of packet error of 0.01 in system B for the single-path static channel. For the same probability of packet error, the detection complexity of system D is given by an average of 1.0024 EE decoding attempts per code word. The complexity increases to an average of 1.78 EE decoding attempts per code word if system J is used instead. Thus the performance improvement that system J provides over systems B and D is achieved at the cost of an increase in the detection complexity of approximately 78% compared with the other two systems.

The value of differential encoding is exploited only if the receiver uses iterative detection, as is illustrated in Figure 5.5. In the figure, the performance of systems D and J is shown for the single-path static channel, the small packet size, and either of two implementations of the corresponding receiver. One implementation employs packet-level iterative detection with no constraint on the number of packet-level iterations. The other implementation constrains the receiver to a single iteration; that is, the receiver employs one-shot detection.

The performance of system J (using differential encoding) is nearly 1.2 dB poorer than the performance of system D (without differential encoding) for a probability of packet error of 0.01 if the receivers use one-shot detection. This is a consequence of the memory introduced by differential encoding and the consequent increase in the probability bit error after differential decoding. Packet-level iterative detection is of benefit in system D for this channel only because of its mitigating effect on the channel-estimation error at the receiver. Thus the performance of system D with packet-level iterative detection exhibits an improvement of only 0.2 dB compared with one-shot detection. Packet-level iteration exploits the memory of differential encoding effectively, however, and the performance of system J is thus improved by 1.85 dB if packet-level iterative detection is used in place of one-shot packet-level detection. Consequently, the performance of system J is better than the performance of system D if packet-level iterative detection is used.

System J achieves a substantial asymptotic performance improvement at a small asymptotic complexity cost compared with systems not employing differential encoding for a single-path channel, as is suggested in Figure 5.4. The performance of system J improves relative to the performance of systems B and D as the signal-to-noise ratio increases and the cost in detection complexity decreases as the signal-to-noise ratio increases. For a probability of packet error of 0.1, the performance of system J is only 0.27 dB better than the performance of system B and the average detection complexity of the former is 2.34 times that of the latter. For a probability of packet error of 0.01, however, the performance improvement increases to 0.48 dB and the average detection complexity decreases is only 1.78 times that of system B. System J provides a performance improvement of 0.68 dB for a probability of packet error of 0.001, and the average detection complexity is 1.41 times the detection complexity of system B. The improvement in performance with system J is 0.90 dB and the detection complexity is only 1.33 times that of system B if the probability of packet error is 10^{-4}.

It is noted in Section 5.2 that for a given packet size, a single-path channel, and ideal channel estimation, differential encoding and packet-level iteration provide an asymptotic improvement over the performance of one-shot detection that increases without bound as the packet size increases. Since the performance of packet-level iteration without differential encoding is no better than that of one-shot detection with ideal channel estimation for a single-path channel, comparable conclusions hold with respect to the asymptotic performance of system J versus that of systems B and D. This is supported by Figure 5.6, in which the performance of systems D and J is shown for the single-path static channel and the small, medium-sized and large packet sizes.

If ideal channel estimates were employed by the receiver, code-symbol decisions in system D would be independent for a single-path channel and the probability packet error would be an increasing function of the packet size. This occurs in practice even though there are channel-estimation errors, as seen in Figure 5.6. In contrast, an increase in the packet size increases the number of known bits that may surround each unknown bit in the trellis after feedback of detected code words in the system with differential encoding. The resulting stochastic increase in the effective minimum distance for unknown bits in the trellis leads to an asymptotic improvement in the probability of packet error with increasing packet size for system J. This is observed in practice at error probabilities of interest, as is also seen in Figure 5.6.

For the small packet and a probability of packet error of 0.01, the performance of system J is 0.42 dB better than the performance of system D, but it increases the detection complexity from an average of 1.0024 EE decoding attempts per code word to an average of 1.78 EE decoding attempts per code word. For the medium-sized packet the improvement in performance of system J over system D is 1.3 dB, and for the large packet the improvement in performance is 1.65 dB. The detection complexity for system J is 2.94 and 3.744 EE decoding attempts respectively per R-S code word at this packet error probability. The corresponding complexity for system D is 1.0002 and 1.00004 EE decoding attempts per code word.

5.3.2 Performance in a Multipath Channel

The performance of systems B, D and J in shown in Figure 5.7 for the small packet size and a two-path static channel. The delays of the two paths are 0 and T, and the second path has magnitude one-half that of the first path. (Thus the channel's impulse response is characterized by the polynomial $h(D) = 1 + 0.5\ D$.) The figure also illustrates the performance of system J with the medium-sized packet. Once again, the performance of system J is superior to the performance of either system B or system D for a probability of packet error of 0.01. For a probability of packet error of 0.01, system B requires an average of 1.002 EE decoding attempts per code word. For the same probability of packet error, system D results in a performance improvement of 0.6 dB over system B at the cost of an average of 1.033 EE decoding attempts per code word. System J results in a performance improvement of 0.75 dB over system B but requires an average of 1.68 EE decoding attempts per code word. For the same probability of packet error, system J with the medium-sized packet results in a performance improvement of 1.4 dB over system B with the small packet size, but the improvement is achieved at the cost of an average of 2.75 EE decoding attempts per code word. It is apparent from Figure 5.7 that the comparison favors system J more highly if it is based on a lower probability of packet error, as was observed above for the single-path channel.

The performance of the SFH systems is shown in Figure 5.8 for a two-path static channel with equal-strength paths. The path delays are 0 and T. As observed previously in Chapter 4 for this channel, system D results in a performance improvement of 1.05 dB over system B for a probability of packet error of 0.01 and the small packet size. There is a corresponding increase in the average number of EE decoding attempts per code word from 1.0047 to 1.43. For the same probability of packet error and packet size, system J results in a performance improvement of 0.8 dB over system B at a cost of an average of 1.57 EE decoding attempts per code word. Also shown in the figure is the performance of system J with the medium-sized packet. The performance of system J with the medium-sized packet results is 1.4 dB better than the performance of system B with the small packet. The detection complexity for system J and this packet size is an average of 2.72 decoding attempts per code word, however. Once again, the comparison is more favorable towards system J if a probability of packet error of 0.001 is considered.

The performance comparison of SFH systems A, B, D and J is shown in Figure 5.9 for the three-path static channel that results in the poorest asymptotic performance of one-shot MLSE equalization. I.e., it is the three-path channel that results in the smallest minimum distance among paths in the equalizer trellis for a given total power in the channel. The impulse response of the channel is characterized by the polynomial $h(D) = 0.5 + (\sqrt{2})^{-1}\ D +$

0.5 D^2. Once again, the performance of each system is considered for a probability of packet error of 0.01. System B results in a performance improvement of 0.7 dB over system A at the cost of an average of 1.016 EE decoding attempts per code word if both use the small packet size. System D has a detection complexity of an average of 1.5 EE decoding attempts per code word for the same packet size, and the performance is 0.7 dB better than that of system B. System J with the small packet results in a performance improvement of 0.75 dB over system B (and an improvement of 1.4 dB over system A) at the cost of an average of 1.56 EE decoding attempts per code word. Thus is results in nearly identical performance to system D with a nearly identical detection complexity. If instead the medium-sized packet is used with system J, however, its performance improvement is 1.45 dB better than the performance of system B with the small packet (and 2.1 dB better system A with the small packet size) . The cost of this performance gain is an average of 3.05 EE decoding attempts per R-S code word.

Figure 5.10 illustrates the performance of systems B, D and J with the small packet size for a static channel consisting of three equal-strength paths with delays of 0, T and $2T$. The performance of system D with the medium-sized packet is also shown. For a probability of packet error of 0.01, system D results in a performance improvement of 0.95 dB over system B. System D requires an average of 1.59 EE decoding attempts per code word at this error probability, and system B requires an average of 1.007 EE decoding attempts per code word. For the same probability of packet error, the performance of system J with the small packet is only 0.4 dB better than the performance of system B even though its detection complexity is 1.46 EE decoding attempts per code word. If the medium-sized packet is used in system J, however, its performance is 1.25 dB better than the performance of system B with the small packet. The cost in complexity for system J in this instance is an average of 3.05 EE decoding attempts per code word.

A similar comparison is provided in Figure 5.11 for a four-path static channel is made The paths have equal strength, and the path delays are 0, T, $2T$ and $3T$. Use of the small packet with system J results in a performance improvement of only 0.6 dB over system B with the small packet for a probability of packet error of 0.01. The complexity is increased from an average of 1.0041 EE decoding attempts per code word for system B to an average of 1.52 decoding attempts per code word for system J. In contrast, system D with the small packet achieves performance that is 1.15 dB better than system B at a cost in complexity of an average of 1.56 decoding attempts per code word. Thus for this channel and the small packet size, system D (without differential encoding) results in much better performance than system J (with differential encoding) even though the detection complexity is similar for the two systems. If instead the medium-sized packet is used in system J, its performance is 1.4 dB better than that of system B with the small packet, though the detection complexity increases to an average of 2.72 EE decoding attempts per code word. Thus system J with the medium-sized packet achieves a small performance improvement over system D with the small packet, but the former has a complexity that is 75% greater than the latter.

From these examples it is clear that even though the use of differential encoding and packet-level iteration provides an asymptotic gain in performance for any static multipath channel, the gains are realized more readily in a static channel if the channel does not have a large delay spread. For a channel with a delay spread of no more than twice the channel-symbol duration, system J achieves better performance than system D even if a small packet size is used with system J. Moreover, the cost in increased complexity is small. Large improvements in performance can be obtained by increasing the packet size in system J (up to a point), though at a cost in increased detection complexity.

For a channel with a delay spread on the order of a few times the channel-symbol duration, system J provides better performance than system D at error probabilities of practical interest only if the packet size of system J is increased sufficiently. Even then, the performance gain is only obtained at the cost of a significant increase in the detection complexity. Furthermore, it is likely that for channels with a sufficiently large delay spread, system J will not achieve comparable performance to system D with the small packet size, regardless of what packet size is used with system J. We have not considered channels with a delay spread sufficiently large to observe the latter phenomenon, however.

Differential encoding improves the performance of packet-level iterative detection over a much wider range of channel delay spreads if the channel exhibits fading. Furthermore, the performance gains are achieved at a small cost in detection complexity. This illustrated in Figure 5.12, which shows the performance of systems B, D and J using the small packet size for a Rayleigh-fading channel that consists of two paths with equal average power. The path delays are 0 and T, and the normalized Doppler spread of the channel is 1.5×10^{-4}. The performance of system J is superior to both system B and system D for a probability of packet error of 0.01. System D results in an improvement in performance of 0.85 dB over system B with a minimal increase in the detection complexity of an average of 1.007 EE decoding attempts per code word for system B. System J results in an improvement in performance of 1.3 dB over system B, with only a 3.6% increase in complexity to an average of 1.036 EE decoding attempts per code word.

In Figure 5.13, the performance of systems B, D and J is shown for a three-path Rayleigh-fading channel. The normalized Doppler spread of the channel is 1.5×10^{-4}, the paths have equal average power, and the path delays are 0, T and $2T$. For a packet error probability of 0.01, system D and system J both result in an improvement in performance of 1.0 dB over system B if all three system use the small packet size. At this probability of packet error, system B requires an average of 1.003 EE decoding attempts per code word, whereas system D require and average of 1.010 attempts and system J requires an average of 1.045 attempts. The performance of system J is improved if the small packet containing twelve R-S code words is replaced with a packet of twenty-five R-S code words. (The latter packet includes 2000 information bits. It has a preamble length of 55 bits, and thus each dwell interval consists of 205 binary channel symbols including the preamble.) The performance of system J with a packet size of $N_s = 25$ results in a performance improvement of 1.4 dB over system B with a detection complexity of an average of 1.08 EE decoding attempts per code word.

The performance of the same three systems with the small packet size is shown in Figure 5.14 for a four-path Rayleigh-fading channel with path delays at 0, T, $2T$, and $3T$ in Figure 5.14. The paths have equal average power, and the normalized Doppler spread of the channel is once again 1.5×10^{-4}. For a packet error probability of 0.01, system J results in performance that is 3.0 dB better than the performance of system B. The detection complexity increases from an average of 1.0009 EE decoding attempts per code word for system B to an average of 1.064 EE decoding attempts per code word for system J. For the same packet error probability, the performance of system D is 0.3 dB poorer than the performance of system J, though it requires an average of only 1.014 EE decoding attempts per code word.

Some multipath channels contain many more propagation paths in proportion to the delay spread of the channel than in the examples we have considered thus far, and such channels are said to have a "dense" delay spectrum. In general, the baseband-equivalent channel responses for frequency slots at a given frequency separation are less correlated if the channel of a given delay spread has a dense delay spectrum than if it has a sparse delay spectrum. We consider one example of a channel with a dense delay spectrum that consists of 41 paths with path delays space uniformly between 0 to $2T$, inclusive, and a normalized Doppler spread of 1.5×10^{-4}. Each path exhibits Rayleigh fading, and the paths have equal average power.

The performance of five SFH systems is shown in Figure 5.15 for the small packet size and the channel with the dense delay spectrum. The five systems include system A (which uses one-shot detection), system D and system J. They also include systems I and J, which employ diagonal code-symbol block interleaving. (Recall that system H uses one-shot detection and system I uses packet-level iterative detection.) The performance of each system is considered for a probability of packet error of 0.01. System H results in a performance improvement of 0.3 dB over system A, whereas system I results in a performance improvement of 0.7 dB over system A at the cost of an average of 1.002 EE decoding attempts per code word. System D results in a performance improvement of 1.25 dB over system A, and the detection complexity increases to an average of 1.0107 decoding attempts per code word. The performance of system J is 1.5 dB better than the performance of system A, and requires 1.1244 EE decoding attempts per code word on average. Thus system J achieves 0.25 dB better performance than system D, though at the cost of an 11% increase in the detection complexity.

The slight performance advantage of system J over system D in the Rayleigh-fading channels we have considered is preserved if the Doppler spread of the channel is increased. Moreover, the performance advantage of system J over system B increase markedly. This is illustrated by considering the three-path, Rayleigh-fading channel with path delays 0, T and $2T$; equal average power in the paths; and a normalized Doppler spread of the channel is given by $D_T = 6 \times 10^{-4}$. (This is the same channel that was considered in the example accompanied by Figure 4.17 in Chapter 4.)

The performance of systems B, D and J with the small packet size is shown for this channel in Figure 5.16. As noted in Chapter 4, system B suffers from an error floor at a probability of packet error of 0.03. In contrast, system D and J have a much lower error floor. For a probability of packet error of 0.01, system J results in a performance improvement of 0.4 dB over system D, though the detection complexity is increased from an average of 1.019 to an average of 1.1012 EE decoding attempts per code word.

5.3.3 Performance of the SFH Systems Employing Differential Encoding with Various R-S Codes

In this subsection, we consider the effect of the rate and the block length of the R-S code on the desirability of using differential encoding in a SFH system with packet-level iterative detection. Two R-S codes of block length 32 are considered in addition to the $(32, 16)$ code. They are a $(32, 12)$ R-S code and a $(32, 20)$ R-S code, and both are considered in conjunction with the small packet size of twelve code words. Thus there are 720 bits of information if the $(32, 12)$ code is employed and 1200 bits if the $(32, 20)$ R-S code is employed. The other parameters are the same for the systems using the $(32, 16)$ code with the small packet size.

The code of larger block length is a $(64, 32)$ R-S code. Both small packets of twelve code words and medium-sized packets of 100 code words are considered with the $(64, 32)$ code. Each packet contains 2304 and $19,200$ bits of information for the small packet and medium-sized packets, respectively. Each parity-encoded code symbol has a binary representation of seven bits. Each dwell interval contains 110 binary channel symbols with the small packet, including a preamble sequence of length 26. For the medium-sized packet, each dwell interval contains 917 binary channel symbols that include a preamble of length 217. There are 64 dwell intervals in each packet transmission, and there are 390 frequency slots in the SFH system. Note that the $(64, 32)$ R-S code has the same rate as the $(32, 16)$ R-S code, though the instantaneous information rate of the packet is slightly greater with the $(64, 32)$ code when the overhead of the transmission format is taken into account.

The performance of several SFH systems using the $(64, 32)$ code is shown in Figure 5.17 for a two-path static channel with equal-strength paths at delays of 0 and T. Systems B, D and J are considered. The results are consistent with those observed for the systems using the $(32, 16)$ code. In particular, the packet size has a similar effect on the performance of system J with either code. For the small packet size and a probability of packet error of 0.01, the performance of system J is poorer than the performance of system D even though the two have nearly the same detection complexity. If a medium-sized packet is used in system J, however, its performance with system J is improved at the cost of an increase in the detection complexity. With either packet size, the performance of system J is better relative to the performance of system D for a lower probability of packet error.

In Figure 5.18, the performance of systems B, D and J with the larger block-length code and the small packet size is shown for the same two-path Rayleigh-fading channel considered above. For a probability of packet error of 0.01, the performance with system J is marginally better than the performance with system D with a small increase in the detection complexity. Once again, this is consistent with the results observed with the $(32, 16)$ code.

The performance of systems D and J with the lower-rate and higher-rate R-S codes and the small packet size is shown in Figure 5.19 for the same two-path static channel considered with the $(64, 32)$ code. Recall from Figure 5.8 that for this channel, the performance of system J is poorer than the performance of system D by 0.25 dB for a probability of packet error of 0.01 if the

$(32,16)$ code is used. If the higher-rate $(32,20)$ R-S code is used, the performance of system J is 0.15 dB worse than the performance of system D, and its performance is 0.3 dB poorer than the performance of system D if the lower-rate $(32,12)$ R-S code is used. Thus the performance of system J relative to the performance of system D improves slightly as the code rate is increased. With each code rate, the performance of system J relative to the performance of system D is better for a lower probability of packet error.

The detection complexity does not depend significantly on the rate of the R-S code for the two-path channel. The complexity of system D, measured in average EE decoding attempts per code word, is 1.38, 1.43 and 1.42 with the $(32,20)$ code, the $(32,16)$ code and the $(32,12)$ code, respectively. The corresponding complexities of system J are 1.54, 1.57 and 1.55.

The performance of systems D and J with the high-rate and low-rate codes and the small packet size is shown in Figure 5.20 the same two-path Rayleigh-fading channel considered with the $(64,32)$ code. Recall from Figure 5.12 that for this channel, the performance of system J is superior to the performance of system D by 0.45 dB for a probability of packet error of 0.01 if the $(32,16)$ code is used. If the higher-rate $(32,20)$ R-S code is used, the performance of system J is 0.5 dB better than the performance of system D, but its performance is 0.1 dB poorer than the performance of system D if the lower-rate $(32,12)$ R-S code is used. Thus as with the static two-path channel, the performance of system J relative to the performance of system D improves slightly as the code rate is increased. The detection complexity of system J is approximately 3.5% greater than the detection complexity of system D for each code rate. Once again with each code rate, the performance of system J relative to the performance of system D is better for a lower probability of packet error.

From Figures 5.19 and 5.8 it is seen that for the two-path static channel, the best performance among the three block-length-32 codes with system J is obtained by the highest-rate code. The best performance among the three block-length-32 codes with system J is obtained by the lowest-rate code if the two-path channel is fading, however, as seen from Figure 5.20 and 5.12. Thus the best choice of the code rate depends on the characteristics of the channel, as is demonstrated in Chapter 4 for the systems that do not use differential encoding.

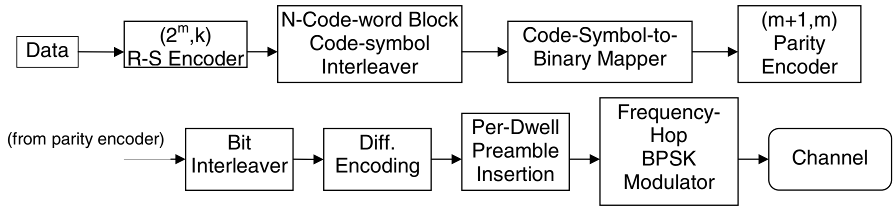

Figure 5.1 Transmitter for the SFH system with differential encoding.

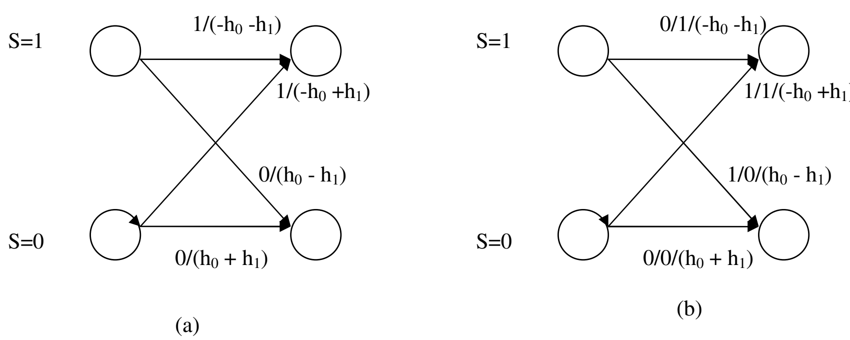

Figure 5.2 Representative time step in a two-state equalizer trellis (a) without differential encoding and (b) with differential encoding.

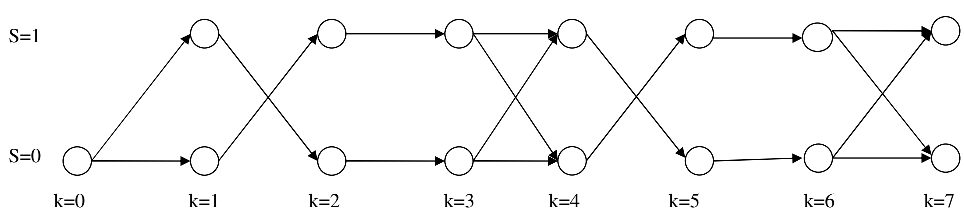

Figure 5.3 A two-state equalizer trellis with pruned branches for the SFH system with differential encoding.

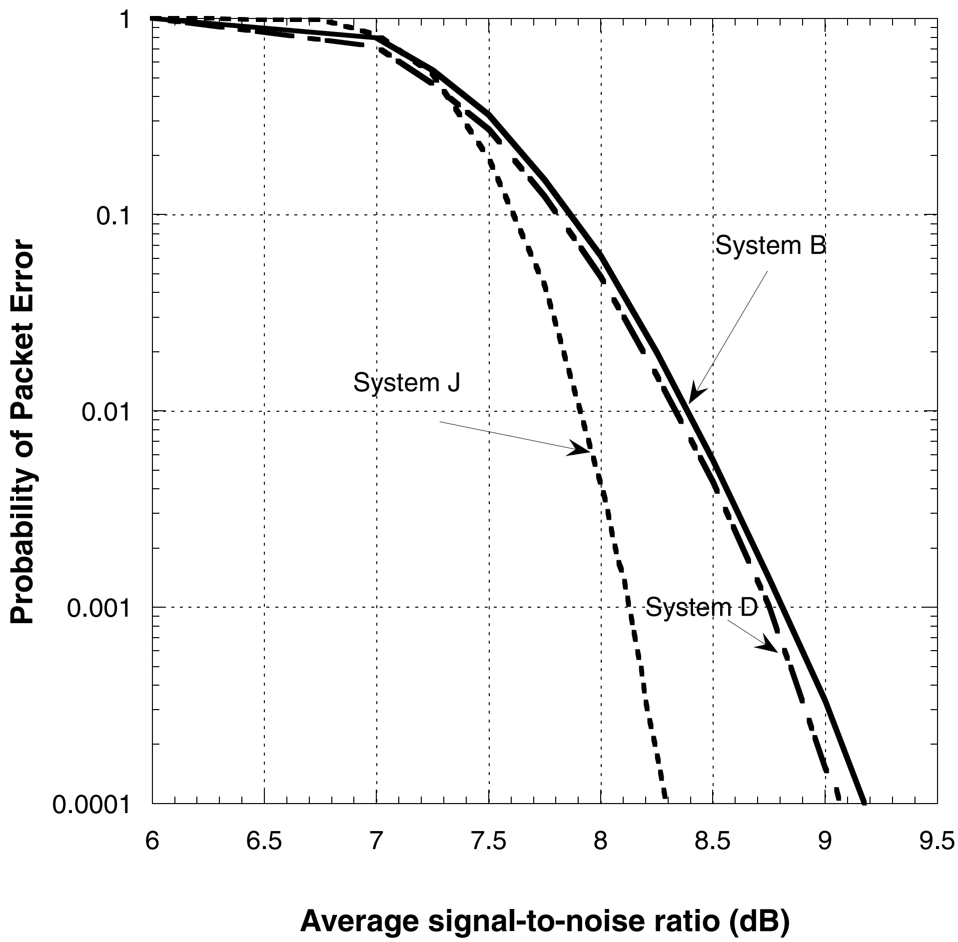

Figure 5.4 Probability of packet error with AWGN channel.

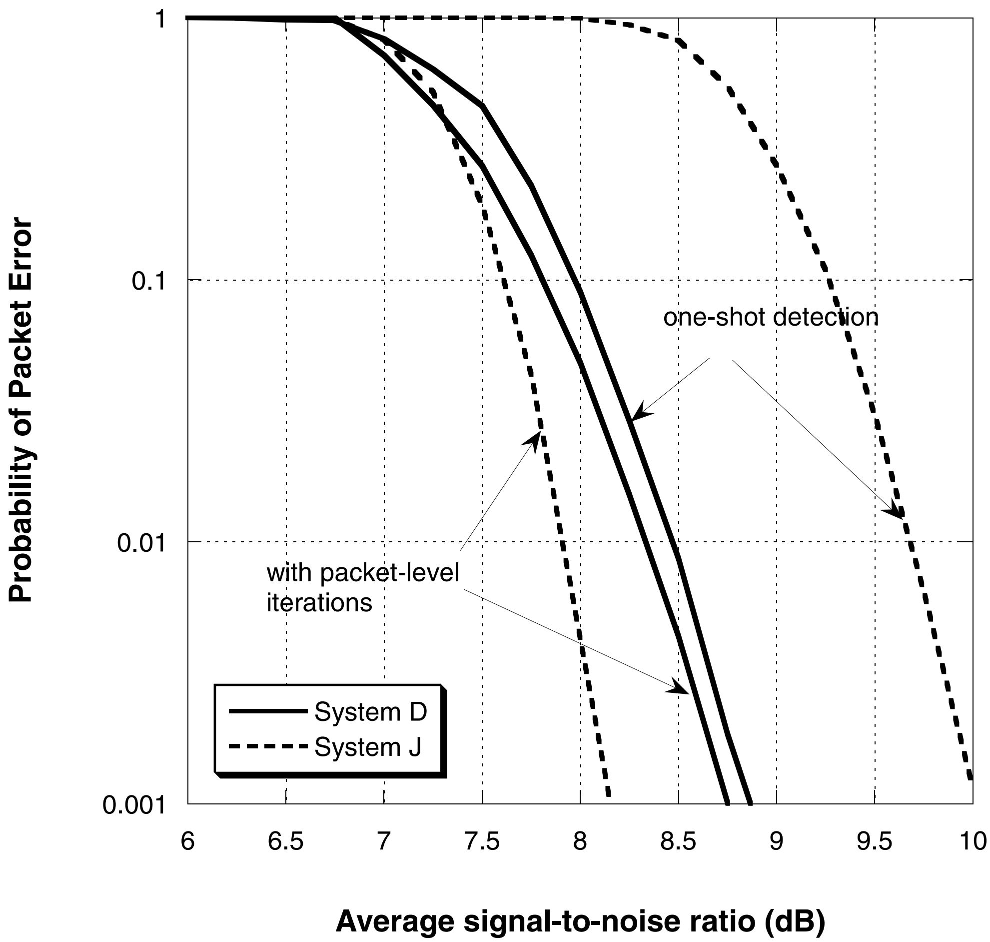

Figure 5.5 Probability of packet error with one-shot detection and packet-level iterative detection.

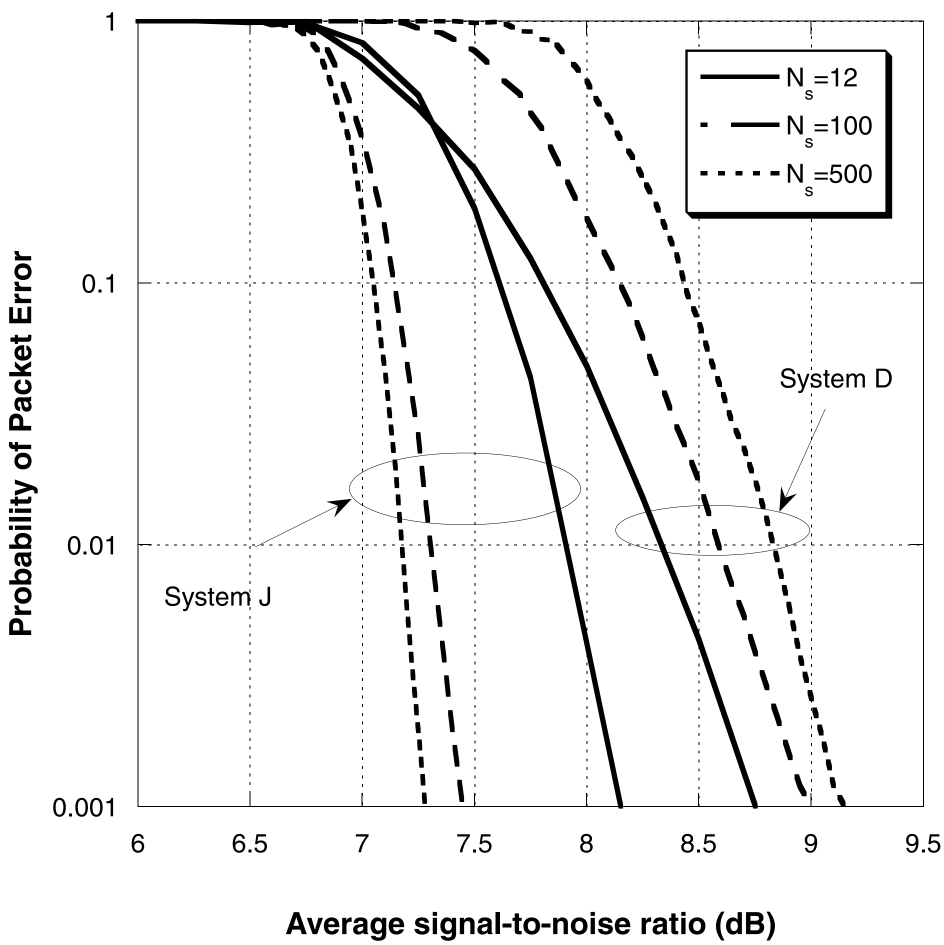

Figure 5.6 Probability of packet error for three packet sizes with AWGN channel.

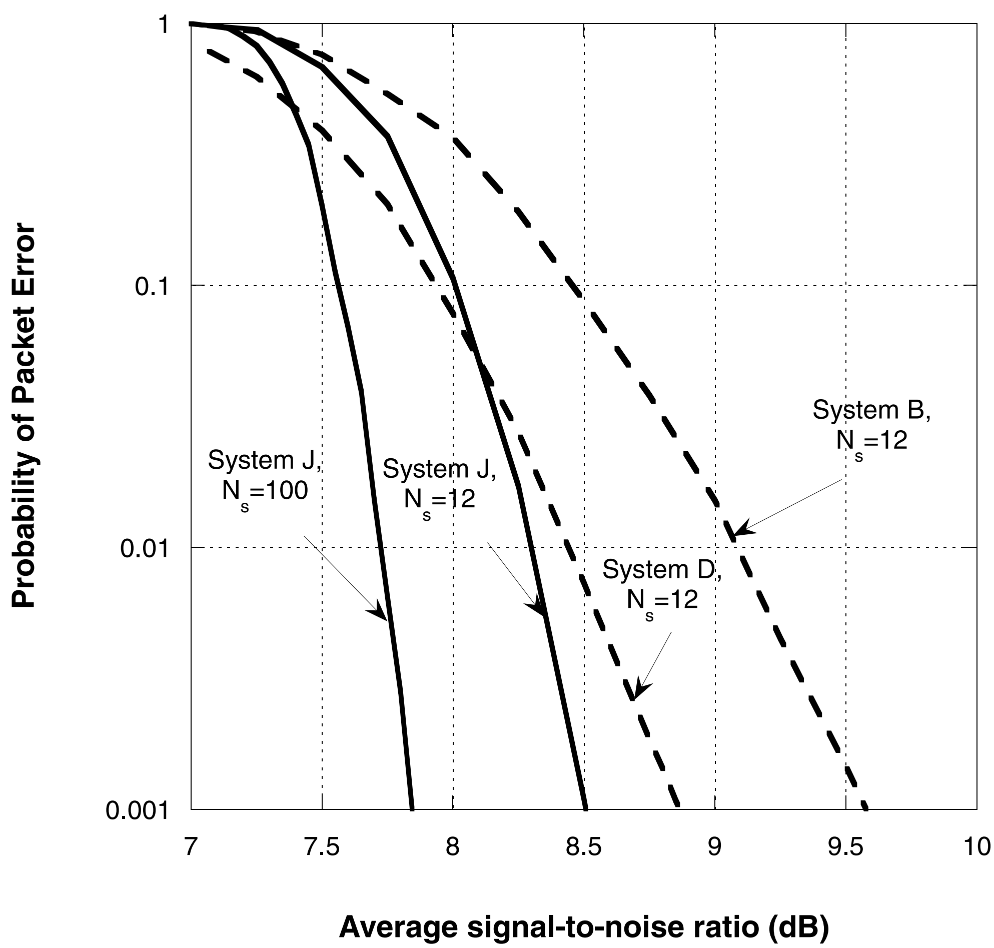

Figure 5.7 Probability of packet error with $1 + 0.5\ D$ static channel.

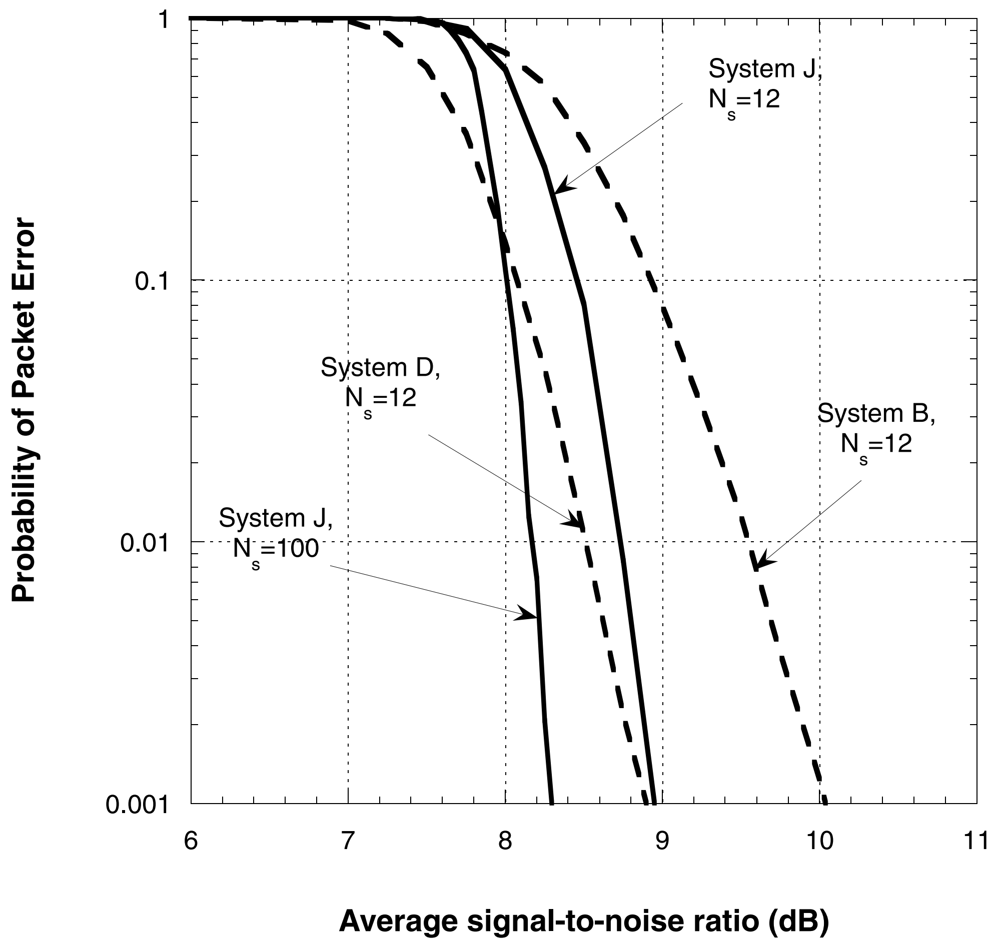

Figure 5.8 Probability of packet error with two-path static channel.

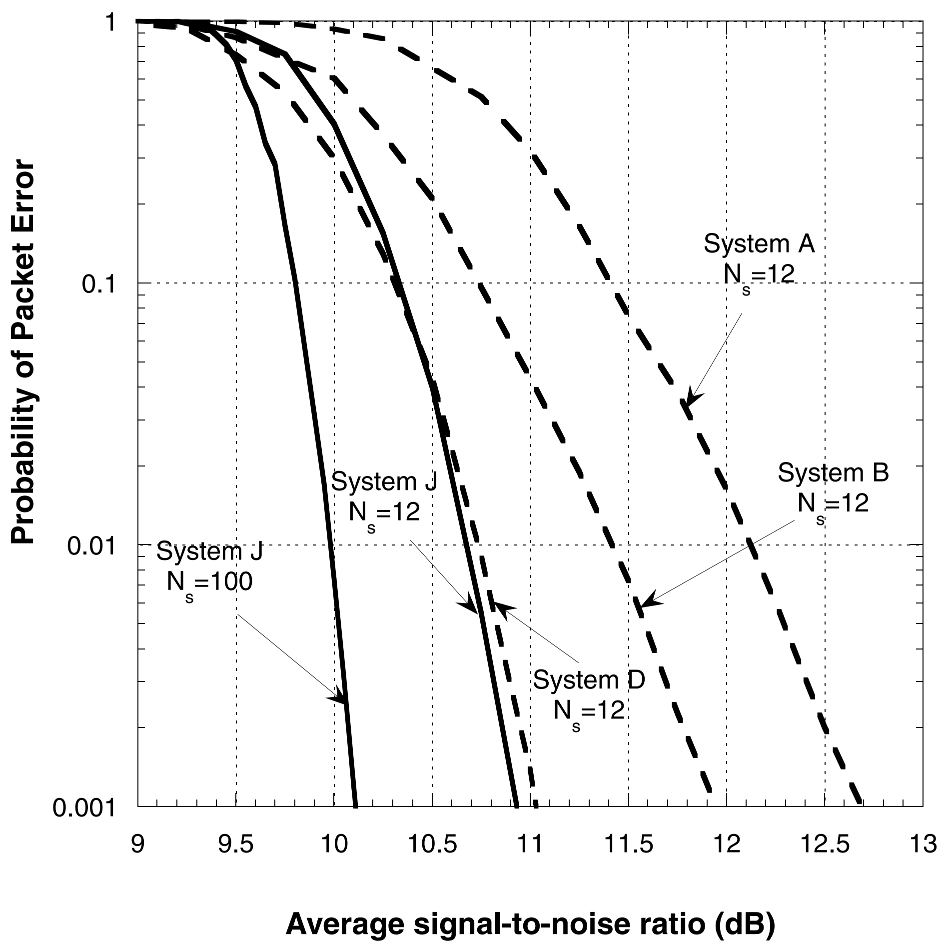

Figure 5.9 Probability of packet error with worst-case three-path static channel.

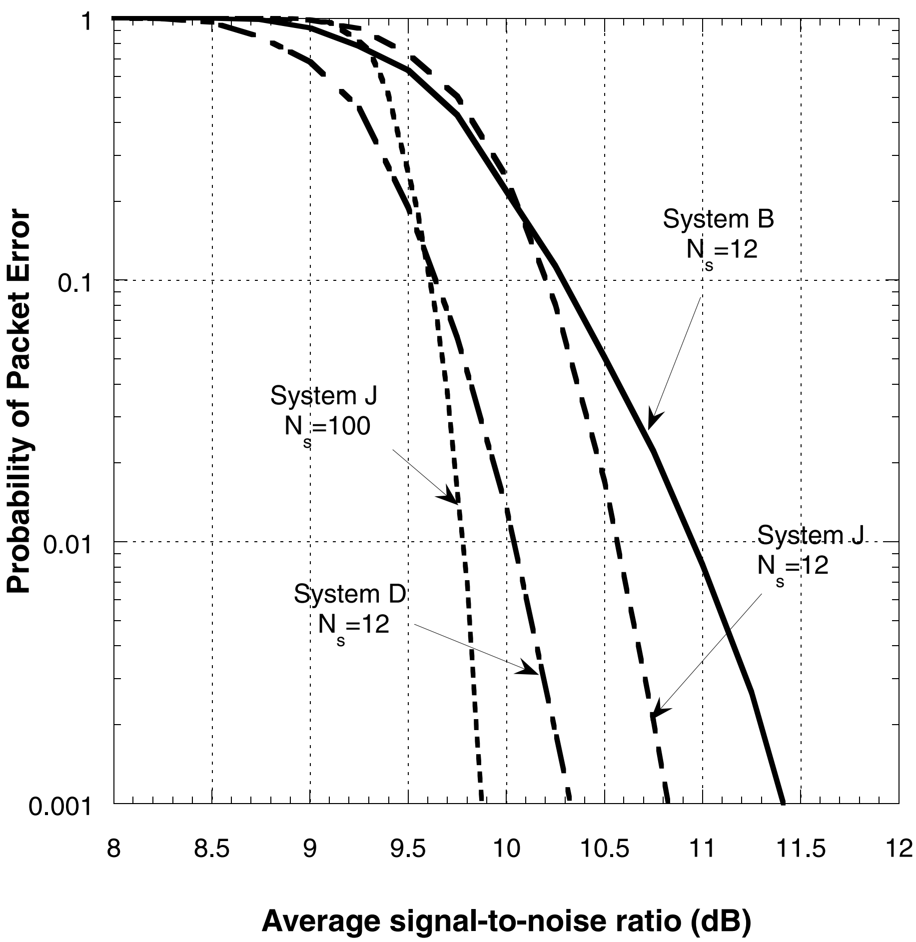

Figure 5.10 Probability of packet error with three-path static channel.

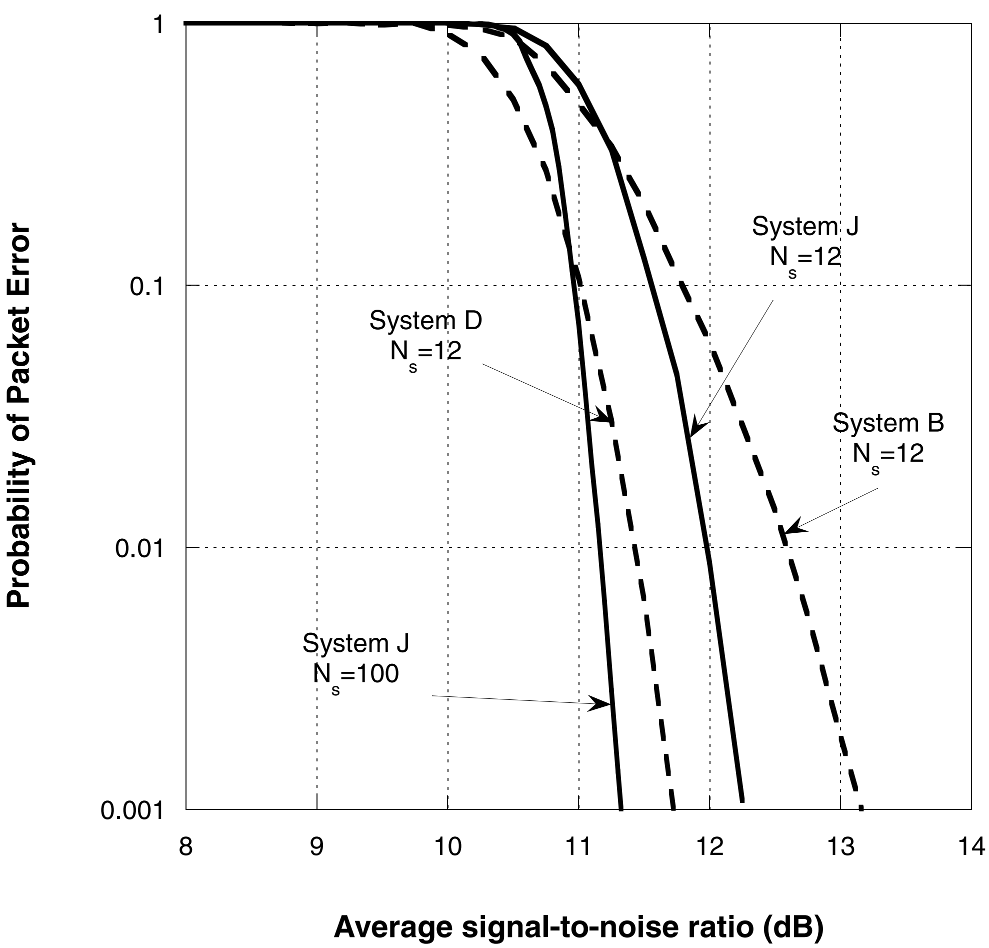

Figure 5.11 Probability of packet error with four-path static channel.

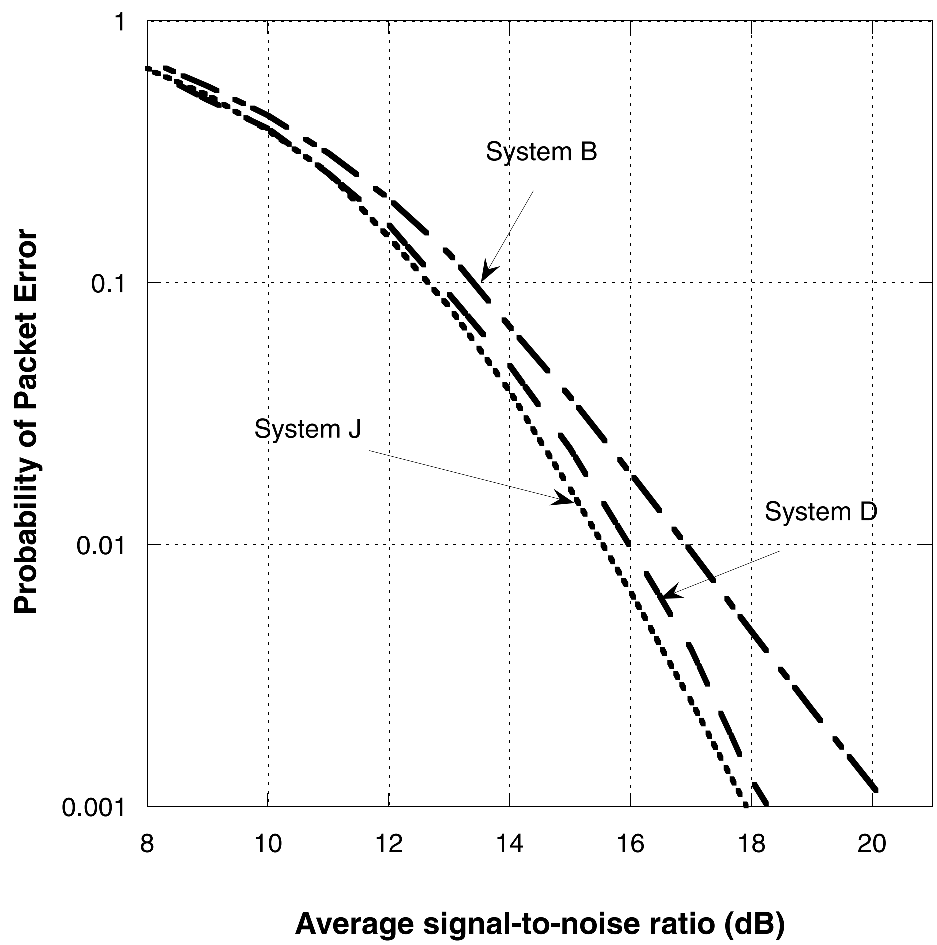

Figure 5.12 Probability of packet error with two-path Rayleigh-fading channel.

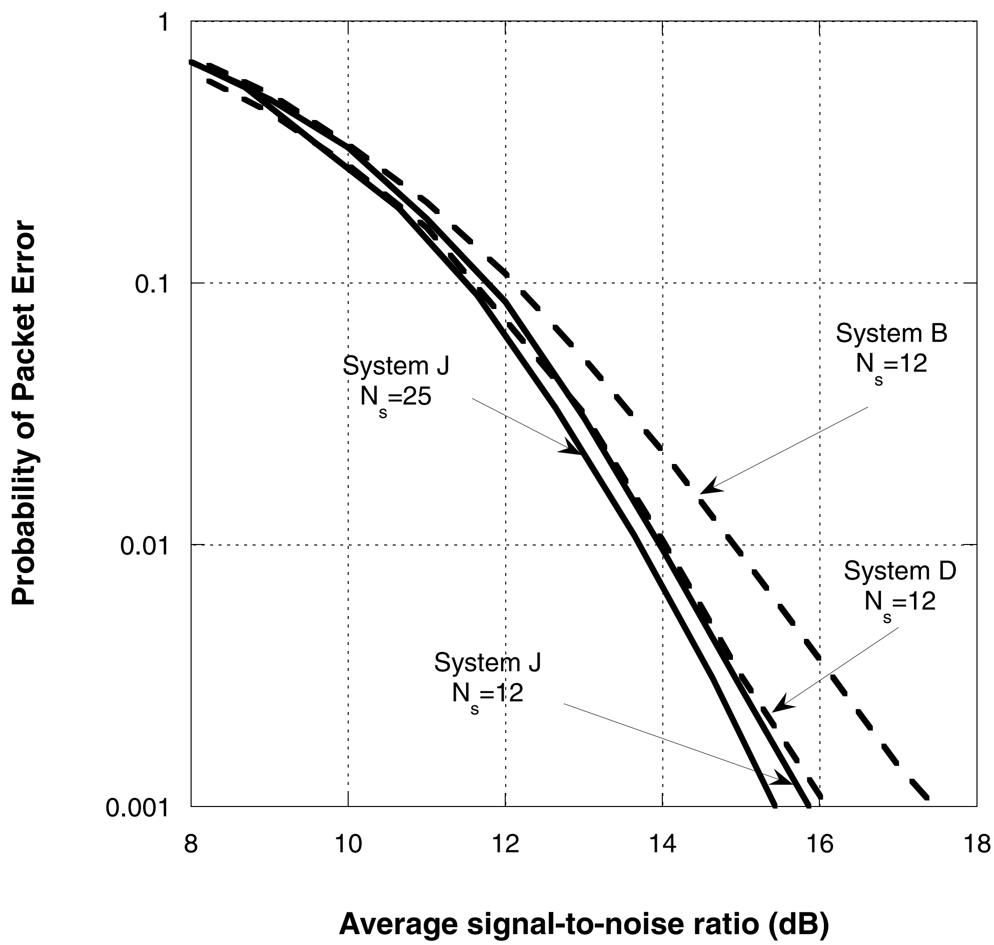

Figure 5.13 Probability of packet error with three-path Rayleigh-fading channel.

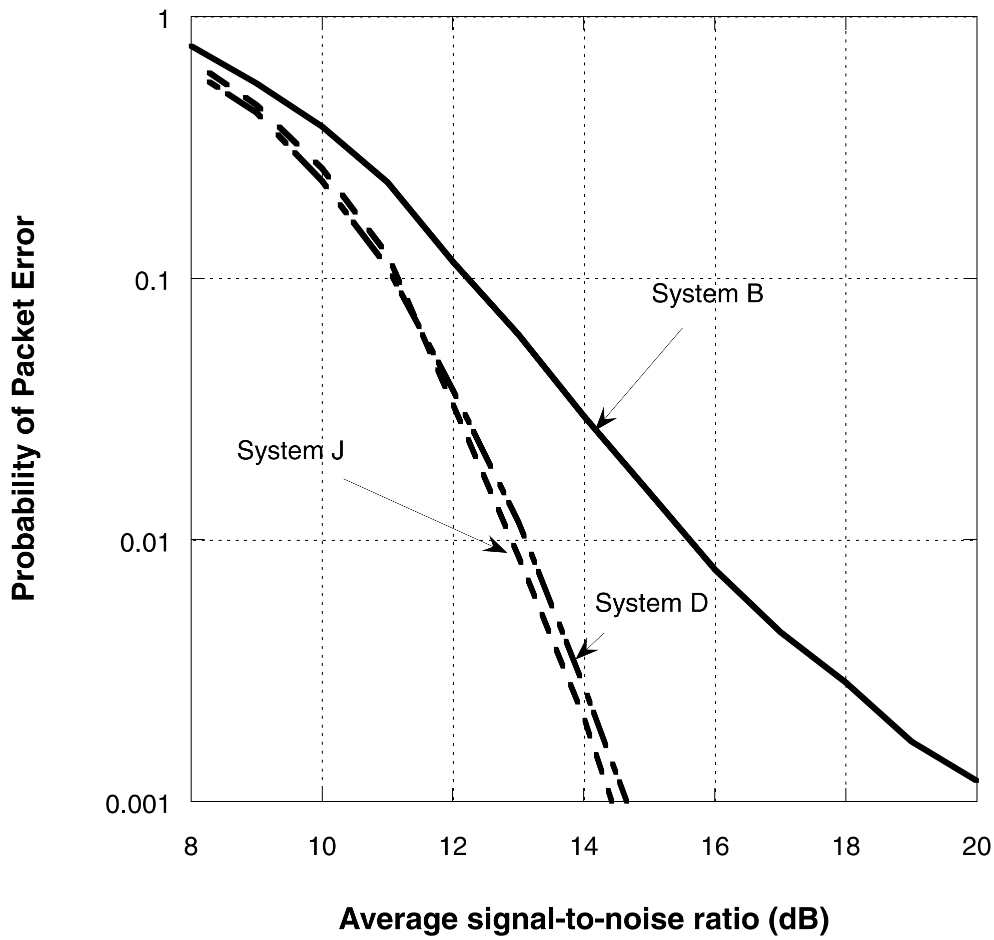

Figure 5.14 Probability of packet error with four-path Rayleigh-fading channel.

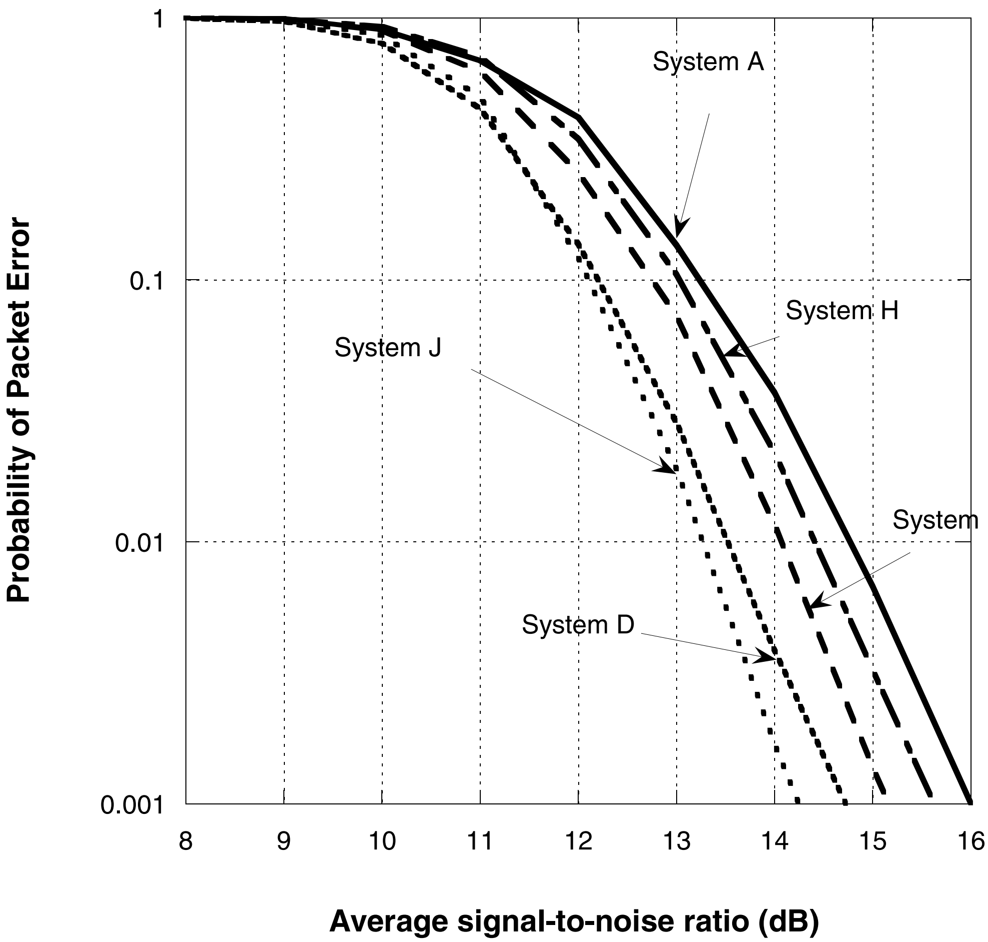

Figure 5.15 Probability of packet error with Rayleigh-fading channel and dense delay spectrum.

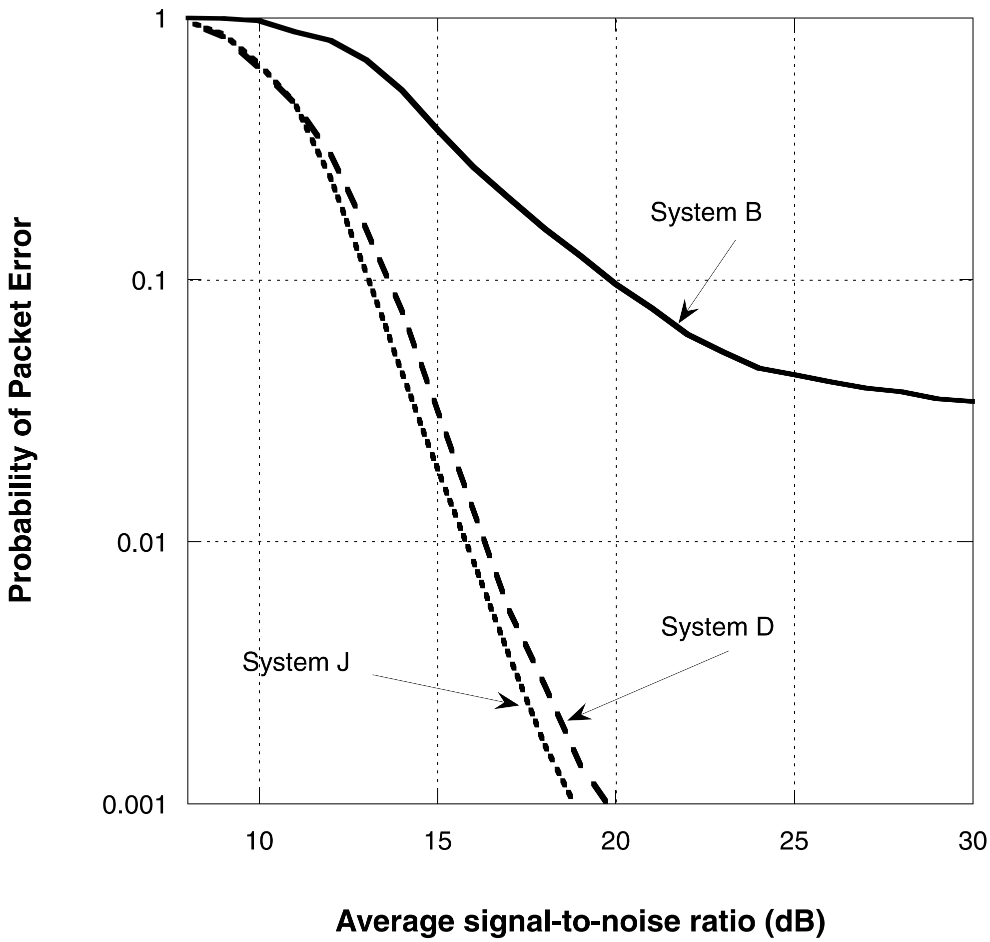

Figure 5.16 Probability of packet error with three-path Rayleigh-fading channel and large Doppler spread.

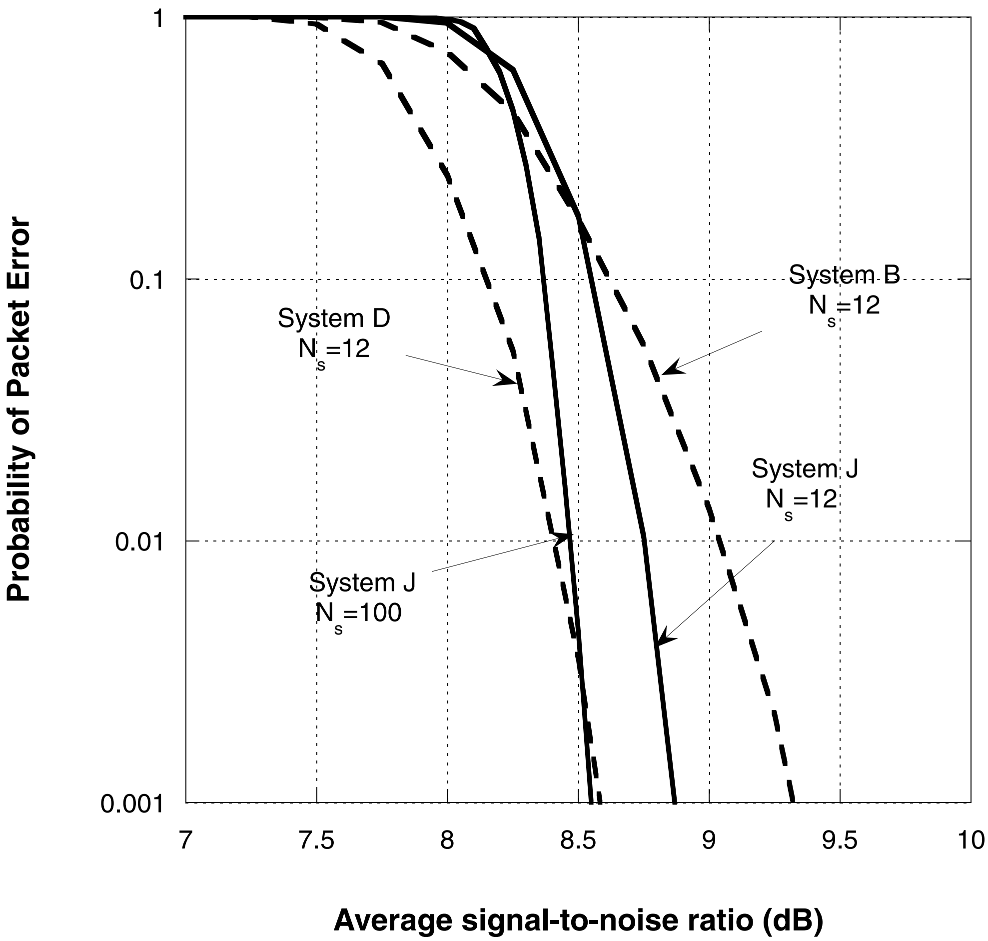

Figure 5.17 Probability of packet error with two-path static channel and (64,32) R-S code.

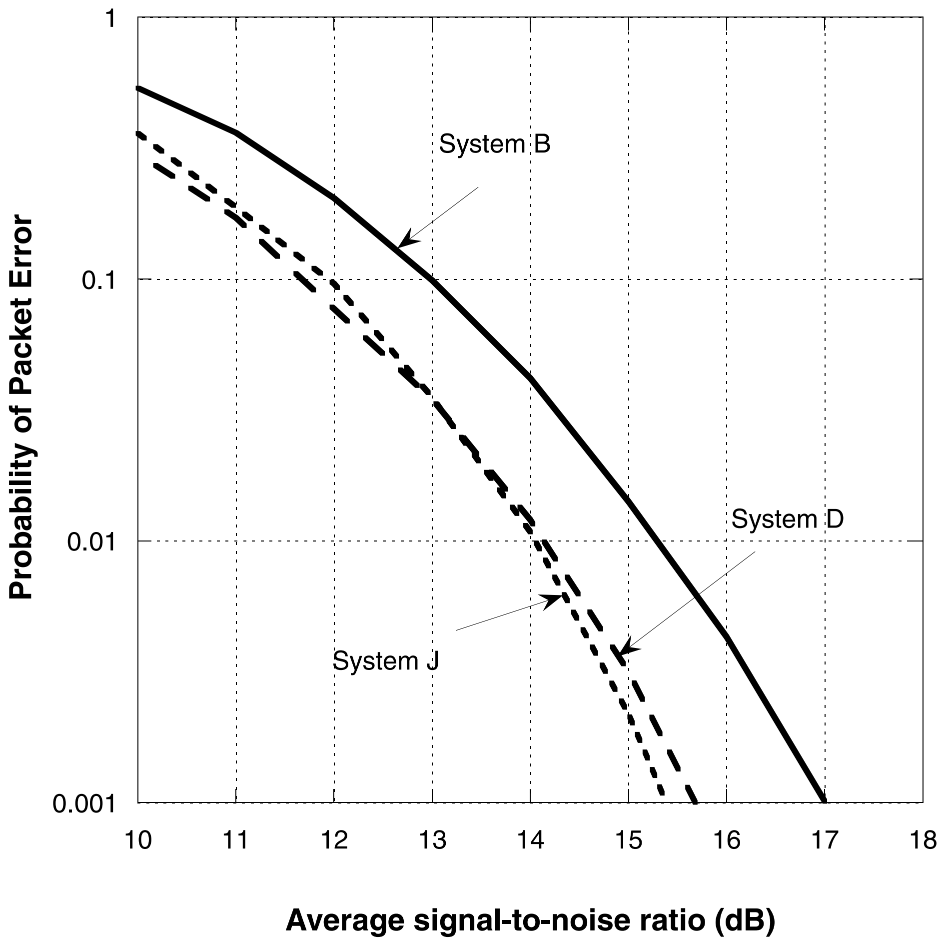

Figure 5.18 Probability of packet error with two-path Rayleigh-fading channel and (64,32) R-S code.

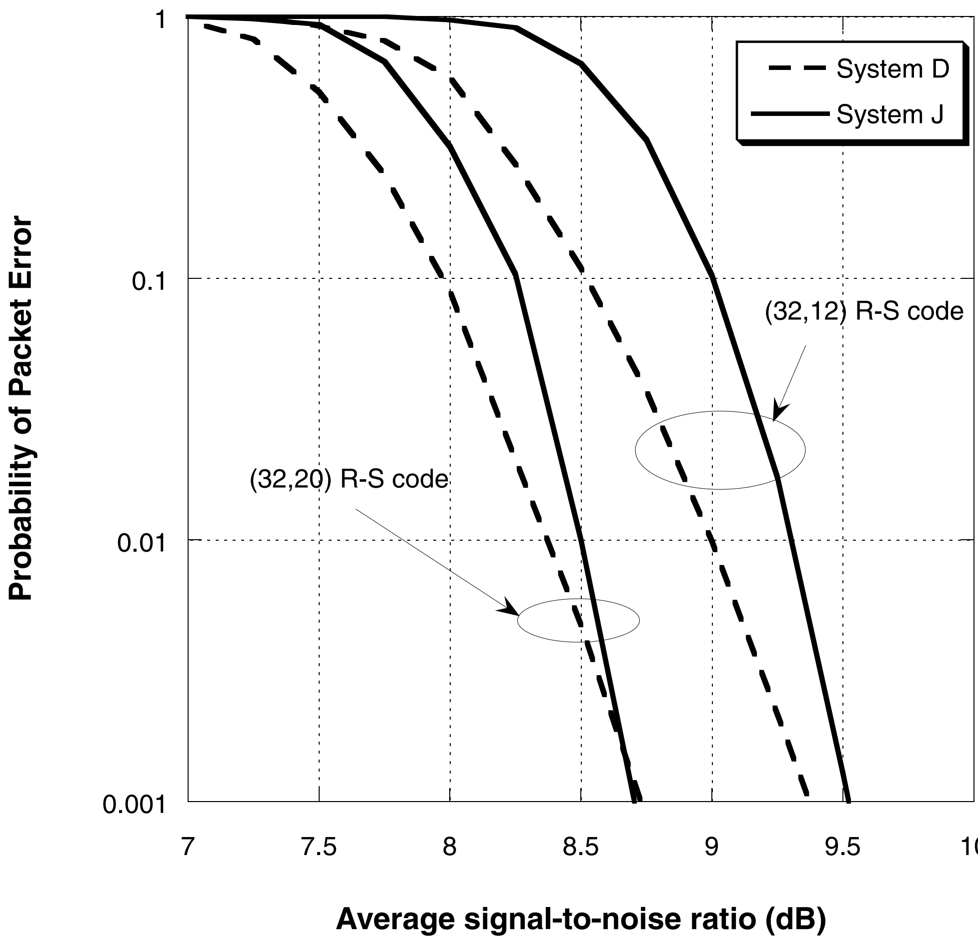

Figure 5.19 Probability of packet error with two-path static channel and other code rates.

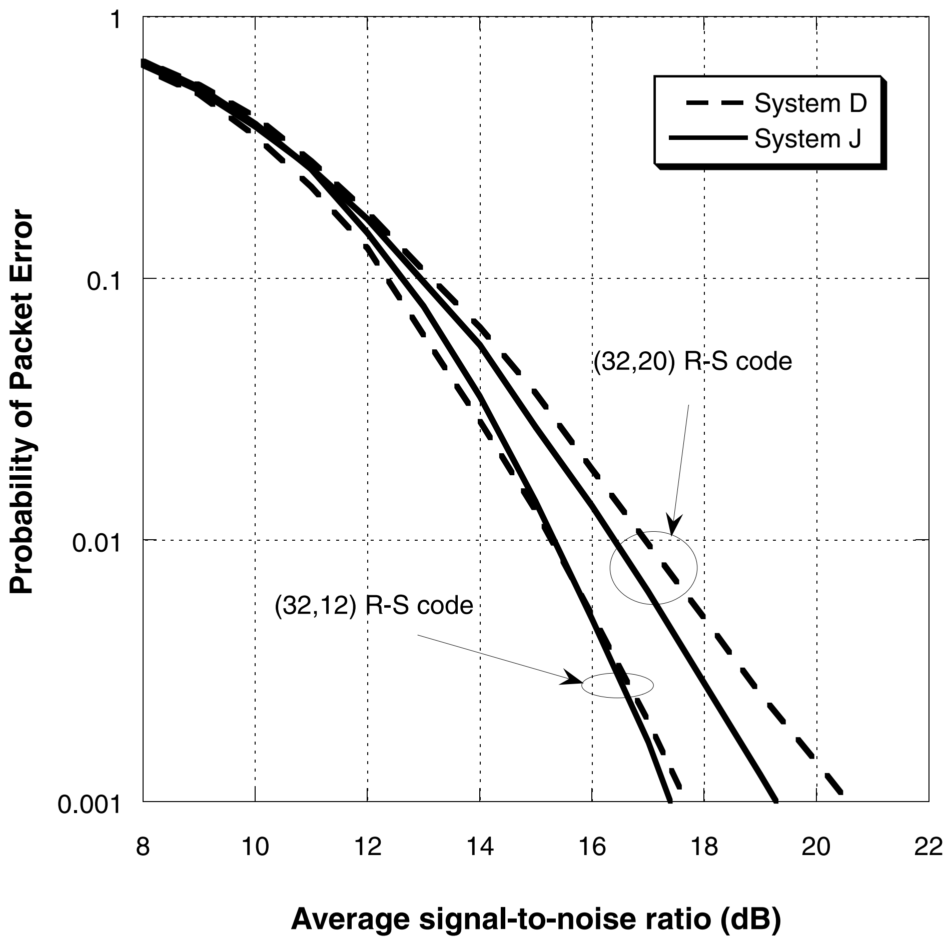

Figure 5.20 Probability of packet error with two-path Rayleigh-fading channel and other code rates.

CHAPTER 6

SFH SYSTEMS WITH PACKET-LEVEL ITERATIVE DETECTION IN CHANNELS WITH PARTIAL-BAND INTERFERENCE

As noted in the introduction, one of the most beneficial characteristics of a properly designed SFH system is its robustness in the face of partial-band channel impairments. In this chapter, the investigation of the performance of SFH systems using packet-level iterative detection is extended to consider their performance in channels that include partial-band interference. The SFH systems considered in this chapter have the same basic features as the systems considered in the earlier chapters, but the scope is expanded to include several variants of the systems already introduced. Among these are both systems using coherent communications (as have been considered up to this point) and systems using noncoherent communications.

6.1 Description of SFH Systems Using Coherent Communications

Four systems (and variants thereof) are the main focus of our investigation of SFH systems using coherent communications in the presence of partial-band interference. Two of them are systems A and B (described in detail in Chapter 4). The third SFH system employs rectangular block code-symbol interleaving, pseudo-random bit interleaving across each full dwell interval (with a different interleaving pattern for each dwell interval), and packet-level iterative detection. Thus it differs from systems C–F of Chapter 4 only in the choice of the per-dwell bit interleaver. It is denoted *system K*. The fourth system differs from system K only in that it applies differential encoding to the bit-interleaved contents of each dwell interval. It is denoted *system L*. Thus system L differs from system J of Chapter 5 only in the choice of the per-dwell bit interleaver. (We choose to focus on systems K and L in lieu of systems D and J in this chapter because the bit interleaving of the former two leads to slightly better performance in the presence of partial-band interference than the bit interleaving of the latter two.) The key characteristics of systems A, B, K and L are summarized in Table 6.1. System G and a variant of system G, both employing packet-wide s-random interleaving (discussed in Chapter 4)), are also considered briefly in Section 6.4.

System	Code-Symbol Interleaver	Bit Interleaver	Differential Encoding	Packet-Level Iteration
A	rectangular	none	no	no
B	rectangular	none	no	yes
K	rectangular	pseudo-random, unrestricted per dwell	no	yes
L	rectangular	pseudo-random, unrestricted per dwell	yes	yes

Table 6.1 Characteristics of coherent SFH systems considered in Chapter 6.

In the receiver for each of the SFH systems considered thus far in the dissertation, an individual R-S code symbol is marked as erased if the detected binary sequence corresponding to the parity-encoded binary representation of the code symbol fails the parity check. The erasure decisions for distinct code symbols are made without reference to one another. If the received signal is subjected to partial-band interference or any other frequency-dependent impairment, however, parity-check failures are more likely to occur in dwell intervals that suffer from more severe channel impairments. Thus the number of parity-check failures in a dwell interval provides information about the reliability of the remaining code-symbol decisions for the dwell interval. This can be exploited by employing threshold-based *dwell erasures* at the receiver [21] in which the receiver erases all the code symbols in a dwell interval if the number of parity-check failures in the dwell interval exceeds a fixed *dwell-erasure threshold* γ.

Among the systems we consider in this chapter are a variant of system K and a variant of system L in which the receiver employs the dwell-erasure technique *in addition to* the erasure of individual code symbols that fail parity check. The respective packet transmission formats are identical to the formats used in systems K and L, and the receiver employs packet-level iterations of MLSE equalization and EE decoding as in those systems. The only difference arises due to the introduction of the dwell-erasure threshold as an additional erasure criterion between equalization and decoding in each packet-level iteration. Note that if $\gamma = N_s$ (the number of code symbols per dwell interval), the dwell-erasure criterion is superfluous. Thus systems K and L using only per-symbol erasures are a special case of their respective dwell-erasure variants.

In each of the SFH systems considered thus far, one parity bit is appended to the binary representation of each R-S code symbol. A more efficient packet format can be realized instead by generating a parity bit for the aggregate binary representation of several R-S code symbols in a dwell interval. In this chapter we consider variants of both system K and system L in which a single bit of even parity is generated for the (m-bit) binary representation of every block of N_p consecutive R-S code symbols in the rectangular block code-symbol interleaver. This is referred to as the *generalized parity-bit method*, and N_p is referred to as the *parity-block size*. (Per-dwell bit interleaving is subsequently applied to each row of the interleaver as in systems K and L, respectively.)

The receiver in the respective generalized-parity-bit variants employs packet-level iterative equalization and decoding as in systems K and L. If the detected binary symbols at the equalizer output result in parity-check failure for a parity-encoded block, the corresponding N_p R-S code symbols are marked as erasures for EE decoding in that packet-level iteration. Note that if $N_p = 1$

(i.e., there is a parity bit for each R-S code symbol), however, per-symbol erasures result. Thus systems K and L using only per-symbol erasures are special cases of their respective generalized parity-bit variants. The generalized parity-bit method is used here only for erasure of individual parity encoded blocks of code symbols, though it could also be used for threshold-based dwell erasures. In the special case in which $N_p = N_s$ (i.e., there is one parity bit per dwell interval), however, the generalized parity-bit method results in a system in which each block erasure is inherently a dwell erasure.

Thus in each of the SFH systems considered in this chapter that use coherent communications, each dwell interval in a packet transmission consists of a preamble sequence of N_t bits followed by the $mN_s + (N_s/N_p)$ bits corresponding to code symbols and parity bits in each dwell interval and a guard interval of N_e bits in which no signal is transmitted. For a packet transmitted at time $t = 0$, the transmission is thus given by

$$s(t) = \sqrt{2P} \sum_{i=0}^{n-1} \sum_{j=0}^{N_t+(m\ N_s+(N_s/N_p)-1} (-1)^{d_{i(N_t+m\ N_s+(N_s/N_p))+j}}$$
$$\times p_T(t - (i(N_t + m\ N_s + (N_s/N_p) + N_e) + j)T) \cos(j2\pi f_i t + \phi_i) \qquad (6.1)$$

where d_l is the lth channel symbol for the corresponding system, $N_p = 1$ for all the systems other those using the generalized parity-bit method, and the other parameters are as defined for equation (5.1) in Chapter 5.

The transmission is subjected to a multipath, fading channel with additive, full-band, Gaussian noise and additive interference as defined in Chapter 3. The interference is a partial-band, Gaussian random process in which a fixed fraction ρ of the frequency slots in the system are subjected to a white, Gaussian interference process with a power spectral density of N_I/ρ (in addition to the noise process). The remaining fraction $1 - \rho$ of the frequency slots have no interference and are subjected only to the noise process. The *average* *signal-to-noise ratio* at the receiver is thus given by

$$\frac{\overline{\mathcal{E}_b}}{N_0} = \frac{PT}{N_0}\frac{n(N_t + m\ N_s + N_s/N_p)}{mkN_s}\sum_{l=0}^{M-1}(\rho_l^2 + 2\sigma_l^2),$$

and the *average signal-to-interference ratio* is given by $\overline{\mathcal{E}_b}/N_I$.

The performance of the SFH system in a multipath channel with partial-band interference depends in general on the particular subset of the frequency slots that are subjected to interference. In the channel model used for the results in this chapter, the presence or absence of partial-band interference in the sequence of frequency slots selected for the SFH transmission is determined by a corresponding sequence of independent, Bernoulli random variables with parameter ρ. In many practical circumstances involving partial-band interference, in contrast, a fixed subset of the frequency slots are subjected to interference. Each example considered in this chapter concerns a channel in which the multipath components differ in delay by an integer multiple of the channel-symbol duration, however. Thus the performance that results with the interference model we employ is identical to the performance that results if any fixed subset of the frequency slots are subjected to interference (assuming the same value of ρ is used in either case).

6.2 Measures of System Performance

In this chapter, the performance of a SFH system is characterized by specifying the range of channel conditions under which a desired probability of packet error is achieved by the system. Specifically, for a given multipath channel and fraction of the band that is subjected to interference (ρ), the performance of the system is given by the signal-to-interference ratio $\mathcal{E}_b/N_I$ that is required to achieve the desired probability of packet error if the average signal-to-noise ratio is $\mathcal{E}_b/N_0 = 20$ dB. (Except where otherwise noted, the desired probability of packet error used in the examples is 10^{-3}.) Thus a larger value of the required signal-to-interference ratio represents poorer performance, and a smaller value of the required signal-to-interference ratio represents better performance. In each example, the required signal-to-interference ratio is considered as a function of ρ for all values of ρ between zero and one.

Two derivative measures are used to characterize the extremal performance of the system for a given multipath channel. The required signal-to-interference ratio for a given multipath channel differs for different values of ρ, and the largest (worst case) required signal-to-noise ratio occurs for some value of ρ. This represents the value of ρ to which the system is most vulnerable (for the given multipath channel), and the corresponding required signal-to-interference ratio is denoted $\mathrm{SIR}_{\mathrm{max}}$. It represents the signal-to-interference ratio that would be required to achieve acceptable performance if the system were confronted with an intelligent partial-band Gaussian interferer using an optimal selection of its interference bandwidth.

The ability of the system to withstand high-power, narrowband interference is measured by the quantity ρ^*. It represents the fractional interference bandwidth below which the system achieves acceptable performance regardless of the total interference power. That is, the system can achieve acceptable performance (for the given multipath channel) even in the presence of infinite received interference power as long as the interference is limited to a fraction of the band no greater than ρ^*. (In the numerical results, we find that the value of ρ^* differs negligibly from the value of ρ for which the required signal-to-interference ratio is 0 dB. Thus the figures in this chapter only illustrate results for values of the required signal-to-noise ratio of 0 dB or greater.) Thus a small value of $\mathrm{SIR}_{\mathrm{max}}$ and a large value of ρ^* is desirable. Note that the right-hand extreme of each graph corresponds to $\rho = 1$, in which case the interference covers the full band.

6.3 Performance of the SFH Systems in Partial-Band Interference

In this section we evaluate the performance of each SFH system described in Section 6.1. Recall that system A uses no bit interleaving and one-shot MLSE equalization and bounded-distance EE decoding. System B uses the same packet format as system A, but its receiver uses packet-level iterative equalization and decoding. The modification of system B that uses pseudo-random bit interleaving in each dwell interval is denoted system K, and the system using both per-dwell bit interleaving and differential encoding is denoted system L.

In each of the examples, we consider a packet consisting of 22 (n, k) extended R-S code words. Except where otherwise noted, a (32,12) R-S encoder is used. Each packet thus contains 1320 bits of information. Each dwell interval includes a preamble sequence of 26 bits, and except where otherwise noted, one bit of parity is added to the binary representation of each R-S code symbol (i.e., $N_p = 1$). Thus there are 158 channel symbols in each dwell interval.

The signal-to-interference ratio required to achieve a probability of packet error of 10^{-3} in SFH systems A, B, K and L is shown in Figure 6.1 as a function of the fractional interference bandwidth ρ for a single-path static, partial-band-interference channel. One-shot detection of a transmission without bit interleaving or differential encoding is characterized by $\mathrm{SIR}_{\max} = 11.0$ dB and $\rho^* = 0.15$, as seen by the results for system A. Instead, the use of packet-level iterative detection with the same transmission format results in a slight improvement in performance for all values of ρ, as seen by comparing the results for systems A and B. The use of per-dwell bit interleaving in conjunction with packet-level iterative reception leads to substantially better performance over the entire range of values of ρ, as seen by the performance of system K.

In particular, the value of $\mathrm{SIR}_{\max}$ is decreased to 9.6 dB, and the value of ρ^* is increased to 0.3.

The use of differential encoding in conjunction with per-dwell bit interleaving and packet-level iterations results in uniformly better performance over the entire range of values of ρ, as seen by comparing the results for system L with those for systems A, B and K in Figure 6.1. The performance of system L is characterized by $\mathrm{SIR}_{\max} = 8.3$ dB and $\rho^* = 0.3$ for this channel. Thus system L provides an improvement of 2.7 dB in $\mathrm{SIR}_{\max}$ compared with system A, which corresponds to much greater robustness with respect to an interferer occupying the worst-case fraction of the band. Moreover, the value of ρ^* is doubled if system L replaces system A. Thus system L can withstand interference from a source with extremely high power over a much larger fraction of the band than can system A. At the other extreme, the performance of system L is approximately 1.0 dB better than any of the other three systems when only full-band Gaussian noise is present (i.e., when $\rho = 1.0$).

Note that if the receiver for the SFH systems had perfect *a priori* knowledge of the channel characteristics and also had perfect *a priori* knowledge of the symbol timing in each dwell interval, systems A, B and K would exhibit identical performance for a single-path static, partial-band-interference channel. This information is in reality unavailable *a priori* at the receiver, and instead the receiver must employ noisy estimates of the multipath channel's baseband-equivalent impulse response in each dwell interval. The receiver in each system considered here is designed to estimate an impulse response of duration up to four times the channel-symbol interval, and the estimates may include errors in the number of taps in the channel model, the relative magnitudes of the tap weights, the phase of each tap weight, and the symbol-rate sample timing. The errors introduce spurious ISI which degrades the performance of the equalizer in each dwell interval.

The packet-level iterative detection in system B provides slightly greater robustness with respect to channel-estimation errors than does the one-shot detection of system A, and the use of bit interleaving in conjunction with packet-level iterative detection in system K results in much greater robustness with respect to channel-estimation errors than is seen with either system A or system B. For values of ρ between 0.15 and 0.3, in particular, the effect of channel-estimation errors precludes acceptable performance with systems A and B whereas it can be achieved with system K. In contrast to all of this, system L results in better performance than the other three systems over all values of ρ even if the receivers are provided with perfect *a priori* knowledge of the channel characteristics and perfect *a priori* knowledge on the symbol timing in each dwell interval.

The detection complexity of system A is one EE decoding attempt per R-S code word, and the detection complexity of system B is only slightly greater (in terms of *average* decoding attempts). The detection complexity of systems K and L is shown in Table 6.2 for a range of values of ρ. The complexity is given in units of average EE decoding attempts per R-S code word. For all values of ρ, system K exhibits a detection complexity which is only a fraction of one percent higher than the complexity of one in system A. In contrast, use of system L results in a moderate increase in the detection complexity over system A. The greatest detection complexity for system L over the entire range of values of ρ is an average of 1.65 average EE decoding attempts per code word. Note that the greatest complexity arises if the interference occupies nearly the full bandwidth, and the complexity is not much greater than one if the fractional interference bandwidth is close to $\rho^* = 0.3$ for system L. Thus the combination of bit interleaving, differential encoding, and packet-level iteration results in a substantially better performance than in a SFH system lacking one or more of these features, and the gains are achieved at a modest complexity cost to the receiver. The additional protection that these features provide against severe partial-band interference (as reflected in an increased value of ρ^*) is achieved at a negligible cost in complexity.

ρ	System K	System L
1.0	1.0001	1.62
0.95	1.0001	1.59
0.9	1.00009	1.65
0.85	1.0001	1.49
0.8	1.0001	1.65
0.75	1.0001	1.58
0.7	1.0015	1.58
0.65	1.0002	1.48
0.6	1.0002	1.56
0.55	1.0002	1.65
0.5	1.0002	1.45
0.45	1.0004	1.4
0.4	1.0004	1.35
0.35	1.0007	1.12
0.3	1.000006	1.0008

Table 6.2 Detection complexity with single-path static, partial-band-interference channel.

The performance of systems A, B, K and L is shown in Figure 6.2 for a two-path static channel with partial-band interference. The paths have equal strength, and their delays are 0 and T. System A results in $\mathrm{SIR}_{\mathrm{max}} = 12.25$ dB and $\rho^* = 0.15$. System B results comparable or slightly better performance for all values of ρ. It results in the same value of ρ^* as system A, but $\mathrm{SIR}_{\mathrm{max}}$ is reduced to 11.6 dB. The use of system K provides a marked improvement in performance over systems A and B for all values of ρ. In particular, $\mathrm{SIR}_{\mathrm{max}} =$ 9.85 dB and $\rho^* = 0.3$ for system K. System L results in slightly to markedly better performance than system K, depending on the value of ρ. The value of $\mathrm{SIR}_{\mathrm{max}}$ is reduced to 9.15 dB in system L, but the value of ρ^* remains unchanged at 0.3. The greatest difference in the performance of systems K and L occurs for $\rho = 0.35$, in which case there is a difference of more than 5 dB in the required SIR.

For the two-path channel, system B has a detection complexity that is once again only slightly greater than that of system A. The detection complexity of systems K and L is shown in Table 6.3. The greatest complexity that arises with system K is an average of 1.14 EE decoding attempts per code word, and the greatest complexity for system L is 1.65. For both systems the greatest complexity arises if the interference occupies nearly the full bandwidth, and the complexity is not much greater than one if the fractional interference bandwidth is close to their common value of ρ^* (which is 0.3).

ρ	System K	System L
1.0	1.14	1.61
0.95	1.13	1.6
0.9	1.08	1.57
0.85	1.09	1.65
0.8	1.07	1.61
0.75	1.06	1.52
0.7	1.05	1.48
0.65	1.04	1.44
0.6	1.038	1.51
0.55	1.028	1.55
0.5	1.013	1.42
0.45	1.009	1.4
0.4	1.008	1.38
0.35	1.004	1.08
0.3	1.0006	1.0008

Table 6.3 Detection complexity with two-path static, partial-band-interference channel.

The performance of systems A, B, K and L is shown in Figure 6.3 for a three-path static channel with partial-band interference. The paths have equal strength, and their delays are 0, T and $2T$. For system A, $\mathrm{SIR}_{\max}$ and ρ^* are 14.16 dB and 0.1 respectively. If system B is used instead, there is a noticeable improvement for all values of ρ. In particular, $\mathrm{SIR}_{\max} = 13.2$ dB and $\rho^* = 0.16$. The value of $\mathrm{SIR}_{\max}$ is reduced further to 10.3 dB with system K, and ρ^* is increased to 0.3. Thus bit interleaving (without differential encoding) and packet-level iteration detection results in much better performance than one-shot detection over the full range of values of ρ with the three-path channel. In particular, $\mathrm{SIR}_{\max}$ is decreased by 2.8 dB and ρ^* is increased three-fold.

Unlike the results for the single-path and two-path channels, the performance of system L is not uniformly superior to the performance of system K for the three-path channel. The performance of system L is 0.8 dB poorer than the performance of system K in the presence of full-band noise only ($\rho = 1$), and consequently the value of $\mathrm{SIR}_{\max}$ is also higher (by 0.5 dB) for system L than for system K. This is consistent with the results in Chapter 5 in which only performance in full-band noise was considered. There it was observed that the value of differential encoding decreases for a system using packet-level iteration as the delay spread of the channel increases and that differential encoding actually results in poorer performance if the delay spread is sufficiently large. The value of ρ^* is 0.35 for system L with the three-path channel, however, which greater than ρ^* for system K. Thus the use of differential encoding provides greater robustness against severe partial-band interference in this channel than does system K. Moreover, the value of ρ^* for system L is greater with the three-path channel than with either the single-path channel or the two-path channel.

The detection complexity of systems K and L is shown in Table 6.4 for the three-path channel. The greatest complexity that arises with system K is an average of 1.8 EE decoding attempts per code word, and the greatest complexity for system L is 1.75. For both systems the greatest complexity arises if the interference occupies nearly the full bandwidth, and the complexity is not much greater than one if the fractional interference bandwidth is close to their respective values of ρ^*. System L exhibits greater complexity than system K for most values of ρ.

ρ	System K	System L
1.0	1.8	1.75
0.95	1.78	1.74
0.9	1.65	1.65
0.85	1.77	1.68
0.8	1.6	1.66
0.75	1.53	1.62
0.7	1.55	1.6
0.65	1.48	1.58
0.6	1.35	1.62
0.55	1.22	1.7
0.5	1.09	1.55
0.45	1.03	1.48
0.4	1.03	1.43
0.35	1.01	1.13
0.3	1.0006	1.0008

Table 6.4 Detection complexity with three-path static, partial-band-interference channel.

The performance of the SFH systems in multipath fading channels is illustrated by considering two Rayleigh-fading channels. In both examples, the performance is characterized by the signal-to-interference ratio required to a achieve a probability of packet error of 10^{-2} if the signal-to-noise ratio is 20 dB. Thus a more modest link performance is targeted in these two examples than in the other examples in the chapter.

The performance of systems A, B, K and L is shown in Figure 6.4 for a two-path, Rayleigh-fading channel with partial-band interference. The paths have equal average strength, their delays are 0 and T, and the normalized Doppler spread of the channel is 1.5×10^{-4}. For system A, $\mathrm{SIR}_{\max}$ and ρ^* are 19.6 dB and 0.05 respectively. If system B is used instead, there is a modest improvement for all values of ρ, with $\mathrm{SIR}_{\max}$ decreasing to 18.75 dB and ρ^* increasing to 0.1. Much better performance results over the full range of ρ if system K is used instead. In particular $\mathrm{SIR}_{\max} = 16.5$ dB and $\rho^* = 0.2$. System L achieves even better performance, and $\mathrm{SIR}_{\max} = 15.55$ dB and $\rho^* = 0.25$. Thus the use of bit interleaving, differential encoding, and packet-level iterative detection results in an improvement of 4 dB in $\mathrm{SIR}_{\max}$ and a five-fold increase in ρ^* compared with one-shot detection.

The detection complexity of both system B and system K is less than 1% greater than the complexity of one-shot detection. The increase in the detection complexity that results from using system L is slightly greater than 1%. Thus for the two-path, Rayleigh-fading channel, the substantial performance gains for all values of ρ with packet-level iterative detection are achieved at very little cost in the average number of EE decoding attempts.

The performance of systems A, B, K and L is shown in Figure 6.5 for a three-path, Rayleigh-fading channel with partial-band interference. The paths have equal average strength, their delays are 0, T and $2T$, and the normalized Doppler spread of the channel is 1.5×10^{-4}. For system A, $\mathrm{SIR}_{\max}$ and ρ^* are 17.1 dB and 0.1 respectively. If system B is used instead, there is a modest improvement for all values of ρ, with $\mathrm{SIR}_{\max}$ decreasing to 16.35 dB and ρ^* increasing to 0.15. The performance improves further over the full range of ρ if system K is used, and $\mathrm{SIR}_{\max} = 14.7$ dB and $\rho^* = 0.25$. System L achieves the best performance of all four systems for each value of ρ, and $\mathrm{SIR}_{\max} = 13.9$ dB and $\rho^* = 0.3$. Thus system L exhibits a 3.2 dB in $\mathrm{SIR}_{\max}$ and a three-fold increase in ρ^* compared with system A. Note that the increased diversity available with the three-path fading channel results in uniformly better performance of all four systems in this channel than in the two-path fading channel. The detection complexity of both system B is less than 1% greater than the complexity of system A, and the complexity of system K is approximately 1% greater than the complexity of system A. The increase in the detection complexity that results from using system L is in the range of 3-4% for the worst-case values of ρ.

6.4 Comparison of Per-Dwell and Packet-Wide Bit Interleaving

In each of the systems considered thus far in this chapter, the bit interleaving (if any) is restricted to interleaving within rows of the block code-symbol interleaver. Packet-wide bit interleaving is considered above in Chapter 4 in the format of system G, which employs packet-wide, s-random bit interleaving but not differential encoding. It is shown that the performance of system G is comparable to or slightly poorer than system D (which uses per-dwell bit interleaving but not differential encoding) in static multipath channels but much poorer than the performance of system D in fading multipath channels.

The key factor in the poorer performance of system G in the latter instance is the fact that an unfavorable channel impulse response in any dwell interval affects the binary representation of a larger number of R-S code symbols if packet-wide bit interleaving is used than if it is not. More specifically, the use of packet-wide bit interleaving results in the unfavorable conditions of a single dwell interval affecting multiple R-S code symbols from some or all R-S code words and thus increasing the probability of decoding failure for those code words. The same effect arises in a channel that is subjected to partial-band interference, with the consequences illustrated in Figure 6.6. The performance is shown in Figure 6.6 for four systems and a single-path static, partial-band-interference channel. One is system K (which uses per-dwell bit interleaving but not differential encoding), and another is system L (which uses per-dwell bit interleaving and differential encoding). The third system is system G (which uses packet-wide, s-random interleaving and no differential encoding) and the fourth is a variant of system G that uses packet-wide, s-random interleaving together with per-dwell differential encoding.

It is seen from Figure 6.6 that regardless of whether or not packet-wide bit interleaving is used, the introduction of differential encoding leads to uniformly better performance. At the same time, per-dwell bit interleaving results in uniformly better performance than packet-wide bit interleaving regardless of whether differential encoding is used. The difference between the performance with packet-wide bit interleaving and the performance with per-dwell bit interleaving is most pronounced in the presence of partial-band interference. Note in particular that neither system with packet-wide bit interleaving is able to achieve acceptable performance in the presence of severe partial-band interference even if the fractional interference bandwidth is very small. There is negligible performance difference for the two interleaving techniques in the presence of full-band Gaussian noise, which is in agreement with the observations in Chapter 4. If differential encoding is used, for example, the replacement of packet-wide bit interleaving with per-dwell bit interleaving results in a decrease in $\mathrm{SIR}_{\max}$ from 10.8 dB to 8.3 dB and an increase in ρ^* from zero to 0.3. The two systems differ in performance by only a small fraction of one decibel in full-band noise, however. Per-dwell interleaving and differential encoding results in uniformly better performance than the other three systems.

6.5 Performance with a Dwell-Erasure Threshold

The performance of packet-level iterative detection with the dwell-erasure technique is examined for two static multipath channels and the dwell-erasure variants of two SFH systems: system K, which uses packet-level iteration and bit interleaving but not differential encoding; and system L, which uses differential encoding as well. (Recall that it is used in addition to per-symbol erasure decisions.) The performance of system K is shown in Figure 6.7 for a single-path static, partial-band-interference channel and various choices of the dwell-erasure threshold γ. The system with a threshold of $\gamma = 22$ corresponds to system K using per-symbol erasures only. For this system, the values of SIR_{max} and ρ^* are 9.6 dB and 0.3 respectively. As the dwell-erasure threshold is decreased, the value of SIR_{max} increases and the value of ρ^* also increases. With a dwell-erasure-threshold of $\gamma = 2$, for example, the value of SIR_{max} is 11.7 dB and ρ^* is 0.55. Thus a more aggressive dwell-erasure policy at the receiver results in improved protection against severe partial-band interference at the price of greater vulnerability to full-band Gaussian noise. For dwell-erasure threshold values of $\gamma = 5$ and $\gamma = 7$, the performance penalty with the respect to SIR_{max} is small and yet have much larger values of ρ^* than does the system with per-symbol erasures only. For system K employing dwell erasures with $\gamma = 5$, a value of $\rho^* = 0.5$ is achieved at the cost of an increase of only 0.1 dB in SIR_{max} compared with per-symbol erasures only.

The performance of system L is shown in Figure 6.8 for the same single-path channel and various choices of the dwell-erasure threshold γ. Once again, the system with a threshold of $\gamma = 22$ corresponds to the use of per-symbol erasures only. The choice of the dwell-erasure threshold provides the same tradeoff between protection against severe partial-band interference and full-band Gaussian noise that was observed above with system K. In this instance, however, if a decrease in γ is sufficient to obtain a significant improvement in ρ^* compared with per-symbol erasures only, it also results in a significant increase in SIR_{max} compared with per-symbol erasures only. Thus it is not possible to choose a dwell-erasure threshold in system L that provides a "nearly free" improvement in the protection against severe partial-band interference provided by per-symbol erasures only.

The introduction of differential encoding results in a higher probability of channel-symbol error during detection in the first packet-level iteration in exchange for a potential improvement in detection performance that results in subsequent packet-level iterations. Thus for a particular choice of the dwell-erasure threshold, a system that employs differential encoding need not result in improved performance over a system in which differential encoding is not employed. Thus is illustrated by comparing Figures 6.7 and 6.8. System L achieves better performance than system K for all values of ρ if per-symbol erasures only are employed or if dwell erasures are employed with $\gamma = 11$. If $\gamma = 7$, the performance of the two systems is similar, and system K results in better performance than system L if a dwell-erasure threshold of $\gamma = 5$ or $\gamma = 2$ is used.

The performance of systems K and L is shown in Figures 6.9 and 6.10, respectively, for various choices of the dwell-erasure threshold γ and the same three-path static, partial-band-interference channel considered in previous examples in this chapter. The same tradeoff between ρ^* and $\mathrm{SIR}_{\max}$ observed with the single-path channel occurs in both systems with the three-path channel as well. If only per-symbol erasures are used, the performance of system K is characterized by $\mathrm{SIR}_{\max} = 10.3$ and $\rho^* = 0.3$. If the dwell-erasure-threshold is $\gamma = 2$ instead, the value of $\mathrm{SIR}_{\max}$ is 14.75 dB and the value of ρ^* is 0.56. Moreover, any choice of the threshold γ that results in a meaningful increase in the value of ρ also results in a significantly higher value of $\mathrm{SIR}_{\max}$.

The performance of system L in the three-path channel is characterized by $\mathrm{SIR}_{\max} = 10.9$ and $\rho^* = 0.35$ if only per-symbol erasures are used. If instead $\gamma = 2$, the values of $\mathrm{SIR}_{\max}$ and ρ^* are 15.1 dB and 0.56, respectively. For a given large dwell-erasure threshold, system L results in a slightly larger value of ρ^* than system K at the cost of a larger value of $\mathrm{SIR}_{\max}$. For a small dwell-erasure threshold, the two systems results in comparable values of ρ^* while system L still exhibits poorer performance in full-band Gaussian noise. Thus the range of channel parameters and erasure threshold for which system L is better than system K is much narrower with the three-path channel than with the single-path channel, which is consistent with the observations in Chapter 5 concerning the effect of differential encoding when communicating over multipath channels.

In either system K or system L, the range of values of ρ can be subdivided into regions in which a given choice of the dwell-erasure threshold γ is optimal. For example for system L and the single-path channel, a threshold of $\gamma = 2$ results in the best performance for values of ρ between zero and 0.55 and a threshold of $\gamma = 22$ (per-symbol erasures only) results in the best performance for values of ρ between 0.55 and one. The best of these performances over the full range of values of ρ is achieved if the receiver employs *parallel detection* [55] on a per-packet basis. That is, the receiver employs two (or more) independent packet-level iterative equalization-and-decoding algorithms with each employing a different value of the dwell-erasure threshold.

Since an undetected decoding error occurs with a low probability in the bounded-distance EE decoder of the R-S code words, parallel decoding produces one of three outcomes with a very high probability: both packet-level iterative detection algorithms detect the (same) correct packet, one algorithm detects the correct packet and the other experiences detection failure, or both algorithms experience detection failure. In each instance, parallel detection results in an unambiguous result of either the correct packet or a failed packet detection. (The probability of incorrect detected-packet decisions from either of the parallel detectors can be made even lower by using a high-rate CRC code as an outer code for the packet contents and a corresponding CRC error-detection decoder.)

Parallel detection using two packet-level iterative detectors with different dwell-erasure thresholds thus results in performance that is given by the lower envelope of the performance curves for the two individual detectors. If parallel detection is used in system K with two parallel detectors using respective thresholds of $\gamma = 22$ and $\gamma = 2$ in the single-path channel, the resulting values of $\mathrm{SIR}_{\max}$ and ρ^* are 9.6 dB and 0.55 respectively. System L with two parallel detectors using the same thresholds results in $\mathrm{SIR}_{\max} = 8.3$ dB and $\rho^* = 0.55$, which is better than the performance of the parallel detector based on system K. The best performance in the three-path channel is obtained with two parallel detectors of system K using respective thresholds of $\gamma = 22$ and $\gamma = 2$. The performance of parallel detection in this instance is characterized by $\mathrm{SIR}_{\max} = 10.3$ dB and $\rho^* = 0.56$.

The detection complexity of parallel detection on a per-packet basis is the sum of the complexities of the constituent packet-level iterative detection algorithms. Thus typical values for the detection complexity of parallel detection is on the order of one to four EE decoding attempts per R-S code word, depending on the system and dwell-erasure threshold for each constituent packet-level iterative detector and the channel parameters. The constituent iterative detectors can be exploited more effectively if they share information after each packet-level iteration of the two detectors. Aside from the effect on the low-probability event of an undetected packet-detection error, this sharing in the parallel detector is guaranteed to result in better performance than parallel detection using independent constituent detectors and to do so with a lower detection complexity than with the independent constituent detectors. It may be possible to obtain additional improvements in performance by also adapting the dwell-erasure decisions in each constituent detector after each packet-level iteration based on the results of previous iterations. (The same adaptive dwell-erasure technique could also be employed with a single packet-level iterative detector.)

6.6 Performance with the Generalized Parity-Bit Method

The performance of packet-level iterative detection with the generalized parity-bit method is examined for two static multipath channels and the corresponding variants of SFH systems K and L. (Recall that with this method, erasure decisions are made only on a per-block basis for each block of R-S code symbols encoded with a single bit of parity.) The performance of system K is shown in Figure 6.11 for a single-path static, partial-band-interference channel and various choices of the parity-block size N_p.

The system with a block size of $N_p = 1$ corresponds to system K using per-code-symbol parity encoding. For this system, the values of $\mathrm{SIR}_{\mathrm{max}}$ and ρ^* are 9.6 dB and 0.3 respectively. As the parity-block size is increased, the value of $\mathrm{SIR}_{\mathrm{max}}$ increases and the value of ρ^* is non-decreasing. Any improvement in ρ^* with an increasing parity-block size N_p is negligible for a block size of eleven or less, however, whereas even an increase in the block size from one to two results in a substantial increase in $\mathrm{SIR}_{\mathrm{max}}$. Thus choices of the parity-block size between two and eleven, inclusive, results in performance that is essentially uniformly poorer than the performance of per-code-symbol parity encoding.

A meaningful tradeoff in performance for system K and the single-path channel is obtained only by considering a parity-block size of $N_p = 22$. (In this instance, there is only one parity bit per row of the block interleaver so that the generalized parity-bit technique results in a type of dwell-erasure technique.) The use of one parity bit per dwell interval results in a value of ρ^* of 0.35, and thus it provides somewhat better protection against severe partial-band interference than the system with per-code-symbol parity encoding. This performance gain is obtained only at the cost of an increase in $\mathrm{SIR}_{\max}$ from 8.3 dB to 12.6 dB, however. Furthermore, a comparison of Figure 6.11 with Figure 6.7 shows that the generalized parity-bit method with one parity-bit per dwell interval results in uniformly poorer performance than the dwell-erasure technique of the previous section with a dwell-erasure threshold of either two, five or seven. Thus the generalized parity-bit method does not provide a useful alternative to the dwell-erasure technique for system K and a single-path channel.

The performance of system L is shown in Figure 6.12 for the single-path static, partial-band-interference channel and various choices of the parity-block size N_p. When a parity bit is used with each R-S code symbol, the values of $\mathrm{SIR}_{\max}$ and ρ^* are 8.3 dB and 0.3 respectively. As was seen with system K, choices of the parity-block size between two and eleven for system L do not provide a useful tradeoff in comparison with the use of per-code-symbol parity encoding. The use of one parity bit per dwell interval instead of one parity bit per code symbol results in an increase in ρ^* from 0.3 to 0.4, but it also results in an increase in $\mathrm{SIR}_{\max}$ from 8.3 dB to 12.0 dB. Once again, however, the use of the generalized parity-bit method with one parity bit per dwell interval results in poorer performance than with the corresponding system using the dwell-erasure technique and a dwell-erasure threshold of either two, five or seven.

The performance of systems K and L is shown in Figures 6.13 and 6.14, respectively, for various choices of parity-block size N_p and the same three-path static, partial-band-interference channel considered in previous examples in this chapter. The same tradeoff between ρ^* and $\mathrm{SIR}_{\max}$ observed with the single-path channel occurs in both systems with the three-path channel as well. Once again for system K, the only alternative to per-code-symbol parity encoding that is of interest is the use of one parity bit per dwell interval. If N_p is increased from one to twenty-two, it results in an increase in ρ^* from 0.3 to 0.35, though at a cost of significant increase in $\mathrm{SIR}_{\max}$. Once again, however, the dwell-erasure technique with an appropriately chosen threshold result in better performance for system K in the three-path channel than does the generalized parity-bit method with one parity bit per dwell interval.

The performance of system L in the three-path channel is characterized by $\mathrm{SIR}_{\max} = 10.9$ and $\rho^* = 0.35$ if per-code-symbol parity encoding is used. If instead $N_p = 22$, the values of $\mathrm{SIR}_{\max}$ and ρ^* are 14.9 dB and 0.35, respectively. For this channel, per-code-symbol parity encoding results in uniformly superior performance in system L to any other choice of parity-block size. From these examples, it is apparent that the generalized parity-bit method by itself does not provide an interesting alternative to the dwell-erasure technique if the SFH system uses packet-level iterative detection. It is possible that the incorporation of the dwell-erasure technique with the generalized parity-bit method will lead to results of greater interest.

6.7 Comparison with Performance of Other SFH Systems in Partial-Band Interference

In this section we compare the performance of SFH systems employing packet-level iterative detection and R-S coding with the performance of several other SFH systems that have been considered in previous work by others. The other systems include two systems that employ one-shot detection and two systems that employ forms of iterative detection. In contrast with all the other results in this dissertation, each of the systems considered in this section employs orthogonal binary frequency-shift keyed (BFSK) modulation and noncoherent demodulation. Moreover, the transmission format of the SFH systems we have previously defined are modified in this section in that the transmission does not include a preamble sequence in any of the dwell intervals. (The modifications from the previous formats are made for the purpose of fair comparison with the other SFH systems.)

6.7.1 Description of SFH Systems Using Noncoherent Communications

Two of the systems using packet-level iterative detection and R-S coding that are described in Section 6.1 are also considered in this section: system K and system L. The transmission formats of the systems are modified by the introduction of BFSK modulation and the elimination of the preamble sequences, however. Thus the transmitted signal for a packet transmission beginning at $t = 0$ is given by

$$s(t) = \sqrt{2P} \sum_{i=0}^{n-1} \sum_{j=0}^{(m+1)\,N_s-1} \cos\left(j2\pi \left[f_i + (-1)^{d_{i\,((m+1)\,N_s)+j}} \frac{1}{2T} \right] t + \phi_{i,d_{i\,((m+1)\,N_s)+j}} \right) \times p_T\left(t - \left(i\left((m+1)\,N_s + N_e\right) + j\right)T\right)$$

where d_l is the lth channel symbol for the corresponding system and the other parameters are as defined for equation (6.1). (Note that $N_p = 1$, implicitly. The generalized parity-bit method is not considered in this section.) A reference polarity of zero is used to differentially encode the first bit of each dwell interval in system L.

The results in this section are restricted to consideration of a single-path static, partial-band-interference channel. Moreover, it is assumed for each of the six systems under consideration that the receiver has *a priori* knowledge of the fact that the channel consists of a single path and *a priori* knowledge of the symbol timing at the receiver. Thus it is not necessary for the receiver in any of the systems to address equalization of the received signal due to possible intersymbol interference, nor is it necessary for the receiver to estimate the optimal sampling time. For systems K and L in particular this eliminates the channel-estimation phase of dwell reception (hence the elimination of the preamble sequence). It results in a memoryless channel and separate per-channel-symbol decisions for each dwell interval in system K, and it in results in a two-state trellis that reflects differential encoding and a memoryless channel for each dwell interval in system L.

In contrast, it is assumed that the receiver in each system does *not* have any *a priori* information about the amplitude or carrier phase of the received signal, the noise and interference power, the presence of absence of interference within any given dwell interval or even the value of ρ. Thus if the receiver in a given system requires knowledge of the signal-to-interference-plus-noise ratio within a dwell interval or the fractional interference bandwidth (or any similar measure of signal quality), it must estimate the value of the parameter.

The packet format for systems K and L in this section consists of twenty-two $(32, 16)$ singly extended R-S code words. The receivers in systems K and L employ noncoherent demodulation and generate two square-law outputs for each of the two possible polarities for each transmitted channel symbol. In system K, the larger of two outputs determines a hard decision for that channel symbol. In system L, the two square-law outputs are used as branch metrics for the correspondingly labeled branches in the corresponding time step of the two-state detection trellis for the dwell interval. The detected channel symbols (or equivalently, the detected differentially encoded bits) are determined by using the Viterbi algorithm to determine the path through the trellis with the largest path metric. The remainder of the operation of packet-level iterative detection for system K and L is the same as for the systems using coherent communications.

One of the other SFH systems uses a packet format with twenty-seven (32,12) R-S code words. Each R-S code symbol is represented by five bits (the parity-bit method is not used), and the rectangular block code-symbol interleaving is employed. Each bit is transmitted using orthogonal BSFK modulation. The receiver employs noncoherent hard-decision detection of each channel symbol, it maps each detected five-bit representation to the corresponding R-S code symbol, and it performs one-shot errors-only (EO) decoding of each R-S code word. The system is referred to in this section as *system EO*, and the numerical results for system EO are taken from [35].

Another of the SFH systems uses the concatenation of a (32,24) R-S outer encoder and a rate-1/2 convolutional inner encoder. The packet format includes fifteen R-S code words and sixteen binary test symbols per dwell interval. Rectangular block code-symbol interleaving of the outer code words is used, and the resulting binary representation of code symbols in each interleaver row is encoded with the inner encoder prior to insertion of the test symbols. The receiver employs a weighted metric based on the number of test symbols resulting in errors in each dwell interval that is used in Viterbi decoding of the inner code for the dwell interval. The hard-decision output of the Viterbi decoder is mapped to detected R-S code symbols for one-shot EO decoding of the R-S code words. The system is referred to in this section as *system RC*. The details of system RC are given in [35], and the numerical results for the system are taken from the same paper.

One of the systems considered in this section employs a rate-1/3 PCC code with constituent (37,21) convolutional encoders of memory order of four, together with iterative MAP decoding of the constituent codes. The final system employs a rate 0.32 turbo product code with constituent (64,36,12) BCH codes together with iterative Fossorier-Lin decoding of the constituent codes. The systems using the PCC code and the turbo product code are described in detail in [26] and [30], respectively, and the numerical results for the systems are taken from the respective papers. They are denoted *system PCC* and *system TPC*, respectively.

The parameters of the six systems considered here are such that they represent a fair comparison with respect to packet transmission time, dwell duration, and information content for a given channel-symbol transmission rate. The key characteristics of systems EO, RC, PCC, and TPC are summarized in Table 6.5.

System	Interleaver	Encoding	Detection Algorithm
EO	rectangular, R-S code symbols	R-S coding	one-shot EO decoding
RC	rectangular, R-S code symbols	concatenated R-S and convolutional	one-shot EE decoding
PCC	packet-wide s-random	parallel convolutional codes	iterative MAP decoding
TPC	rectangular	BCH turbo-product code	Lin-Fossorier iterative algebraic decoding

Table 6.5 Characteristics of the additional SFH systems considered with noncoherent communications.

6.7.2 Performance in Partial-Band Interference for SFH Systems Using Noncoherent Communications

The introduction of differential encoding into a SFH system with packet-level iterative detection results in improved performance over a wide range of conditions in the partial-band-interference channel even in the absence of the channel-estimation errors discussed in Section 6.3. This is illustrated by comparing the performance of systems K and L with noncoherent communications for a single-path, partial-band-interference channel under the condition of perfect *a priori* knowledge of the symbol timing and the number of paths in the channel. The performance is shown in Figure 6.15. The performance of system K is characterized by $\mathrm{SIR}_{\max} = 14.6$ dB and $\rho^* = 0.23$. The value of ρ^* is approximately the same for system K and system L, but system L achieves substantially better performance than system K for all values of ρ that are greater than ρ^*. Indeed, the value of $\mathrm{SIR}_{\max}$ is only 12.0 dB for system L. The detection complexities of the two systems using noncoherent communications are almost identical to the complexities of the corresponding systems using coherent communications for the same single-path channel and each value of ρ.

The performance of system L using noncoherent communications with the dwell-erasure technique is shown in Figure 6.16 for the same single-path channel and several values of the dwell-erasure threshold γ. Recall that a dwell-erasure threshold of $\gamma = 22$ corresponds the use of per-symbol erasures only, and the resulting performance is given by $\mathrm{SIR}_{\max} = 12.0$ dB and $\rho^* = 0.23$. As was true for the system using coherent communications, a decrease in the dwell-erasure threshold in the system using noncoherent communications results in an improvement (increase) in ρ^* but a degradation in $\mathrm{SIR}_{\max}$.

Better performance can be obtained in system L with parallel detection of constituent packet-level iterative detectors with respective dwell-erasure thresholds of two and twenty-two (per-symbol erasures only). The resulting performance is characterized by $\mathrm{SIR}_{\max} = 12.0$ dB and $\rho^* = 0.45$. The worst-case detection complexity over all values of ρ is an average of only slightly more than one EE decoding attempt per code word for system L with a dwell-erasure threshold of two. The worst-case detection complexity over all ρ increases to an average of 1.7 EE decoding attempts per code word is system L uses per-symbol erasures only. Parallel detection with system L and erasures thresholds of two and twenty-two for the constituent detectors results in a worst-case detection complexity over all ρ of an average of 2.67 EE decoding attempts per R-S code word. As noted in Section 6.5, better performance can be obtained with lower detection complexity by sharing of information between the constituent detectors at each packet-level iteration.

The performance of system L with per-symbol erasures only is compared in Figure 6.17 with the performance of the other two systems using R-S codes: systems EO and RC. Clearly the use of packet-level iterative detection in system L results in better performance than either of the two systems using one-shot detection. System L results in an increase in ρ^* from 0.1 to 0.22 and an improvement of 4.2 dB in $\mathrm{SIR}_{\mathrm{max}}$ compared with system EO. It results in an improvement in ρ^* from 0.15 to 0.22 and a 2.0 dB decrease in $\mathrm{SIR}_{\mathrm{max}}$ compared with system RC. In full-band Gaussian noise, the performance of system L is 2.3 dB better than the performance of system EO and 0.6 dB better than the performance of system RC.

The performance of system L with two choices of the dwell-erasure threshold is compared in Figure 6.18 with the performance of system PCC and the performance of system TPC. The performance of system L with per-symbol erasures only results in performance that is uniformly poorer than the performance of either of the other two system. It results in a decrease in ρ^* from 0.285 to 0.22 and a degradation of 3.8 dB in $\mathrm{SIR}_{\mathrm{max}}$ compared with system TPC. Furthermore, it results in a decrease in ρ^* from 0.31 to 0.22 and a degradation of 2.55 dB in $\mathrm{SIR}_{\mathrm{max}}$ compared with system PCC. In full-band Gaussian noise, the performance of system L with per-symbol erasures only is 3.0 dB poorer than the performance of system TPC and 1.73 dB poorer than the performance of system PCC.

In contrast, the use of a dwell-erasure threshold of $\gamma = 2$ with system L provides a tradeoff between better protection against severe partial-band interference with system L and much better performance in full-band Gaussian noise with either system PCC or system TPC. In particular, the value of ρ^* for system L with an erasure threshold of two is 0.45, which is much greater than the corresponding values for systems PCC and TPC. The value of SIR_{max} is 7.3 dB greater for this variant of system L than for system PCC, however, and it 8.0 dB greater than for system TPC. In full-band Gaussian noise, the performance of system L with an erasure threshold of two is 6.5 dB poorer than the performance of system TPC and 5.3 dB poorer than the performance of system PCC.

The use of packet-level iterative detection with R-S coding is most competitive with the other codes using iterative decoding if it is employed with parallel detection. This is illustrated in Figure 6.19, which shows the performance of system PCC, the performance of system TCC, and the performance of system L with the parallel detector using constituent packet-level iterative detectors with dwell-erasures thresholds of two and twenty-two. The parallel detector results in much better protection against severe partial-band interference than either system PCC or TPC at the cost of a performance penalty in the presence of wide-band interference or noise that is much less severe than the penalty incurred using only an erasure threshold of two. As noted in Section 6.5 and earlier in this section, even better performance with parallel detection may be achieved if the receiver employs sharing of information between the constituent detectors and adaptation of the dwell-erasure threshold.

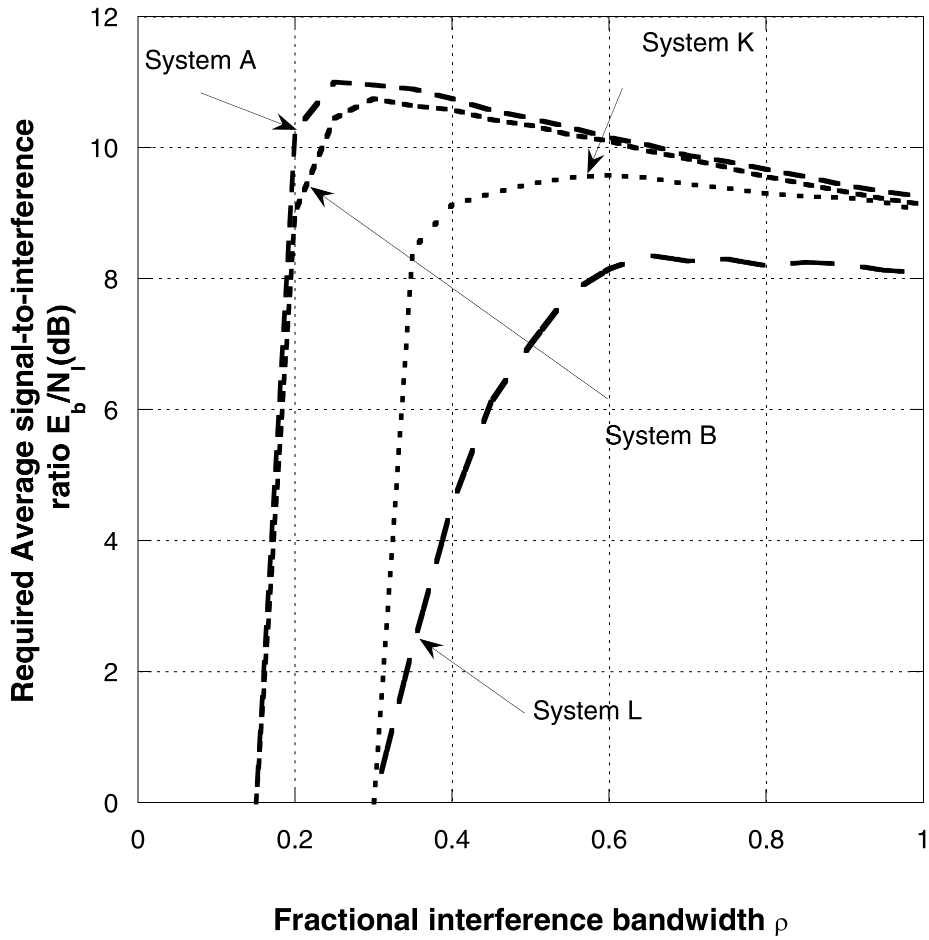

Figure 6.1 Performance in a single-path static, partial-band-interference channel.

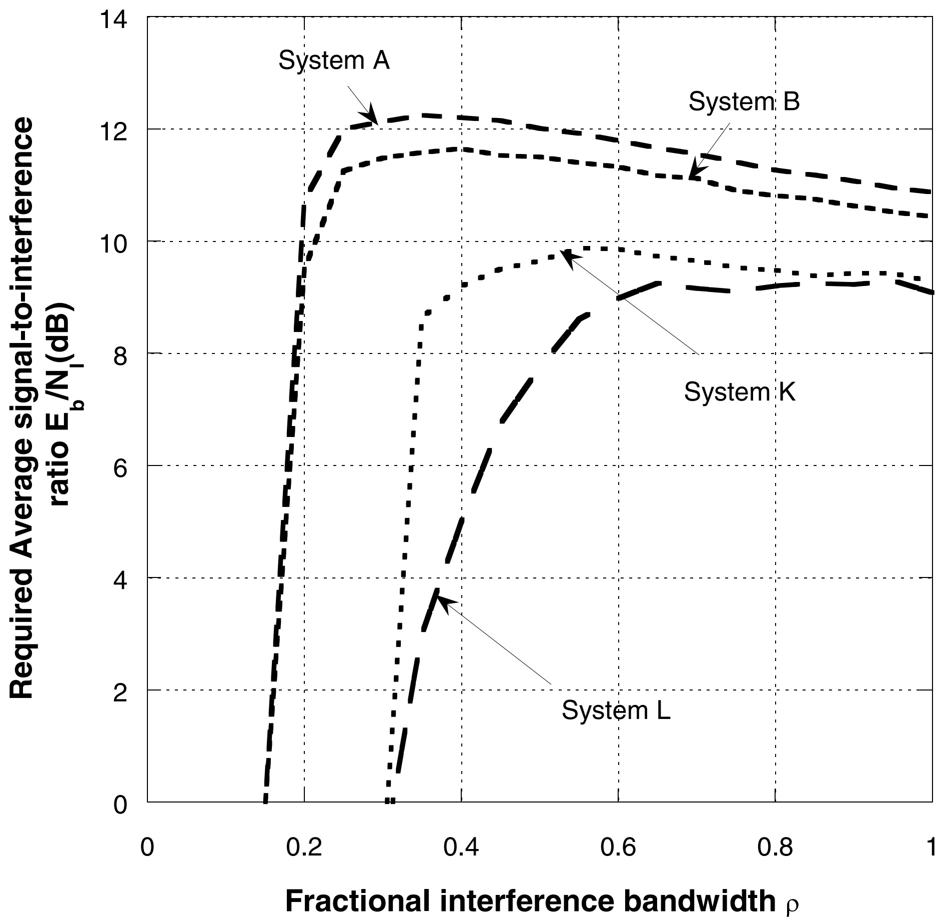

Figure 6.2 Performance in a two-path static, partial-band-interference channel.

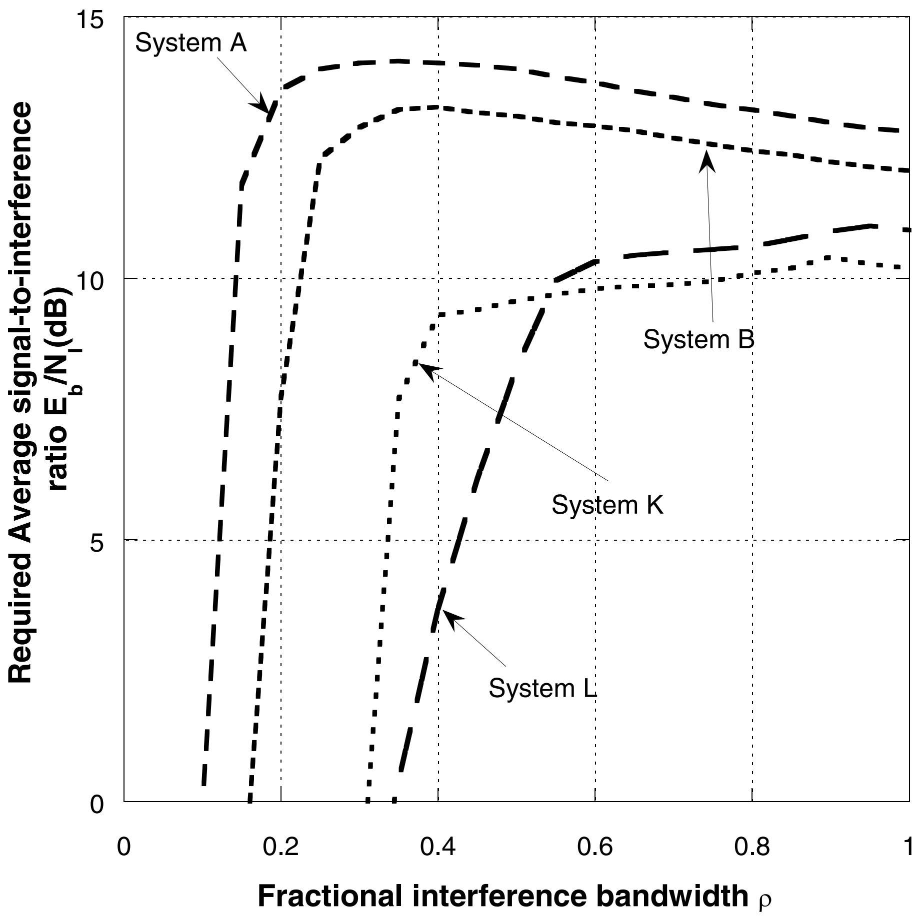

Figure 6.3 Performance in a three-path static, partial-band-interference channel.

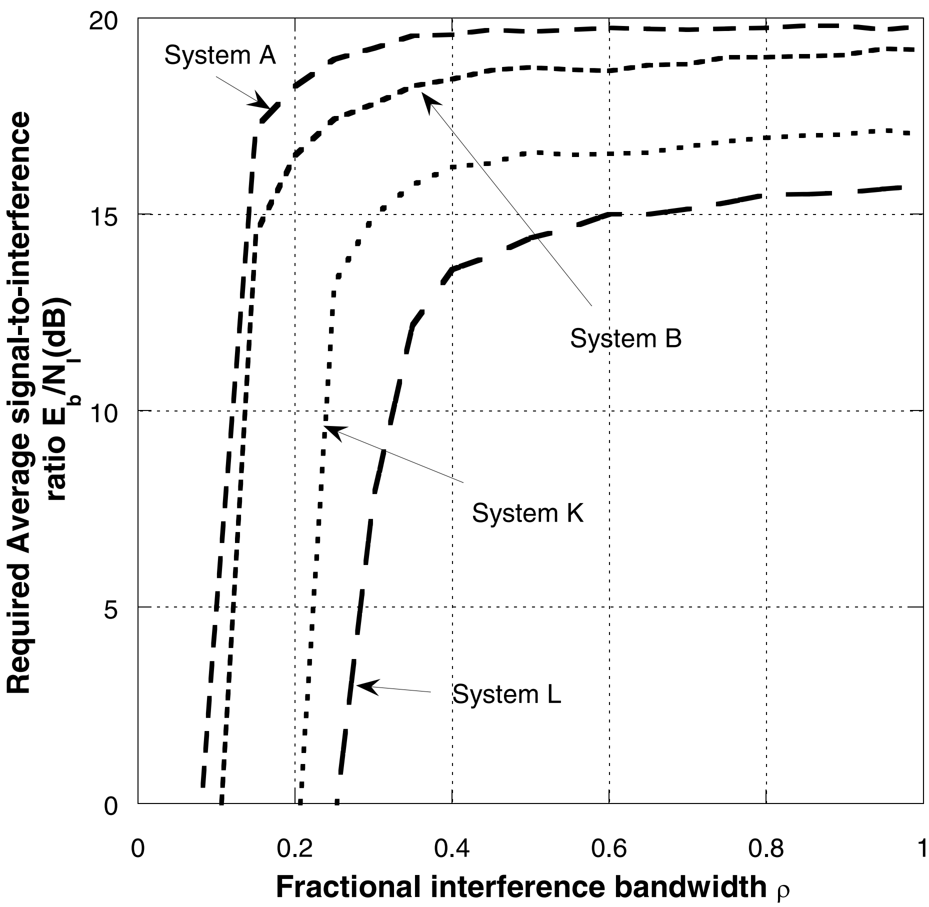

Figure 6.4 Performance in a two-path Rayleigh-fading, partial-band-interference channel.

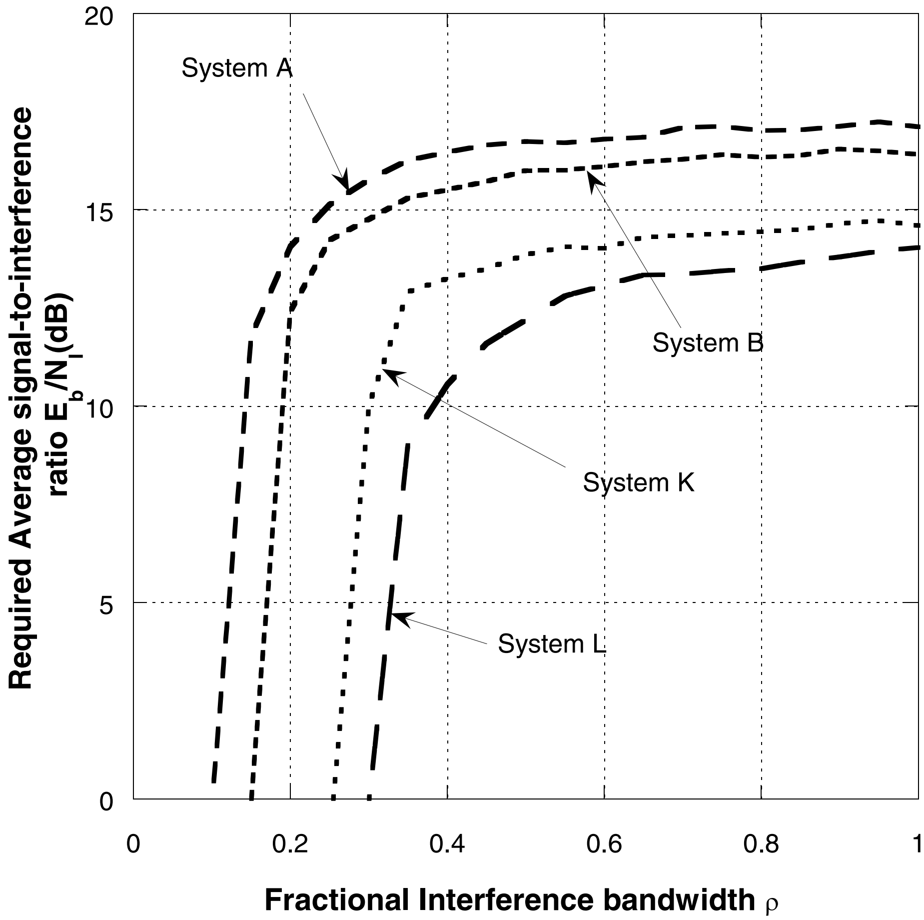

Figure 6.5 Performance in a three-path Rayleigh-fading, partial-band-interference channel.

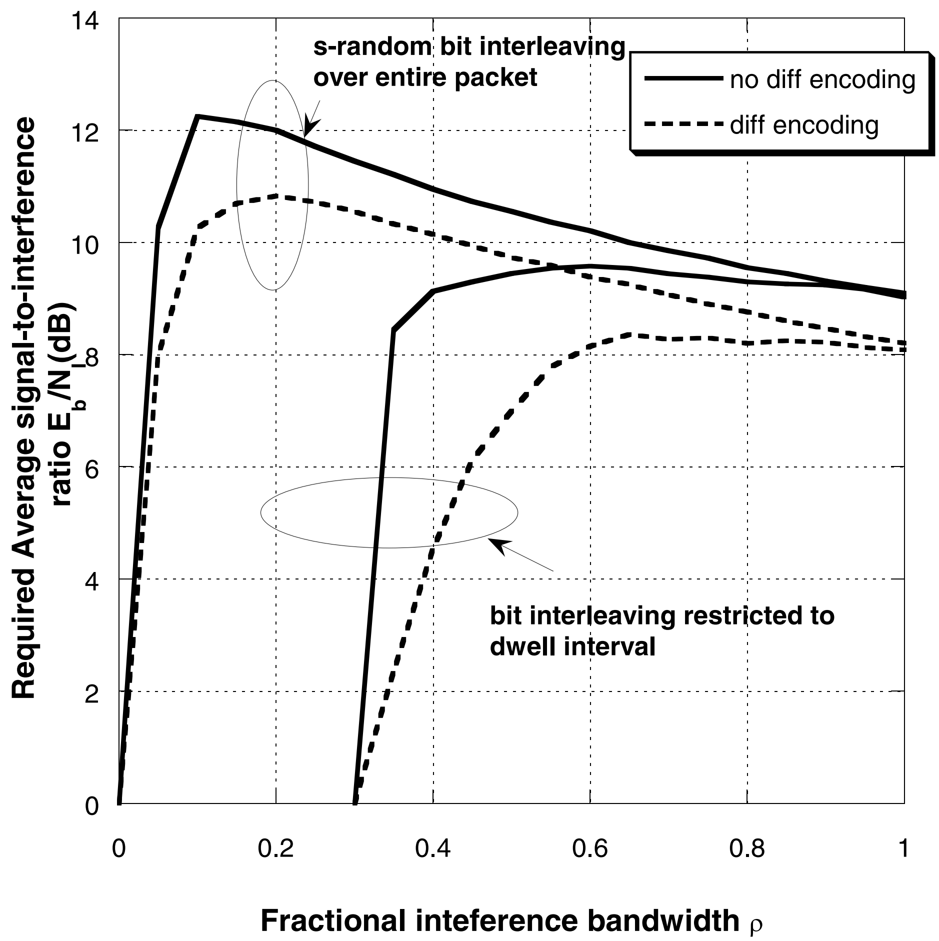

Figure 6.6 Performance in a single-path static, partial-band-interference channel with two types of interleaving.

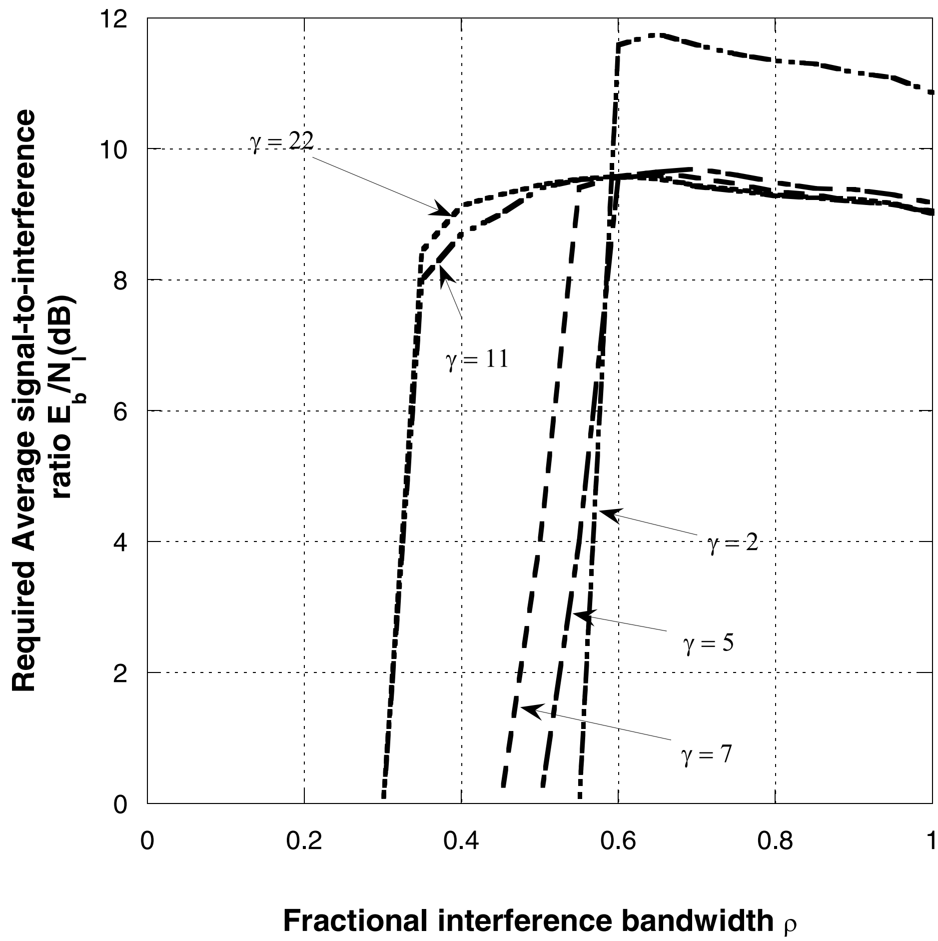

Figure 6.7 Performance of system K with dwell erasures in a single-path static, partial-band-interference channel.

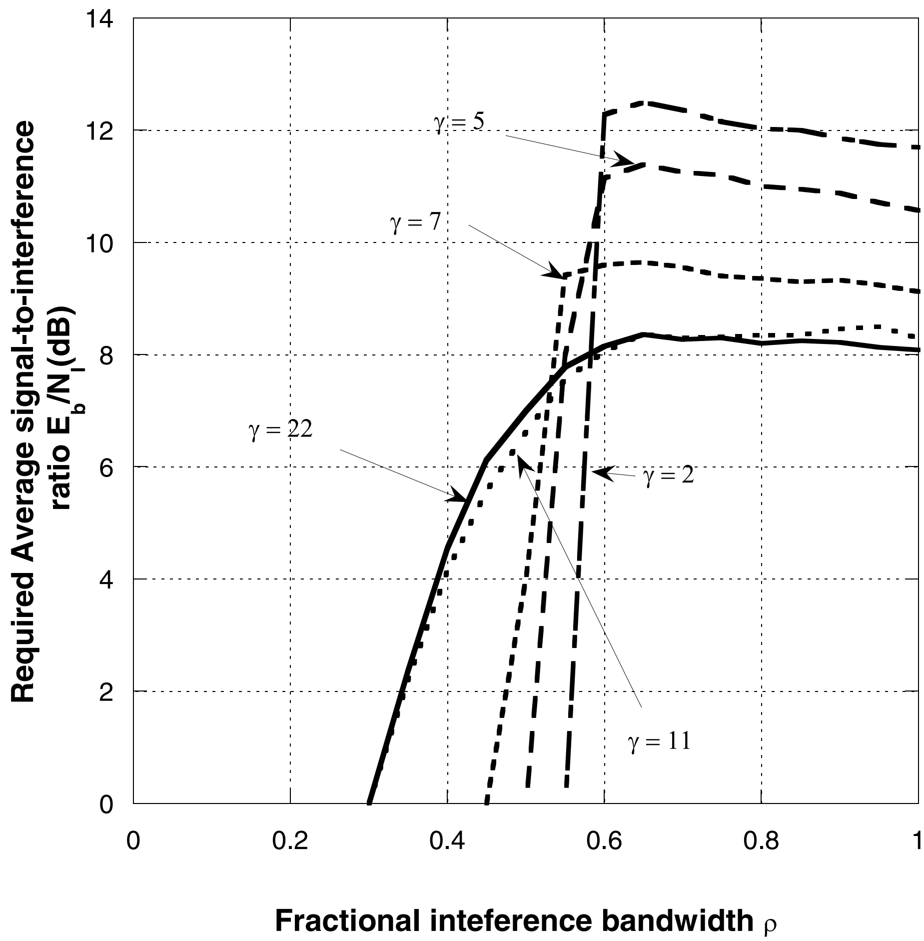

Figure 6.8 Performance of system L with dwell erasures in a single-path static, partial-band-interference channel.

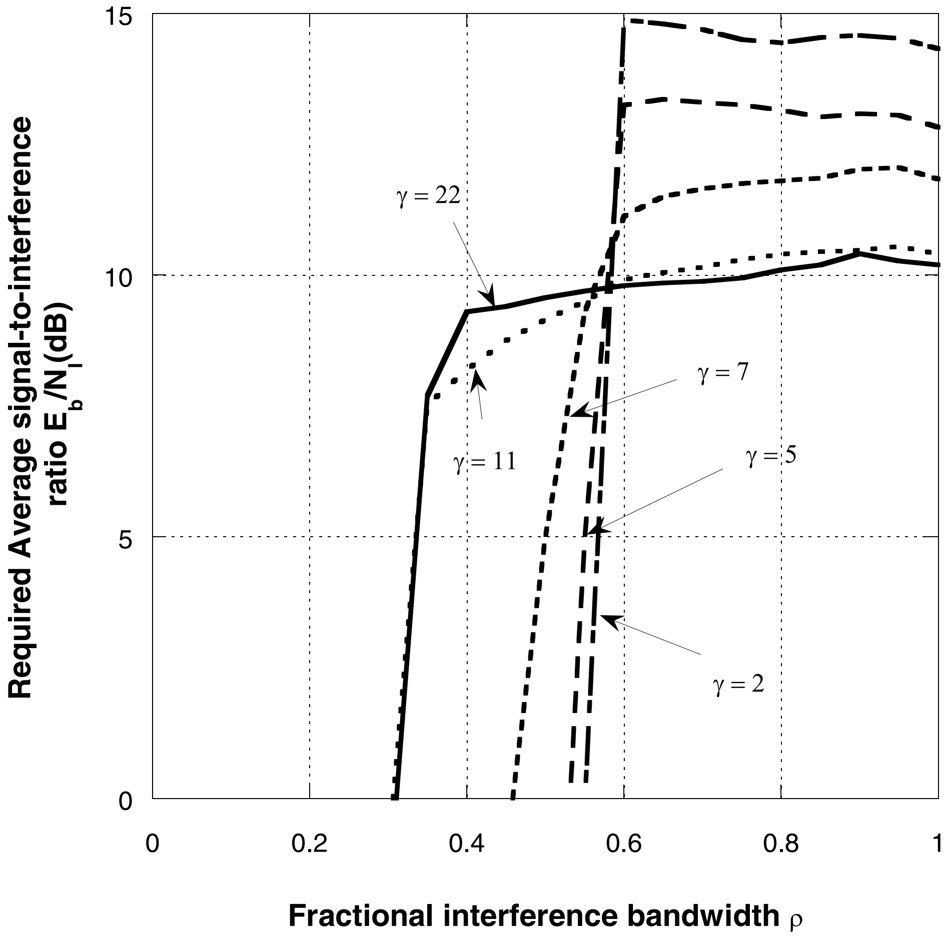

Figure 6.9 Performance of system K with dwell erasures in a three-path static, partial-band-interference channel.

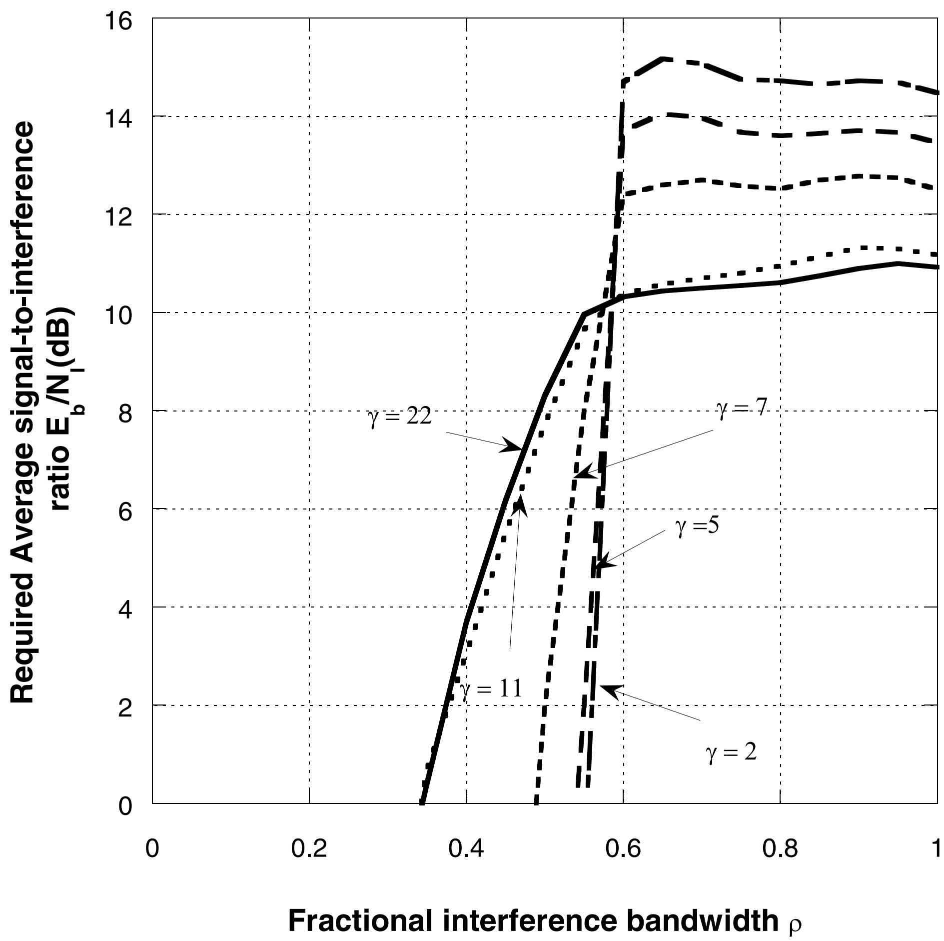

Figure 6.10 Performance of system L with dwell erasures in a three-path static, partial-band-interference channel.

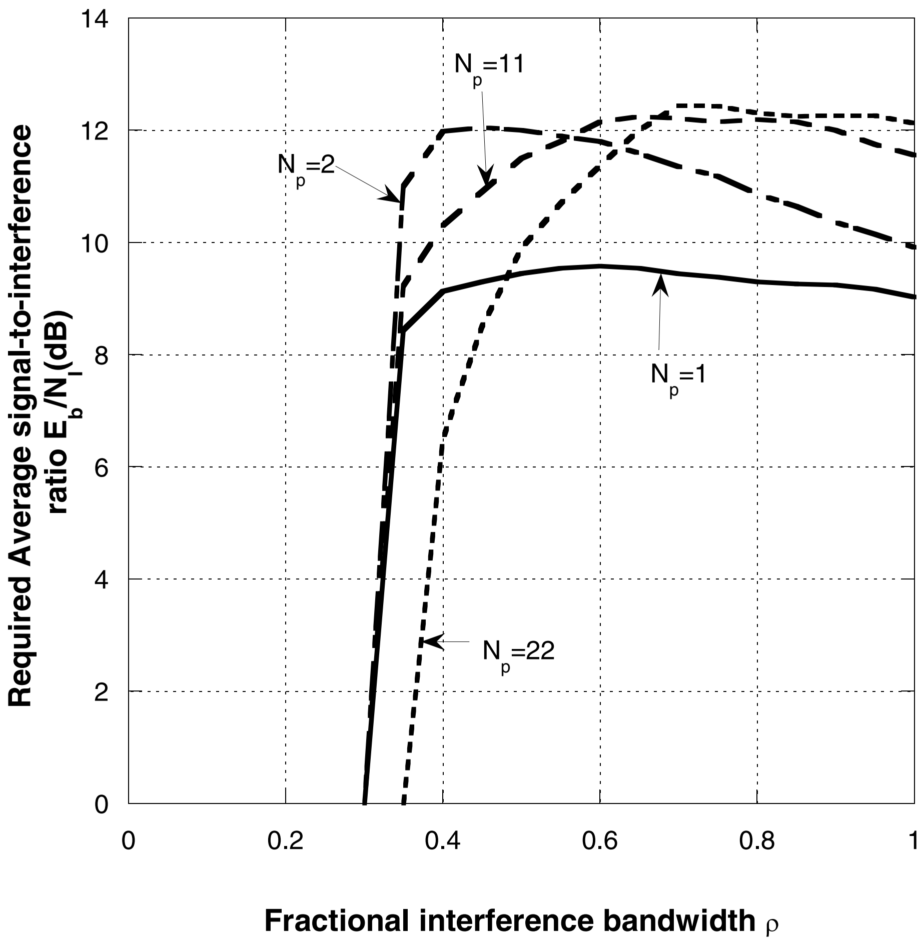

Figure 6.11 Performance of system K with generalized parity-bit method in a single-path static, partial-band-interference channel.

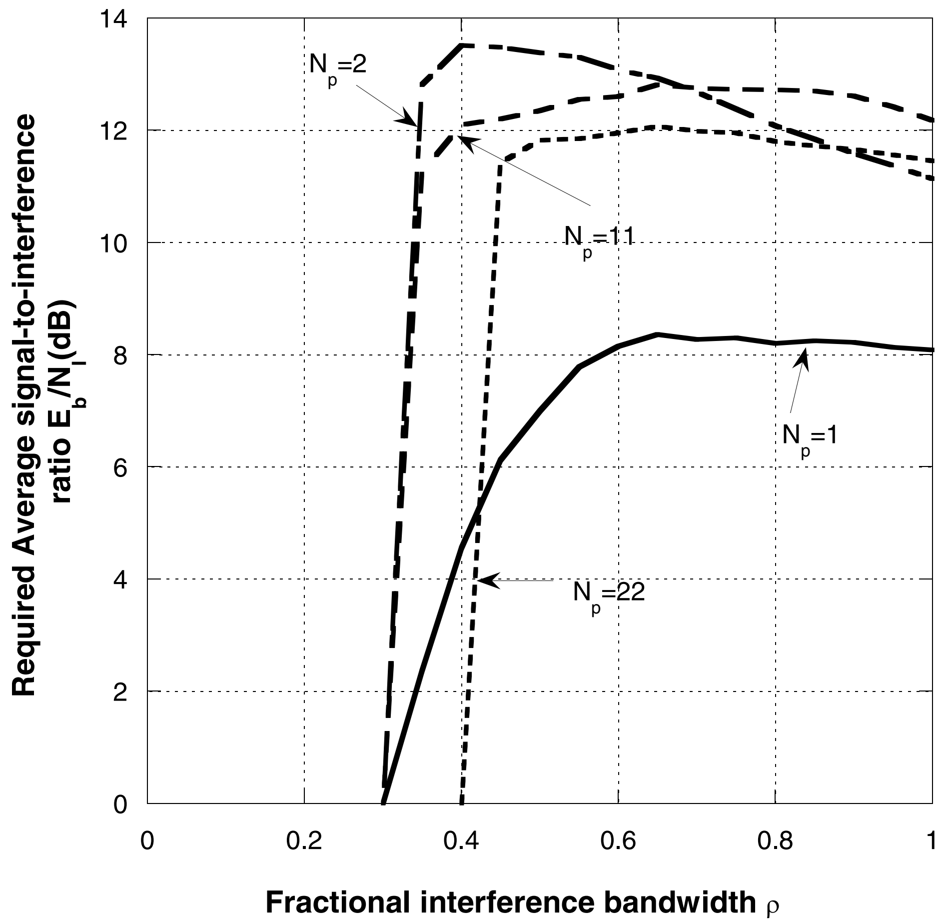

Figure 6.12 Performance of system L with generalized parity-bit method in a single-path static, partial-band-interference channel.

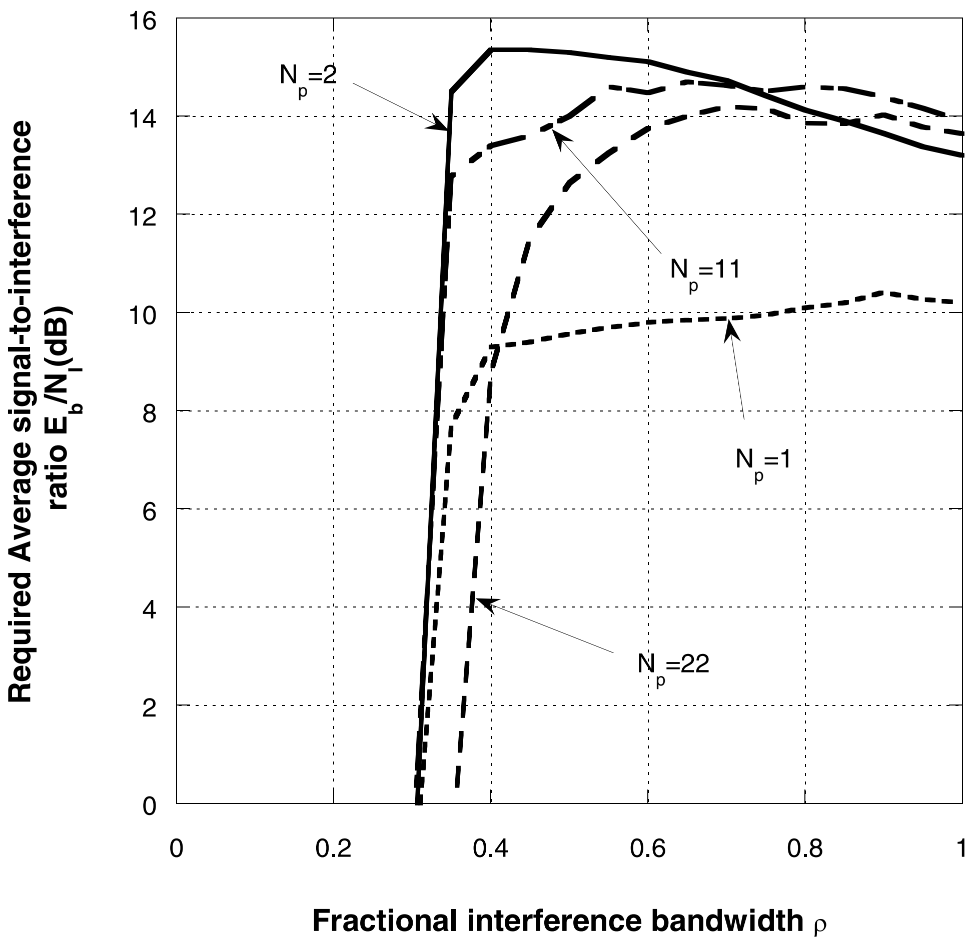

Figure 6.13 Performance of system K with generalized parity-bit method in a three-path static, partial-band-interference channel.

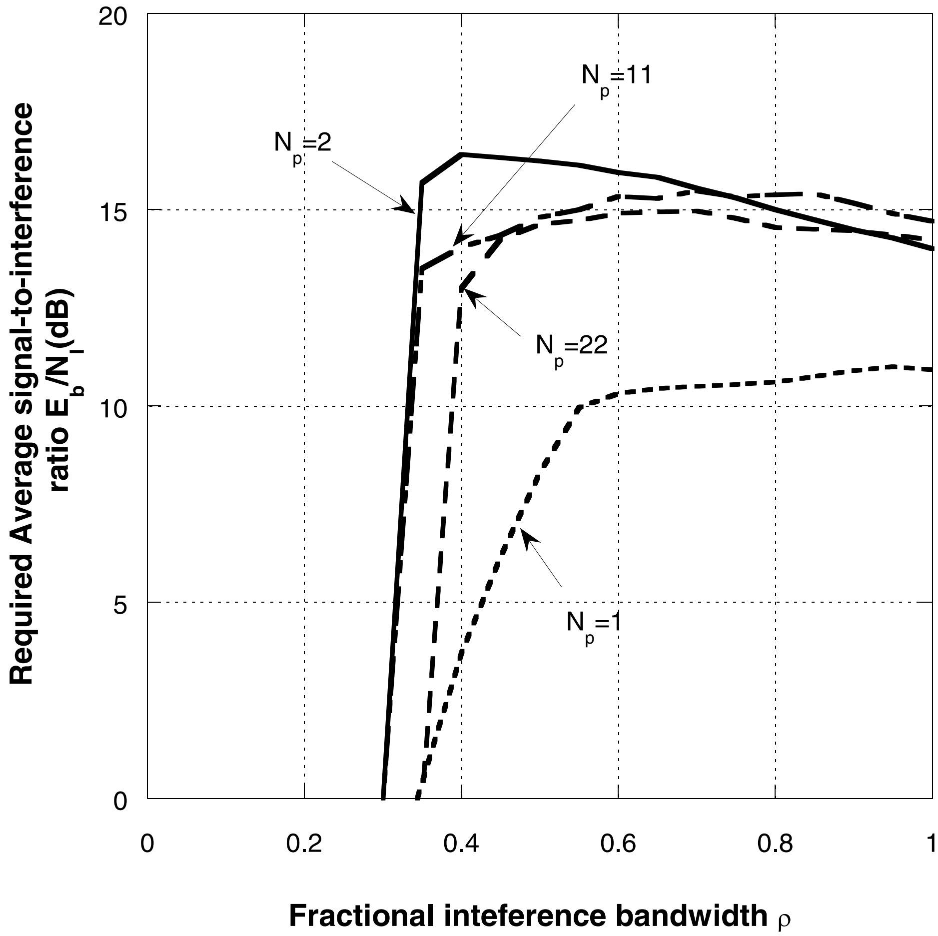

Figure 6.14 Performance of system L with generalized parity-bit method in a three-path static, partial-band-interference channel.

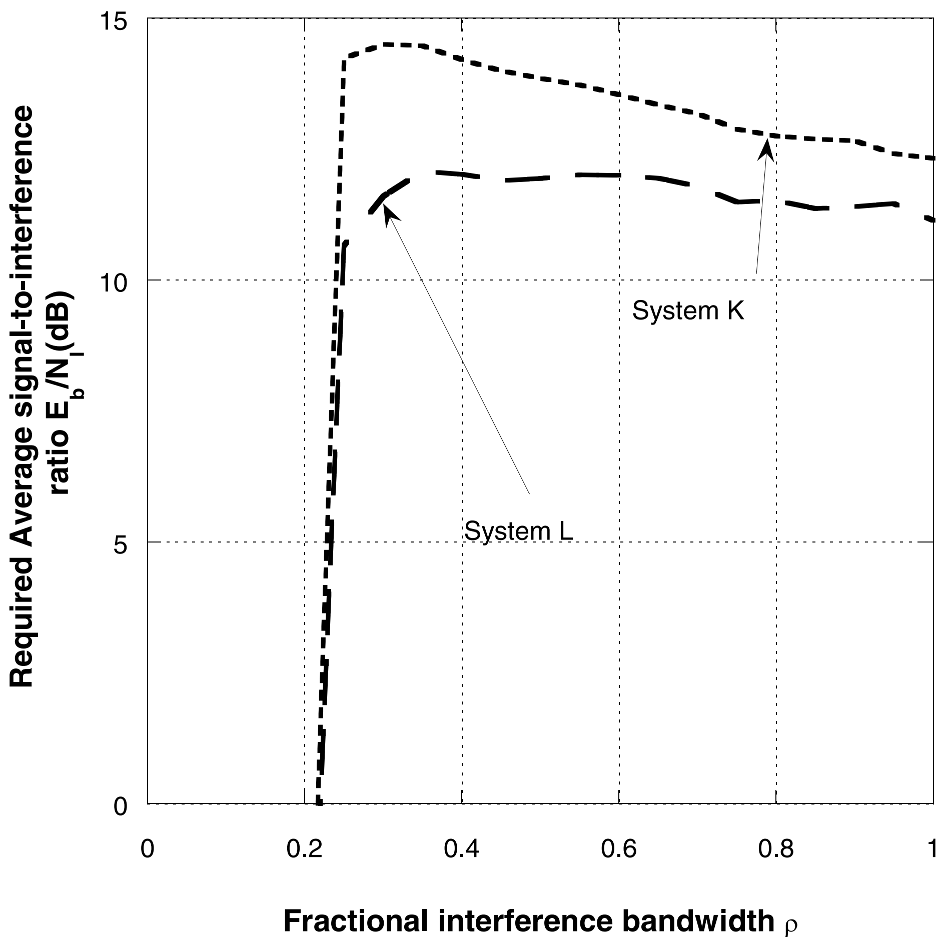

Figure 6.15 Performance with noncoherent communications and packet-level iterative detection and decoding in a single-path static, partial-band-interference channel.

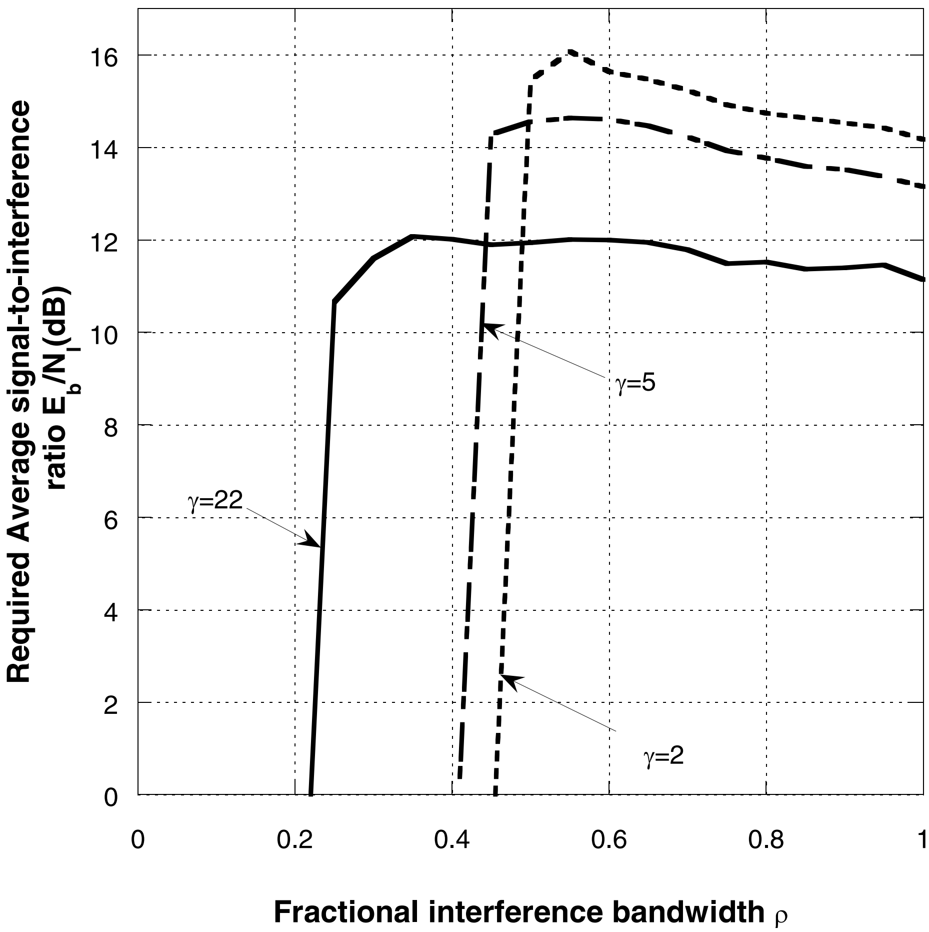

Figure 6.16 Performance of system L with noncoherent SFH communications and dwell erasures in a single-path static, partial-band-interference channel.

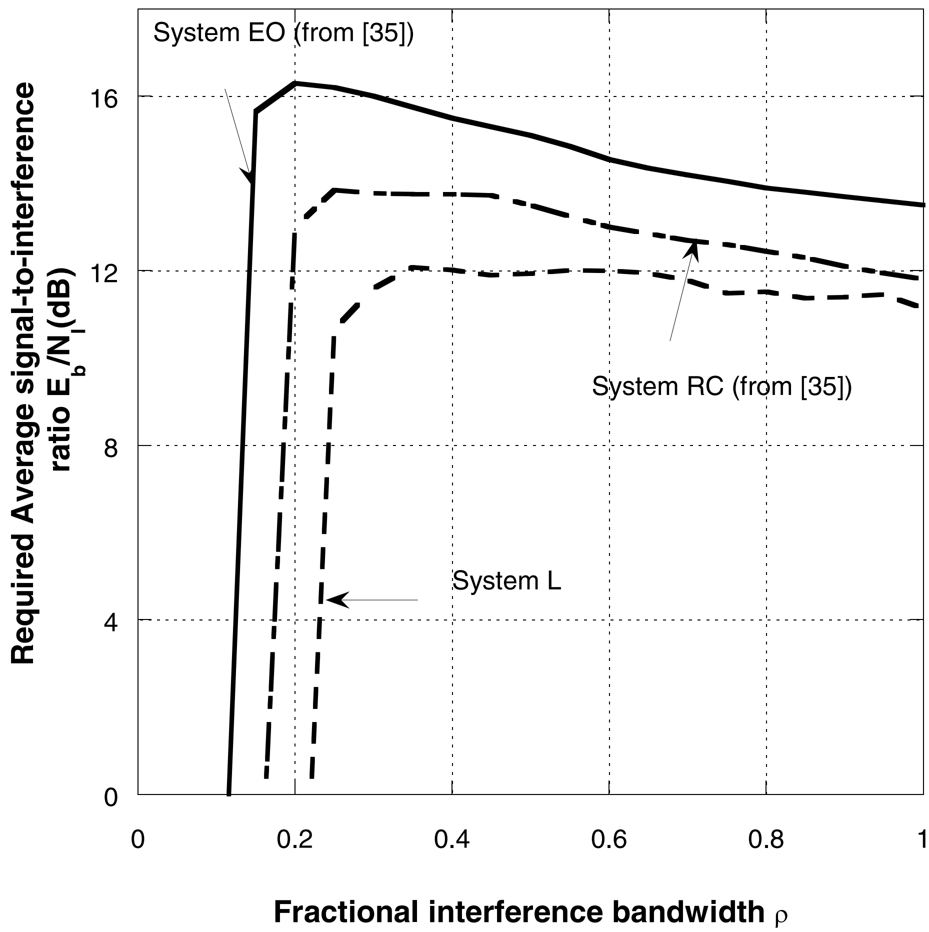

Figure 6.17 Performance of three noncoherent SFH systems using R-S codes.

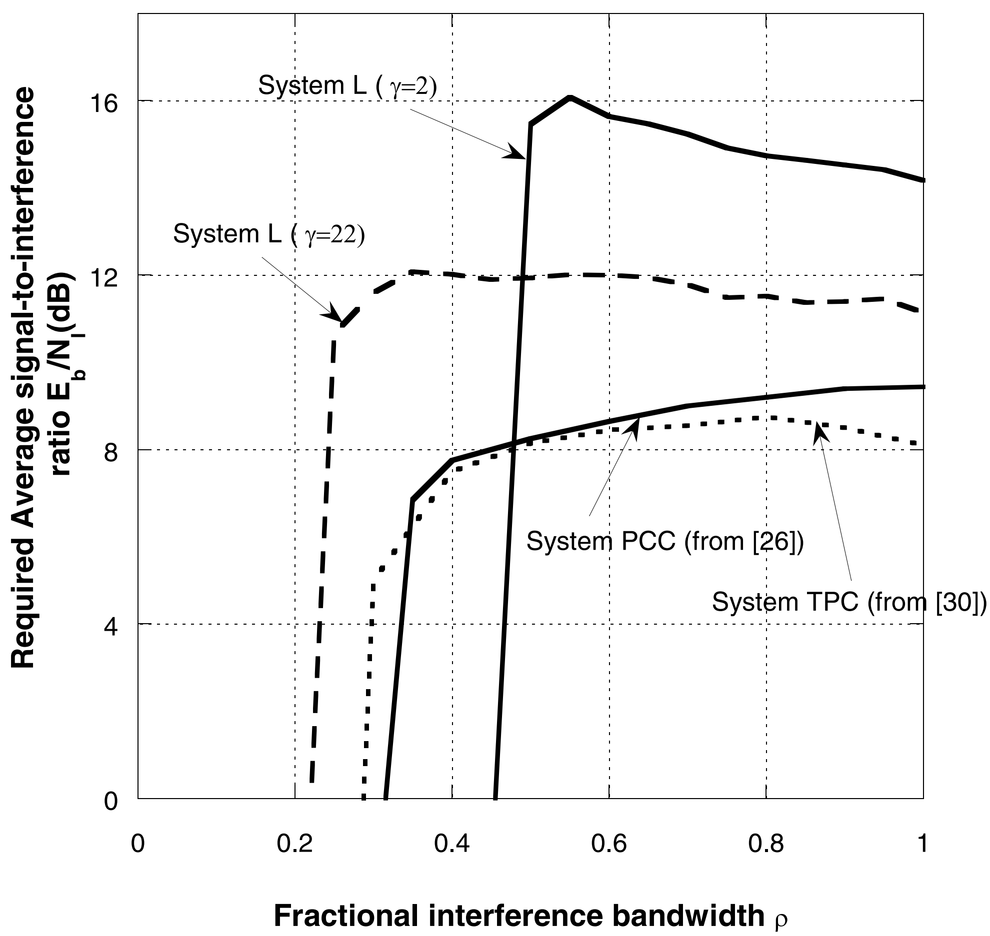

Figure 6.18 Performance of system L with dwell erasures and two other noncoherent SFH systems with iterative decoding.

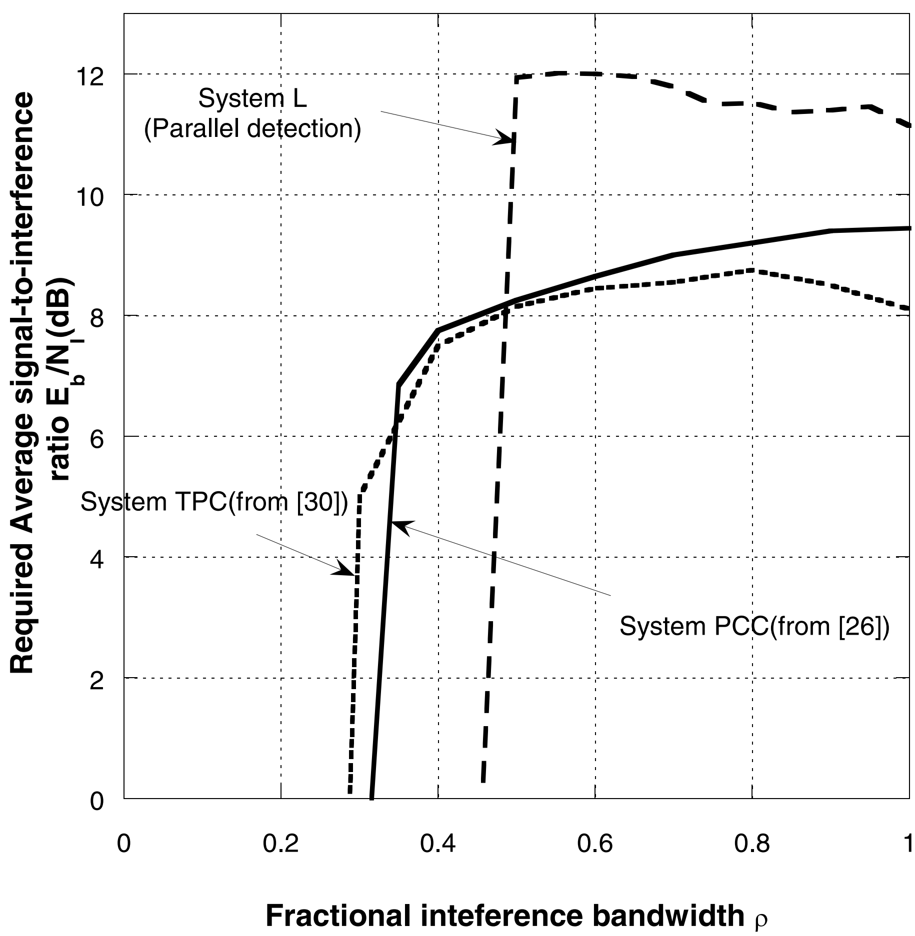

Figure 6.19 Performance of system L with parallel detection and two other noncoherent SFH systems with iterative decoding.

CHAPTER 7

CONCLUSIONS

In this dissertation, the performance of packet-level iterative MLSE equalization and EE decoding is evaluated for a variety of ISI channels. The technique results in a significant improvement in system performance compared with one-shot equalization and decoding at the cost of only a modest increase in detection complexity. The best performance with the technique is achieved if appropriate bit interleaving is employed. Performance gains on the order of 1.5 dB are obtained in static channels at the cost of a 60% increase in detection complexity, and gains on the order of $2-3$ dB are obtained in fading channels with an increase of only a few percent in the average detection complexity.

The use of differential encoding is also investigated for SFH systems using packet-level iterative detection. It is shown that differential encoding results in better asymptotic performance in an AWGN channel, and it results in only a modest increase in the detection complexity. For the packet sizes and error probabilities of interest for packet radio communications, differential encoding also yields performance improvements in static channels with moderate ISI. Differential encoding improves the performance of packet-level iterative detection over a much wider range of channel delay spreads if the channel exhibits fading with a modest increase in the detection complexity.

The performance of SFH systems using packet-level iterative detection is also evaluated for channels with partial-band interference. It is shown that the use of differential encoding with symbol-by-symbol erasures provide significantly higher robustness with respect to both partial-band and wideband interference than does one-shot channel-symbol detection and decoding. It also results in better performance than a system which employs concatenated

R-S and convolutional decoding with one-shot channel-symbol detection and decoding.

The use of dwell erasures is also considered in conjunction with packet-level iterative detection. It is shown that the choice of the dwell-erasure threshold provides a tradeoff between performance in partial-band interference and performance in full-band noise. Parallel decoding with packet-level iteration using the dwell-erasure technique in one decoder and only symbol-by-symbol erasures in the other decoder is also considered. It is shown that it results in performance that is better than packet-level iteration with symbol-by-symbol erasures only regardless of the fraction of the band that is subjected to interference, and the detection complexity is increased only about two-fold.

The performance of parallel decoding with R-S coding and packet-level iterative detection is also compared with the performance of two modern turbo codes and iterative decoding algorithms for a SFH system with noncoherent detection. It is shown that the system with R-S coding and packet-level iteration results in much better protection against partial-band interference at the cost of a moderately poorer performance in full-band noise. It is also noted how the performance of the parallel decoding system can be improved further by a more sophisticated use of the feedback in the packet-level iterations.

REFERENCES

1. M. B. Pursley "The role of spread spectrum in packet radio networks," *Proc. IEEE*, vol. 75, no. 1, pp. 116 – 134, Jan. 1987.

2. M. B. Pursley, "Reed-Solomon codes in frequency-hop communications," pp. 150–174 in *Reed-Solomon Codes and Their Applications*, V. K. Bhargava and S. B. Wicker, eds., New York: IEEE Press, 1994.

3. A. J. Viterbi, "A robust ratio-threshold technique to mitigate tone and partial-band jamming in coded MFSK systems," in *Proc. 1982 IEEE Military Commun. Conf.* (Boston, MA), pp. 22.4.1–22.4.5, Oct. 1982.

4. A. W. Lam and D. V. Sarwate, "A comparison of two methods for generation of side information in frequency-hop spread-spectrum multiaccess communications," in *Proc. 21st Annual Conf. Inform. Sci. Syst.* (Baltimore, MD), pp. 869–877, Mar. 1987.

5. C. W. Baum and M. B. Pursley, "Bayesian methods for erasure insertion in frequency-hop communications with partial-band interference,"*IEEE Trans. Commun.*, vol. 40, no. 7, pp. 1231–1238, July 1992.

6. D. E. Kammer, "SINCGARS - The new generation combat net radio system," in *Proc. 1986 Tactical Commun. Conf.* (Ft. Wayne, IN), pp. 64–72, Apr. 1986.

7. B. J. Hamilton, "SINCGARS system improvement program (SIP) specific radio improvements," in *Proc. 1996 Tactical Commun. Conf.* (Ft. Wayne, IN), pp. 397–406, Apr. 1996.

8. H. Ramchandran and D. L. Noneaker, "Adaptive equalization and Reed-Solomon coding in high-data-rate frequency-hop spread-spectrum communications," *Internat. J. Wireless Inform. Networks*, vol. 8, no. 2, pp. 61–74, Apr. 2001.

9. G. D. Forney, Jr., "Maximum-likelihood sequence estimation of digital sequences in the presence of intersymbol interference," *IEEE Trans. Inform. Theory,* vol. IT-18, no. 3, pp. 363–378, May 1972.

10. E. Paaske, "Improved decoding for a concatenated coding system recommended by CCSDS," *IEEE Trans. Commun.,* vol. 38, no. 8, pp. 1138–1144, Aug. 1990.

11. O. M. Collins and M. Hizlan, “Determinate state convolutional codes,” *IEEE Trans. Commun.,* vol. 41, no. 12, pp. 1785–1794, Dec. 1993.

12. H. Ramchandran and D. L. Noneaker, “A comparison of two iterative equalization-and-decoding techniques in frequency-hop spread-spectrum communications using Reed-Solomon coding,” in *Proc. of 2004 IEEE Vehicular Tech. Conf.* (Los Angeles, CA), pp. 1713–1717, Sept. 2004.

13. H. Ramchandran and D. L. Noneaker, “ Interleaver designs for low-complexity packet-level iterative equalization and decoding in SFH spread spectrum communications,” in *Proc. 8th Int. Symp. Comp. Theory and Appl.* (Ambleside, UK), pp 392–397, July 2005.

14. F. Magee and J. Proakis, “An estimate of the upper bound on error probability for maximum-likelihood sequence estimation on channels having a finite-duration impulse response,” *IEEE Trans. Inform. Theory*, vol. IT-19, no. 5, pp. 699–702, Sept. 1973.

15. J. G. Proakis, *Digital Communications*, 4th ed., New York: McGraw-Hill, 2001.

16. R. Anderson and G. Foschini, “The minimum distance for MLSE digital data systems of limited complexity,” *IEEE Trans. Inform. Theory*, vol. IT-21, no. 5, pp. 544–551, Sept. 1975.

17. S. Benedetto et al., “Serial concatenation of interleaved codes: performance analysis, design, and iterative decoding,” *IEEE Trans. Inform. Theory,* vol. 44, no. 3, pp. 909–926, May 1998.

18. K. R. Narayanan and G. L. Stüber, “A Serial Concatenation Approach to Iterative Demodulation and Decoding,” *IEEE Trans. Commun.,* vol. 47, no. 7, pp. 956–961, July 1999.

19. H. Ramchandran and D. L. Noneaker, “Packet-level iterative errors-and-erasures decoding for SFH spread-spectrum communications with Reed-Solomon codes and differential encoding,” in *Proc. of 2005 IEEE Military Commun. Conf.* (Atlantic City, NJ), vol.4, pp. 2610–2616, Oct. 2005.

20. H. Ramchandran and D. L. Noneaker, “Packet-level iterative detection for SFH communications with Reed-Solomon coding in partial-band interference,” in *Proc. 2006 IEEE Military Commun. Conf.* (Washington D.C), Oct. 2006.

21. M. B. Pursley, “Tradeoffs between side information and code rate in slow-frequency-hop packet radio networks,” in *Proc. of IEEE Int. Conf. Commun.* (Seattle, WA), vol. 2, pp. 947–952, June 1987.

22. C. Douillard et al., “Iterative correction of intersymbol interference: Turbo equalization,” *European Trans. Telecomm.*, vol. 6, no. 5, pp. 507–511, Sept.-Oct. 1995.

23. M. Tüchler, R. Koetter, and A. C. Singer, “Turbo equalization: Principles and new results,” *IEEE Trans. Commun.*, vol. 50, no. 5, pp. 754–767, May 2002.

24. J. L. Cromwell, G. Paparisto, and K. M. Chugg, “On the design and hardware demonstration of a robust, high-speed frequency-hopped radio for severe battlefield channels,” in *Proc. 2002 IEEE Military Commun. Conf.* (Anaheim, CA), pp. 899 –903, Oct. 2002.

25. J. H. Kang and W. E. Stark, “Turbo codes for coherent FH-SS with partial band interference,” in *Proc.1997 IEEE Military Commun. Conf.*(Monterey, CA), vol. 2, pp. 5–9, Nov. 1997.

26. J. H. Kang and W. E. Stark, “Turbo codes for noncoherent FS-SS with partial-band interference,” *IEEE Trans. Commun.*, vol. 46, no. 11, pp. 1451–1458, Nov. 1998.

27. J. H. Kang and W. E. Stark, “Iterative estimation and decoding for FH-SS with slow Rayleigh fading,” *IEEE Trans. Commun.*, vol. 48, no. 12, pp. 2014–2023, Dec. 2000.

28. H. Kim et al., “Anti-jamming performance of slow FH-CPM signals with concatenated coding and jamming estimation,” in *Proc. 2003 IEEE Military Commun. Conf.* (Boston, MA), pp. 1120–1125, Oct. 2003.

29. W. G. Phoel, “Iterative demodulation and decoding of frequency-hopped PSK in partial-band jamming,” *IEEE J. Selected Areas Commun.*, vol. 23 , no. 5, pp. 1026–1033, May 2005.

30. Q. Zhang and T. Le-Ngoc, “Turbo product codes for FH-SS with partial-band interference,” *IEEE Trans. Wireless Commun.*, vol. 1, no. 3, pp. 513–520, July 2002.

31. M. B. Pursley and J. S. Skinner, “Turbo product coding in frequency-hop wireless communications with partial-band interference,” in *Proc. 2002 IEEE Military Commun. Conf.* (Anaheim, CA), vol. 2, pp. 774–779, Oct. 2002.

32. S. Cheng and M. C. Valenti, “Turbo-NFSK: Iterative estimation, noncoherent demodulation, and decoding for fast fading channel,” in *Proc. 2005 IEEE Military Commun. Conf.* (Atlantic City, NJ), pp. Oct. 2005.

33. H. El Gamal and E. Geraniotis, "Iterative channel estimation and decoding for convolutionally coded anti-jam FH signals," *IEEE Trans. Commun.*, vol. 50, no. 2, pp. 321–331, Feb. 2002.

34. M. B. Pursley and W. E. Stark, "Performance of Reed-Solomon coded frequency-hop spread spectrum communications in partial-band interference," *IEEE Trans. Commun.,* vol. 33, no. 8, pp. 767–774, Aug. 1985.

35. C. D. Frank and M. B. Pursley, "Concatenated coding for frequency-hop spread-spectrum with partial band interference," *IEEE Trans. Commun.,* vol. 44, no. 3, pp. 377–387, March 1996.

36. T. G. Macdonald and M. B. Pursley, "Staggered interleaving and iterative errors-and-erasures decoding for frequency-hop packet radio," *IEEE Trans. Wireless Commun.,* vol. 2, no. 1, pp. 92-98, Jan. 2003.

37. G. W. Zeoli, "Coupled decoding of block-convolutional concatenated codes," *IEEE Trans. Commun.,* vol. COM-21, no. 3, pp. 219–226, Mar. 1973.

38. L.-N. Lee, "Concatenated coding systems employing a unit-memory convolutional code and a byte-oriented decoding algorithm," *IEEE Trans. Commun.,* vol. COM-25, no. 10, pp. 1064–1074, Oct. 1977.

39. S. B. Wicker, "Deep Space Applications," in *Handbook of Coding Theory* (V.Pless and W. P. Huffman, eds.), Amsterdam: Elsevier, 1998.

40. R. M. Pyndiah, "Near-optimum decoding of product codes: Block turbo codes," *IEEE Trans. Commun.*, vol. 46, no. 8, pp. 1003–1010, Aug. 1998.

41. M. K. Cheng and P. H. Siegel, "Iterative soft-decision Reed-Solomon decoding on partial response channels," in *Proc. 2003 IEEE Global Commun. Conf.* (San Francisco, CA), pp. 1588–1592, Dec. 2003.

42. M. Lamarca, J. Sala, and A. Martinez, "Advanced decoding algorithms for Reed-Solomon/convolutional concatenated codes," *Annals Telecommun.*, vol. 60, nos. 1-2, pp. 45–78, Feb. 2005.

43. D. Chase, "A class of algorithms for decoding block codes with channel measurement information,"*IEEE Trans. Inform. Theory,* vol. IT-18, no. 1, pp. 170–182, Jan. 1972.

44. R. Koetter and A. Vardy, "Algebraic soft-decision decoding of Reed-Solomon codes,"*IEEE Trans. Inform. Theory,* vol. 49, no. 11, pp. 2809–2825, Nov. 2003.

45. J. Jiang and K. R. Narayanan, "Iterative soft decoding of Reed-Solomon codes," *IEEE Commun. Letters*, vol. 8, no. 4, pp. 244–246, Apr. 2004.

46. M. El-Khamy and R. J. McEliece, "Iterative algebraic soft-decision list decoding of Reed-Solomon codes," *IEEE J. Selected Areas Commun.*, vol. 24, no. 3, pp. 481–490, Mar. 2006.

47. P. A. Bello, "Characterization of randomly time-variant linear channels," *IEEE Trans. Commun. Syst.*, vol. CS-11, no. 4, pp. 360–393, Dec. 1963.

48. P. A. Bello and B. D. Nelin, "The effect of frequency selective fading on the error probabilities of incoherent and differentially coherent matched filter receivers," *IEEE Trans. Commun. Syst.*, vol. CS-11, no. 2, pp. 170–186, June 1963.

49. M. B. Pursley, *Introduction to Digital Communications*, Appendix C, Upper Saddle River, NJ: Prentice-Hall, 2005.

50. F. D. Nesser and J. L. Massey, "Proper complex random processes with applications to information theory," *IEEE Trans. Inform. Theory*, vol. 39, no.4, pp. 1293–1302, July 1993.

51. P. A. Bello and B. D. Nelin, "The influence of fading spectrum on the binary error probabilities of incoherent and differentially coherent matched filter receivers," *IRE Trans. Commun. Syst.*, vol. CS-10, no. 2, pp. 160–168, June 1962.

52. S. B. Wicker *Error Control Systems for Digital Communication and Storage*, Chapter 8, Englewood Cliffs, NJ: Prentice-Hall, 1994.

53. A. J. Viterbi, "Convolutional codes and their performance in communication,"*IEEE Trans. Commun.*, vol. 19, no. 5, pp. 751–772, Oct. 1971.

54. D. Divsalar and F. Pollara, "Turbo codes for PCS applications," in *Proc. of 1995 IEEE Intern. Conf. Commun.* (Seattle, WA),pp. 54–59, June 1995.

55. M. B. Pursley, "Coding and diversity for channels with fading and pulsed interference," in *Proc. Conf. Inform. Sciences Syst.* (Princeton, NJ), pp. 413-418, Mar. 1982.